DEVELOPMENT OF THE *FR 13* RISK FRAMEWORK – DEMONSTRATED WITH ONE- AND TWO-STEP STEADY-STATE MEMBRANE PROCESSING OF JUICES

by

Mr Wei ZOU

School of Chemical Engineering

The University of Adelaide

A thesis submitted for examination for the degree of

Master of Philosophy (Chemical Engineering)

December – 2015

STATEMENT OF DECLARATION

I, Wei Zou, certify that this work contains no material which has been accepted for the award of any other degree or diploma in any university or other tertiary institution and, to the best of my knowledge and belief, contains no material previously published or written by another person, except where due reference has been made in the text.

I give consent to this copy of my thesis when deposited in the University Library, being made available for loan and photocopying, subject to the provisions of the Copyright Act 1968.

The author acknowledges that copyright of published works contained within this thesis[1] resides with the copyright holders of those works.

I also give permission for the digital version of my thesis to be made available on the web, via University's digital research repository, the Library catalogue and also through web search engines, unless permission has been granted by the University to restrict access for a period of time.

Signature:

Date:

---

[1] Davey, K.R., Zou, W., 2015. Fruit juice processing and membrane technology application (*sic*) – A response. Food Eng. Rev. – submitted Oct. 2015.

Zou, W., Davey, K.R., 2014. A *Friday 13th* risk model for failure in cross - flow membrane filtration of passion fruit juice. In: Proc. 26th European Modelling and Simulation Symposium - EMSS 2014, Sept. 10 – 12, Bordeaux, France, paper 106. ISBN: 9788897999386

Zou, W., Davey, K.R., 2014. A novel *Friday 13th* stochastic assessment of failure of membrane filtration in juice clarification. In: Proc. 44th Australasian Chemical Engineering Conference (Processing Excellence, Powering our Future). Sept. 27 – Oct. 1, Perth, WA, Australia, paper 1259. ISBN/ISSN: 1922107387

Zou, W., Davey, K.R., 2015. An integrated two-step *Fr 13* synthesis – demonstrated with membrane fouling in combined ultrafiltration-osmotic distillation (UF-OD) for concentrated juice. Chem. Eng. Sci. – submitted on Nov. 2015.

EXECUTIVE SUMMARY

Steady-state processing is used extensively in foods and chemical, engineering, and more widely. Importantly, however there will be naturally occurring, random fluctuations in parameter values about an apparent steady-state 'set' mean. These are not sufficient, on their own, to be considered transient i.e. unsteady-state. Generally, random small change in one parameter is 'off-set' by a corresponding change in another - with the output seemingly remaining steady. Traditional chemical engineering does not address these random fluctuations explicitly.

However, Davey and co-workers (e.g. Abdul-Halim and Davey, 2015 a, b; Davey, 2015 a; Davey et al., 2016) have reasoned that process failures can result from the accumulation of these fluctuations within an apparent steady-state process itself. Their hypothesis is that naturally occurring chance fluctuations can unexpectedly combine and accumulate in one direction and leverage significant change across a binary 'not failure - failure' boundary. That is to say, even with good design and operation of plant, there can be unexpected (surprise and sudden) occasional failures. This they titled *Fr 13* (*Friday 13th*) to underscore the nature of the event. A current limitation of the *Fr 13* framework however that is it has been largely limited to one-step (single) unit-operations. It was not known therefore if there was any benefit in developing the framework as a useful tool for integrated multi-step foods and chemicals engineering unit-operations.

A research program was therefore undertaken with the aim to advance the *Fr 13* framework to gain unique insight into how naturally occurring fluctuations in apparent steady-state plant parameters can be transmitted and impact in progressively complex (in the context of 'integrated' not 'complicated') multi-step processes, and to assess the *Fr 13* framework as a new design tool.

A logical and stepwise approach was implemented as a research strategy.

Because steady-state membrane clarification and concentration of fruit juices is becoming a widespread alternative to traditional thermal treatments, a two-step membrane concentration was selected as a timely and stringent test of development of the *Fr 13* risk thesis.

Two, preliminary single-step *Fr 13* membrane models, 'dead-end' and 'cross-flow', were initially synthesized and tested with independent experimental data for clarification of orange (n = 25) and blood orange (n = 34) juice. *Fr 13* simulations of the key input parameters, transmembrane pressure (ΔP), filtration time (t) and volumetric flow rate (Q), revealed that some 16.8 % of dead-end and 4.0 % of cross-flow membrane filtrations, over an extended time, will fail to meet the required operational flux plus a practical tolerance (2 %) as a design margin of safety. If each filtration is thought of as a daily batch-continuous operation, then an unexpected fouling failure could result every six (6) and 26 days, respectively, in batch–continuous processing.

A more commercially representative integrated two-step *Fr 13* membrane global model was then synthesized for combined ultrafiltration (UF) - osmotic distillation (OD) (UF-OD), and validated with extensive independent data (n = 27) for pomegranate (*Punica granatum*) juice. Overall global failure of the integrated two-step UF-OD was defined as a fouled (unwanted) OD flux. *Fr 13* simulations showed that the integrated UF-OD is expected to be vulnerable to surprise fouling failure in 10.5 % of all operations over an extended time. This translates to 39 surprise failures per year with a 3 % design tolerance. In completing this work an important error in the membrane literature was discovered, corrected and addressed[2].

Fr 13 simulations of these newly synthesized models underscored that the three (3) apparent steady-state membrane processes should be more correctly thought of as a combination of successful and failed operations. This new insight is not available from traditional risk and hazard analyses, with or without sensitivity analyses.

Findings were applied in 'second-tier' studies to assess re-design of membranes processing of juices. The aim was to improve process reliability and reduce vulnerability to unexpected failure. For example, repeat *Fr 13* simulations revealed that for the integrated

[2] The permeate flux (J_0) used for measuring membrane permeability was found to be widely incorrectly defined e.g. by Schafer et al. (2005), Boerlage et al. (2002) and Echavarria et al. (2011) in which it was not possible to reconcile the form or units in engineering science. The effect was to significantly overestimate the predicted vulnerabilities to *Fr 13* fouling failure, in the preliminary work. This is being addressed by Davey and Zou (2015) (*see* Appendix C).

UF-OD, reducing variance about the mean value of transmembrane pressure ($\Delta P_{UF\ 1\text{-}1}$) and filtration time ($t_{UF\ 1\text{-}1}$) of UF significantly reduces overall UF-OD failures (p_2). Practically, this suggests costs for increased precision control to limit fluctuations in the UF parameters could be readily justified.

Further, second-tier simulations of the integrated UF-OD showed that the addition of an enzymatic treatment step prior to UF could significantly reduce the overall UF-OD failures through a reduction in the required (design) operational UF flux ($J_{UF\ 1\text{-}1,\ required}$).

These findings will aid an enhanced understanding of factors that contribute to unwanted fouling as membrane failure, and to increased confidence in steady-state membranes operations.

It is concluded that the *Fr 13* framework is generalizable to an integrated two-step, steady-state processes. Additionally, there appears no methodological barriers to advancement. Therefore results auger well for further advancement of the *Fr 13* framework to a range of steady-state processes of increasing complexity and inter-connectedness. If properly developed, it is thought that *Fr 13* could become a new decision tool, in both design analysis and synthesis, for improved understanding of process behaviour outcomes.

This research is original and not incremental work. Outcomes are of immediate interest to researchers in risk analyses and processors and manufacturers of membrane equipment.

ACKNOWLEDGMENTS

I would like to express my gratitude to Dr K R (Ken) Davey (FIChemE), my principal supervisor from the School of Chemical Engineering, The University of Adelaide, for his patience, instruction, encouragement and time in guiding and helping throughout my candidature. I especially acknowledge his immense help and support in addressing various issues that arose. Also I wish to thank Dr Brian O'Neill, my co-supervisor from the School of Chemical Engineering, The University of Adelaide, for providing guidance and advice.

I would also like to thank Professor Peter Ashman, Head of the School, and to all staff members in the School of Chemical Engineering, for giving me the opportunity to complete my research degree.

I am greatly indebted to my parents who gave me the opportunity to come to Australia and I would also like to thank them for providing me with the financial assistance for doing so.

I would also like to thank my colleagues, especially Saravanan, Priyantha, Nadiya, James, and all my friends here in Adelaide for being there when needed, and for providing moral support.

I hope that the results of my efforts justify the expectations and confidence of the people concerned, and the interest, help, and encouragement of all my family, friends and colleagues.

TABLE OF CONTENTS **PAGE**

LIST OF FIGURES **PAGE**

LIST OF TABLES **PAGE**

CHAPTER 1

INTRODUCTION

The foods industries are the world's largest manufacturing sector and one of the most stable (Davey, 2001). Batch-continuous, steady-state processing is widely practiced. Advantages include ease of control and a uniform product quality (Ghasem and Henda, 2008; McCabe et al., 2001).

Davey and co-workers however have demonstrated that naturally occurring, random fluctuations about 'set' parameter values can result in process and product failures. These fluctuations are overlooked in traditional chemical engineering as being problematic; this is because they are not sufficient on their own to be considered transient i.e. unsteady-state (Zou and Davey, 2015; Sinnott, 2005; Amundson et al., 1980). Their underlying hypothesis is that random fluctuations in process parameter values can accumulate in one direction in amounts sufficient to leverage significant change about a carefully defined (binary) boundary and thereby make apparently well-operating processes vulnerable to random (surprise) *failure*[3]. They titled their approach *Fr 13* (*Friday 13th*) to illustrate the surprise nature of behaviour of the process or resultant product. A *Fr 13* risk assessment requires an underlying systems unit-operation model, together with a carefully defined risk factor and a refined Monte Carlo (r-MC) sampling. Carefully selected distributions are used to realistically mimic naturally occurring fluctuations in plant parameters.

Published studies of application to one-step unit-operations included vulnerability to pitting (corrosion) of metals at sea (Davey et al., 2016) as a result of naturally occurring fluctuations in sea temperature and salinity; the failure of thermal efficiency in a coal-fired-boiler (Davey, 2015 a) due to fluctuations in coal feed quality; a sudden shift from 'safe to unsafe' in Clean-In-Place milk processing (Davey et al., 2013; 2015); an unexpected and sudden shift from potable to non-potable water with ultraviolet irradiation (Abdul-Halim and Davey, 2015 a, b); a surprise shift from stable to unstable i.e. washout in fermenter operation (Patil et al., 2005; Patil, 2006); and, a sudden shift from sterile to non-sterile UHT milk (Cerf and Davey, 2001; Davey and Cerf, 2003).

The recent Blackett Review (Anon., 2012) has reported that these low-probability high-impact failures are an emerging challenge for governments and operators of processes;

[3] *see* Appendix A for a definition of important terms used in this study. The first use appears in the text italicized.

and is compounded due to increasing inter-connectedness of product and processes world-wide. For example, despite conservatively being twice UHT (steady-state) pasteurized (130 ^{O}C, 4 s) low-fat milk unexpectedly remained contaminated, and was used in manufacture of other milk products within 24 h resulting in 13,420 cases of poisoning before recall (Asao et al., 2003).

A current drawback with development of the *Fr 13* framework in addressing these issues however that is the work has been largely limited to single, i.e. one-step, unit-operations. It is not known conclusively if there is a benefit to apply the approach, or to develop the framework as a useful design tool, in progressively integrated multi-step manufacturing processes.

Thus, this research program was undertaken to advance the *Fr 13* framework for integrated multi-step processes. The goal was to test the framework for an integrated two-step manufacturing process – these are widely practiced in the foods and chemicals industries.

Because the steady-state membrane processing of fruit juices is becoming a widespread alternative to traditional thermal treatments, an integrated two-step ultrafiltration-osmotic distillation (UF-OD) membrane concentration was selected as a timely and stringent test of development of the *Fr 13* framework. Fouling failure of membranes is defined as a failure to meet the required (design), operational flux plus a practical tolerance as a design margin of safety, under auto-set processing conditions.

The principle aim of this research is to gain new insights, initially, into failure of single (one-step), and to build on this to investigate integrated (two-step), membrane processes, to stringently test the *Fr 13* framework as a useful design tool for multi-step processes in a steady-state global plant.

A justification is that results could not only be used to improve membranes design and operations, together with improved process efficiency, and potentially plant safety, but also results be generalized and be more widely applied.

A logical and stepwise approach was implemented as the research strategy.

Relevant literature is reviewed in Chapter 2 which summarizes the *Fr 13* framework with recent developments, applications and limitations. As membranes processing was

judiciously selected as a focus for this research, membrane properties and associated membranes unit-operations and fouling mechanisms are reviewed, and; unit-operations models of membranes are identified and evaluated.

In Chapters 3 and 4 a preliminary one-step *Fr 13* membrane model for, respectively, both a steady-state dead-end (*MF*) and cross-flow (*UF*) filtration is synthesized and tested with independent data for clarification of orange and blood orange, juice.

In Chapter 5 a novel integrated two-step *Fr 13* synthesis is developed for the first time. It is demonstrated with membrane fouling in a combined *UF-OD* global model for concentrated juice. Second-tier studies are undertaken to assess re-design for improved process efficiency and plant safety.

This thesis concludes with a summary and conclusions together with possible future developments, in Chapter 6.

A definition of important terms used in this research is listed and carefully defined at the end of the thesis. All symbols used are defined in relevant Nomenclature.

Refereed publications arising from this research are given in Appendix D.

CHAPTER 2

LITERATURE REVIEW

2.1 Introduction

An unexpected (surprise) and sudden failure, or *Friday 13th* (*Fr 13*), event, is a notion that has long persisted in the industrial West (Suddath, 2009) – and something anecdotally widely acknowledged in steady-state (Rosen, 2009) foods and chemicals manufacturing and processing. These unexpected surprise (and sometimes catastrophic) failures are inclined to be mistakenly blamed on 'human error' or 'faulty fittings', usually after exhaustive official hearings (Davey, 2011).

However, Davey and co-workers are developing a quantitative *Fr 13* risk framework to illustrate that process failures can actually be the result of accumulation of random fluctuations within the process itself. This framework has been successfully applied to a number of steady-state one-step *unit-operations* (e.g. Davey et al., 2016; Abdul-Halim and Davey, 2015 a, b; Davey, 2015 a; Davey et al., 2015; Zou and Davey, 2015).

In this chapter, a detailed review of the *Fr 13* framework, recent developments, applications, benefits and limitations is presented and a comparison made with traditional unit-operations solutions and alternative risk techniques.

Membrane processing of fruit juices was selected to test and advance the framework as this process used extensively in the foods process industry. Moreover, integrated membrane clarification and concentration of fruit juices is becoming a widespread alternative to traditional thermal treatments. The properties of membranes, and membranes unit-operations and fouling failure mechanisms are reviewed in this chapter and membrane unit-operations models are identified and evaluated.

To conclude this chapter, two (2), single-step steady-state membrane models are selected for *Fr 13* investigation for the first time.

2.2 Traditional single value assessment (SVA) solution

The traditional method to computationally solving foods and chemicals engineering unit-operations is a single point, deterministic approach, with or without a sensitivity

analysis (Sinnott, 2005). Cerf and Davey (2001) (Davey and Cerf, 2003) defined this methodology as Single Value Assessment (*SVA*).

In this traditional approach, model inputs are linked together with outputs via mathematical expressions such as multiplication, subtraction, addition and exponentiation. The equations can be conveniently solved in mathematical software e.g. Microsoft Excel™ spread sheeting.

A single or 'best estimate' value of input parameters is used to solve for a single 'best estimate' outcome. A variation (± 1 to 5, %) is used around the mean value of inputs to test the robustness of model results, for *uncertainty* in process parameters. Almost all chemical unit-operations used in food and bio-processing can be addressed with this method (Foust et al., 1980; McCabe et al., 2001).

However, naturally occurring random fluctuations on inputs and possible impact(s) on plant outcome behaviour are not accounted for implicitly with this traditional chemical engineering.

2.3 Development of the *Fr 13* framework

The term *Fr 13* was coined and pioneered by Davey and co-workers to explain reoccurring and unexpected failure in otherwise well-operated and well-regulated foods and chemicals processing.

The central idea is that a combination and accumulation of naturally occurring, random fluctuations in key parameter 'set' values, can accumulate unexpectedly in one direction. In some instances the result is to leverage highly significant, and often catastrophic, changes in process or product (Davey, 2015 a; Davey, 2011). This can lead to a product or process being unsafe, unstable or inefficient (Davey and Cerf, 2003; Davey et al., 2015; Davey, 2015 a; Abdul-Halim and Davey, 2015 a, b; Zou and Davey, 2015).

2.3.1 A *Fr 13* risk assessment

Notably, the structure of the *Fr 13* framework is identical to traditional SVA because all multiplications, additions, exponentiations and other mathematical operations that connect the model parameters are the same (Davey, 2015 a; Davey et al., 2016), other than a probability distribution which is used in place of the single 'best' guess to define the key input parameters.

There are five (5) identifiable components to a *Fr 13* risk assessment of steady-state unit-operation processes. These are:

i. Synthesis of an underlying unit-operations model

An underlying unit-operations model must be established. This is normally achieved through synthesis and validation of key process parameters in a computational model and software for particular plant throughputs

ii. Selection of probability distribution

A *probability* distribution is a used for all practically possible values that process parameters may take, together with the likelihood that a parameter will take a single value. Generally, there are some 40 theoretical probability distributions that could be used including Normal, Triangle, Beta-subjective. However, Davey and co-workers reported that the number of *Fr 13* failures is not sensitive to a range of distributions. This might not always be the case however (Law, 2011). A possibility is that these distributions could also be based on expert experience or even opinion (Davey, 2010; Law, 2011)

iii. Establishment of an unambiguous definition of process (or product) failure

A practical and unambiguous definition of failure of process (or product) must be established. In foods and chemicals processing this is usually an unwanted reduction in process efficiency (e.g. Davey 2015 a; Zou and Davey, 2015), or the unwanted survival of contaminant pathogens (Davey and Cerf, 2003), or spoilage microbes (Abdul-Halim and Davey, 2015 a, b)

iv. Sampling using refined (*Latin Hypercube*) Monte Carlo (r-MC)

Monte Carlo (MC) is a statistical technique used to investigate the impact of risk by using randomly selected 'what if' scenarios for simulation. It involves the random sampling of each probability distribution within a parameter to produce 1,000 or 100,000 of iterations. Each probability distribution is sampled in a manner that reproduces the shape of the distribution. Uncertainty and *variability* are two major components of Monte Carlo Assessment (MCA) (Vose, 1998; Vose, 2008).

A refined MC, r-MC with *Latin Hypercube* sampling is used in *Fr 13* because 'pure' MC can over- and under-sample from the distribution. This refinement ensures samples cover the entire distribution. If the number of samples is sufficiently large, the output mean of a product of a large number of independent positive parameters with different distribution functions will be approximately normally distributed (Vose, 2008).

Overall, because a large number of r-MC samples are used in the *Fr 13* simulation, it is argued (e.g. Abdul-Halim and Davey, 2015 a, b; Davey, 2015 a) that it can reasonably be assumed that all process scenarios that can actually occur in practical operation, including failures, are included

v. Interpretation of process behaviour plant outcome behaviour with second-tier studies

The outcome from a *Fr 13* simulation is a distribution of all possible process behaviour configurations, including failures.

A major advantage claimed for *Fr 13* risk assessment is that repeat simulations can be used to investigate process intervention strategies and re-design of the physical plant i.e. 'second-tier' studies (*see* e.g. Abdul-Halim and Davey, 2015 a, b; Davey, 2015 a; Zou and Davey, 2015) to reduce unexpected risk, and it can be applied at both the analysis and synthesis stages.

The overall approach descried above has been formulated as a detailed 5-step algorithm that can be readily applied.

2.3.2 The 5-step *Fr 13* risk algorithm

The generalized algorithm for a *Fr 13* risk assessment was proposed by Davey (Davey, 2010) and subsequently used by Davey and co-workers (e.g. Patil et al., 2005; Abdul-Halim and Davey, 2015 a, b; Davey, 2015 a). This generalized algorithm is thought to be applicable to any steady–state unit-operations process.

The established steps of the algorithm are:

1. Select an identifiable unit-operation and process
    a. Synthesize and validate key process parameters in a computational model and software for particular plant throughputs
    b. Establish a clear definition (s) of process or product failure
2. Identify key process parameters on process (or product) failure(s) using traditional engineering SVA approaches
3. Define and investigate plausible probability distributions for identified key process parameters
4. Simulate the unit-operation and process using *Fr 13* with r-MC (Latin Hypercube) samplings
5. Distill insights to improve design of selected unit-operations with reduced vulnerability to failure
    a. Sensitivity analysis of input parameters and rank significance on failure
    b. Investigate effects of ‘what if’ scenarios and consequences of proposed intervention strategies. Evaluate risk and potential opportunities.

2.3.3 *Fr 13* applications

Table 2-1 presents and summarizes a chronological listing of six (6) unit-operations models published to date in the refereed literature for *Fr 13* assessment of one-step steady-state unit-operations. Contributions made by researchers are reviewed in this section in the chronological order tabulated.

Table 2-1: Summary and chronological listing of published *Fr 13* risk assessments for steady-state, single-step unit-operations processing

	Unit-operation	***Fr 13* model**	**Reference(s)**
1	UHT milk sterilization	Failure of UHT sterilization defined as non-sterility of a 1 L pack of UHT milk. UHT parameters (D_r, z, T, t, C_0) were defined by probability distributions. 16 of 100,000 scenarios were identified as failed operations. Risk was shown to be 16 times greater than industrially accepted criteria (= 10^{-5})	Davey and Cerf (2003)
2	Monod Fermentation	Failure defined as unexpected 'washout' of *E. coli*. Investigated impact of variation (5 to 15 %) of micro-organism growth characteristics i.e. μ_{max}, $Y_{x/s}$, K_s, on the output dilution rate, D_{max}. Results underscored that small random changes in microbiological parameters significantly affect productivity of fermentation	Patil et al. (2005); Patil (2006)
3	Clean-In-Place (CIP) processing	A 2- and 3-stage CIP model was developed to illustrate *Fr 13* failure which defined as failure to remove whey protein on metal surfaces within auto-set cleaning time, i.e. $t'_T < t_T$. Results revealed 4.2 % of 2-stage (T = 50 ^{O}C) and 2 % of 3-stage (T = 75 ^{O}C) CIP operations fail despite a tolerance as a margin of safety. CIP was shown to be a combination of successful and failed operations	Davey et al. (2013; 2015); Chandrakash (2013)
4	UV irradiation for potable water	UV irradiation of *E. coli* in potable water (turbulent flow) was assessed using *Fr 13*. Failure was defined in terms of design and actual reduction of *E. coli*. Simulation of parameters (I_0, k, Q) showed 16 % of UV operations failed to reduce *E. coli* to a regulatory level ($10^{-4.35}$), with a 10 % tolerance. Increased control of physical system e.g. Q and I_0 was shown to reduce failure vulnerability	Abdul-Halim and Davey (2015 a, b)
5	Coal-fired boiler (CFB)	*Fr 13* was used to investigate fuel-to-steam efficiency of CFB. 20 parameters included coal feed and quality. 73 (per 10000) failures (as $\eta' < \eta$ = 77.82 %) were found, equivalent to 3 failures per year. Repeat simulations highlighted pre-mixing of coal as a practical strategy to reduce vulnerability to CFB efficiency failures	Davey (2015 a)
6	Pitting of metals at sea	*Fr 13* was applied to predict risk of metals (AISI 316L) pitting at sea. Demonstrated for Bass Strait. Pitting potential (E_{PIT}) with key parameters i.e. T and $[Cl^-]$, was simulated. 463 (9.26 %) failures as pitting initiation ($E_{PIT} < E_{OCP}$ + *tolerance%*) were found in 5000 iterations. Creation of original 'isorisques' i.e. contours of risk probability, established new atlas of pitting risk	Davey et al. (2016)

The *Fr 13* risk assessment was first applied to explain the vulnerability to failure in an otherwise well-operated UHT milk plant (Davey and Cerf, 2003). Failure of sterilization was defined as a non-sterile 1 L pack of UHT milk with viable micro-organisms, such as *Bacillus stearothermophilus* and *B. thermodurans*, which might pose a serious risk to public health.

The concentration of contaminant spores (C_0), decimal reduction time (D_r), thermal resistance (z), heating temperature (T) and residence time (t) were identified as key sterilization parameters and simulated with r-MC samplings. *Fr 13* simulation showed that the underlying risk value of non-sterility of UHT milk packs (1.6×10^{-4}) predicted from *Fr 13* was respectively, 1.6×10^{5} times greater than that from the SVA of 10^{-9}, and 16 times greater than the industrially accepted value of 10^{-5} for the non-sterility of UHT milk packs. It could be concluded that a higher proportion of the number of non-sterile UHT milk packs would be practically existed, caused by unexpected, random fluctuation within the UHT sterilization itself.

Patil et al. (2005) applied the *Fr 13* framework to a model of batch-continuous Monod fermenter using *Escherichia coli* to investigate the impact of random variation (5 to 15, %) of micro-organism growth parameters on output dilution rate, D_{max}. Failure to 'washout' was defined as an unwanted low dilution rate compared to the value of $D_{max\ output}$ from SVA (i.e. $D_{max} < D_{max\ output}$). Simulations showed that variability (15 % of set mean value) in input microbiological parameters (μ_{max}, $Y_{x/s}$,K_s) significantly affected the productivity of the fermentation process. This practical insight into an otherwise well-operated continuous fermenter contrasted sharply with SVA analysis in which natural variability in microbiological parameters was not accounted for.

A *Fr 13* risk analysis of steady-state, 2- and 3-stage Clean-In-Place (CIP) models was conducted by Davey et al. (2013; 2015). The aim was to gain insight into random errors that may lead to surprise sudden failures of an otherwise well-operated CIP plant. CIP failure was defined as the failure to remove whey protein deposits on wet or metal surfaces in an auto-set processing time i.e. $t'_T < t_T$. Results revealed that for the two-stage CIP process (*bird model*) with a cleaning fluid at a $T = 50\ ^{o}C$, CIP will fail in 4.2 % of all operations, plus a 5% tolerance; and for the three-stage CIP process (*xin model*), with a

cleaning fluid of T = 75 ^{o}C some 2 % of all alkali CIP operations will fail, plus a 2% tolerance, over the long term. Second-tier studies were conducted to find intervention strategies to improve process reliability and safety e.g. improved precision control of cleaning fluid temperature (T).

Abdul-Halim and Davey (2015 a, b) developed a *Fr 13* failure model to assess unexpected risk in steady-state UV irradiation of *Escherichia coli* in potable water. UV failure was defined in terms of design and actual reduction of *E. coli*, together with an assumed tolerance. Simulation of key parameters (I_0, k, Q) revealed that 16 % of successful UV operations can fail to achieve reduction in viable *E. coli* of $10^{-4.35}$ due to random effects, plus a 10 % tolerance. Abdul-Halim and Davey (2015 b) demonstrated that although UV efficacy for potable water was initially reduced by the presence of suspended solids in feed water (as both UV shielding and absorbing agents), fluctuations in the concentration of these however did not meaningfully impact overall vulnerability to failure to produce potable water. UV efficacy was shown to be impacted highly significantly by fluctuation in feed water flow (Q). The study concluded this is strong quantitative evidence to emphasize that solids should be removed prior to UV reactor, and that an improved flow control be used to reduce variance on feed flow, rather than just increasing UV dose.

Davey (2015, a) used *Fr 13* to analyse the fuel-to-steam thermal efficiency of a coal-fire-boiler (CFB) to determine risk of reduced CFB efficiency in the face of naturally occurring fluctuations in key parameters. Simulation of 20 efficiency parameters revealed 73 failures in CFB efficiency per 10,000 operations were found which equals three (3) failures per year on average, over an extended time. The second-tier simulations concluded that coal could be pre-mixed and pre-sized to a consistent blend from batch to batch to provide a standardized feed to a CFB to minimize the unwanted impact of fluctuations in CFB thermal efficiency about a required value.

Further, the underlying probabilistic *Fr 13* method has been applied successfully by Davey et al. (2016) to metals (AISI 316L) pitting at sea (in the Bass Strait). Pitting potential (E_{PIT}) with key parameters i.e. sea surface temperature (T) and salinity ($[Cl^-]$) were defined as Normal and Truncated probability distributions. Simulations showed that 463 (9.26 %) failures as pitting initiation ($E_{PIT} < E_{OCP}$ + *tolerance%*) were found in 5,000

scenarios. An unanticipated but highly constructive outcome was the invention of ‘isorisques’. These were defined as contours of equal probability of risk of pitting of metal as impacted by naturally occurring, chance fluctuations in surface sea temperature (down to 20 m) and sea salinity. It is intended these be used to determine the change in pitting risk after a sudden shift in sea surface temperature or salinity following a major storm or ice (salt-free) melt, or to simulate the impact of (slow) climate change.

Additionally, the framework is currently being successfully applied to original investigations of the impact of naturally occurring, random fluctuations in traffic flow (as occupancy) on energy optimization in maintaining auto-set air temperatures in large buildings (Chu and Davey, 2015; Chu, 2015).

Clearly, the data of Table 2-1 demonstrate that the idea of *Fr 13* has gained acceptance in the literature. Anecdotally at least, some more traditional food and chemical engineers do not like the probabilistic effect of chance, but preferring a more deterministic and traditional SVA approach.

2.3.4 *Fr 13* and other risk approaches

The *Fr 13* framework is predicated on well-established unit-operations model with r-MC samplings. It looks to quantify the impact of accumulation of random fluctuations in parameters on the behaviour of steady-state processes.

The impact that fluctuations in physical parameters in an expected steady-value can have is also the subject of recent risk assessment approaches of Aven (2010), Haimes (2009), Haimes (2004) and others including Milazzo and Aven (2012). For example, Milazzo and Aven (2012) used a quantitative risk approach for surprise failures of the rupture of pipes in the chemical industry. These authors suggested that while a probabilistic approach is useful, uncertainties still remain as to whether data used is applicable to a specific scenario (circumstance). Two techniques to overcome this drawback were proposed. The first was to use chance (uncertainty) distributions (e.g. Beta-distribution; Triangular distribution or Uniform distribution) for plant parameters together with an event tree model to propagate the uncertainties for risk *p*. This is similar to that of the

Fr 13 risk framework. However, their preference was to use a quantitative risk approach, together with a qualitative risk technique, e.g. 'score system' (of Low, Medium, and High) to further investigation of process uncertainties.

A drawback was that this approach remains largely qualitative (subjective) relying on a 'scored' system and is therefore not rigorously quantitative. As acknowledged by Milazzo and Aven (2012) this approach restricts attention to the most credible scenarios.

Because the *Fr 13* framework is imbedded in established unit-operations processing (Foust et al., 1980; Ozilgen, 1998; McCabe et al., 2001) it is openly quantitative and, in principle, generalizable (Davey, 2015 b) and provides a picture of all, practically possible process scenarios, including (carefully defined) failures. Significantly however both approaches share the goal 'to place stronger emphasis (on the impact of) … uncertainties' (Milazzo and Aven, 2012 pp. 1ff).

A criticism of the term *Fr 13* is that it might be more widely considered to refer to a catastrophic event. Importantly, *Fr 13* as defined by e.g. Abdul-Halim and Davey (2015 a) and others does not imply actual breakage or 'faulty fittings' (or even human error), but a sudden and surprise shift across a (binary) boundary.

Importantly, these insights claimed for *Fr 13* and probabilistic methods of Aven and others are not available from traditional risk and hazard analyses such as microbiological risk assessment, Hazard Analysis Critical Control Point (HACCP), HAZard and OPerability (HAZOP) and Reliability Engineering (Notermans and Mead, 1996; Giaccone and Ferri, 2005). As pointed out recently by Abdul-Halim and Davey (2015 a, b) and others including Davey (2011) and Davey (2015 a), this is because the random element is not explicit in these risk and hazard methods.

2.3.5 *Fr 13* as terminology

Although *Fr 13* is carefully defined by Davey and co-workers as a particular plant outcome behaviour i.e. as that portion of a probability distribution of the numerical difference between the value of a key parameter outcome and the actual instantaneous value, plus an acceptable tolerance as a design margin of safety (mathematically this is $p > 0$), it is

acknowledged that *Fr 13* might be thought of as referring to a catastrophic event.

Pointedly, the origin of the terminology was in HTST sterilization of raw milk (as 1 L cartons) (Davey and Cerf, 2003) where there could possibly be a catastrophic legacy, with or without fatalities. *Fr 13* was coined to quantitatively explain surprise failures that could arise from the impact of naturally occurring random fluctuations in key parameter values about a process steady-state 'controlled' mean. The probabilistic element in *Fr 13* is to quantitatively mimic naturally occurring chance fluctuations. It was demonstrated that chance impact through unanticipated accumulation and combination of these fluctuations could lead to unsterile (failed) milk - faulty fittings or human error did not need to be invoked as an explanation.

Suggestions for an alternate terminology include those based on Root Cause Analysis (RCA) (e.g. DNV's Taproot® methodology) - although this does not involve probability assessment, and is typically undertaken after an event has occurred - or further, renamed as an *Iterative Random-impacts Assessment* (IRA) to predict (and fix) probable events before they occur (Zou and Davey, 2015). If advancement of the framework is successful, and adopted as a valuable design tool, IRA might be taken up.

2.3.6 Benefits and limitations of *Fr 13*

The *Fr 13* framework has a number of advantages over alternative probabilistic methods e.g. Aven (2010), Haimes (2009), Haimes (2004) and others (Milazzo and Aven, 2012).

In particular, is that it is based on sound underlying unit-operations, a principle well-established in chemical engineering (Foust et al., 1980; Ozilgen, 1998; McCabe et al., 2001). Further, the *Fr 13* probabilistic element provides a quantitative picture of all, mathematically practical possibilities (i.e. non-subjective), process scenarios, including failures. A result is the quantitative capacity of framework to distinguish the effect of targeted intervention strategies or design changes in second-tier simulations on plant behaviour.

Once established, a major benefit of the *Fr 13* framework is that it can be used in second-tier simulations to make physical changes to a process or operating practices to

reduce vulnerability to failure. This can be undertaken in both analysis and synthesis stages. For example, Davey (2015 a) concluded that coal could be pre-mixed and pre-sized to a consistent blend from batch to batch to provide standardized feed to a coal-fired-boiler to minimize the impact of fluctuations in process thermal efficiency about a required value.

A current drawback with development of the *Fr 13* framework is that the work is largely limited to single, i.e. one-step, unit-operations. Therefore it is not known if there is benefit in applying the approach or developing the framework as a useful tool for multi-step foods and chemicals unit-operations and processes.

Notably, membranes processing is becoming widely used as an alternative to traditional thermal treatments for a range of foods, particularly juices.

For this research, an integrated membrane process of UF-OD was therefore selected as a timely and stringent test of development of the *Fr 13* framework to multi-step unit-operations processing.

2.4 Membranes

Membranes were first discovered by Loeb and Souriragin in the early 1960 s. Membranes normally comprise a thin surface layer which provides required permselectivity[4] and an open, thicker porous support layer which provides mechanical stability and strength. This can be conveniently described as a traditional filter with small-pores to permit the separation of fluids and micro-molecules (D'Souza and Mawson, 2005).

2.4.1 Structure

There are two types of membranes based on structure: micro-porous membranes and asymmetric membranes (Cui et al., 2010).

Micro-porous membranes have an open and random structure with inter-connected micro-pores designed to reject all species above structured membrane pore size. The

[4] Restriction of permeation of macromolecules across membranes on the basis of molecular size and physical configuration.

separation of macromolecules is a function of molecular size and pore size distribution of membranes. In general, only molecules that differ in size can be efficiently separated by micro-porous membranes (Mulder, 1996).

Asymmetric membranes consist of a number of selective skin layers with different structures and permeability at the interface of membranes (Cui et al., 2010). The permeability of asymmetric membranes is determined exclusively by interface layers, (macro-pores), and the body offers mechanical support with virtually, no separating function.

Compared to traditional micro-porous membranes, asymmetric membranes have an advantage of greater transmembrane flux, and therefore block less.

2.4.2 Materials

In terms of materials, depending on applications and self-properties, membranes can be classified into organic (polymeric) and inorganic (ceramic), membranes (Goulas and Grandison, 2008).

Organic membranes are produced using various materials, such as cellulose acetate (CA), poly-(vinylidene fluoride) (PVDF), polyamide (PA), polysulfone (PSF), polyethersulfone (PES), polypropylene (PP) and poly-carbonate (PC), etc. Organic membranes are widely used in juice and beverage industries due to advantages of low cost, easy to produce and being hydrophilic to a wide range of pore size (Goulas and Grandison, 2008). However, a strict operational condition is the major limitation of organic membranes. For example, CA is a typical organic membrane material (thickness 0.1 - 1.0 µm) with the disadvantage of temperature limits of 30 – 40 ^{o}C, narrow pH range (2 – 6) and low chlorine tolerance of free chlorine (~ 1 mg L^{-1}) (Cui et al., 2010).

Inorganic membranes are produced using inorganic materials, including carbon, borosilicate glass, zirconia and alumina, together with narrow particle-size distributions. Compared with organic membranes, inorganic membranes have greater resistance to extreme process conditions such as high temperature, pH, mechanical strength and thermal

stability (Cui et al., 2010). The major limitations are significant-cost and narrow range of pore sizes (Cheryan, 1998).

2.4.3 Module

The membrane module is membrane configuration into devices and hardware to separate the feed stream into permeate and *retentate flux* streams (Cui et al., 2010).

In particular, four (4) membrane modules are widely applied: tubular, hollow fibre, plate-frame and spiral-wound, module. These modules are designed and manufactured to offer a large membrane surface area for effective separations (Goulas and Grandison, 2008).

The tubular module is composed of numerous porous tubes, which may be made from stainless steel, cardboard or plastic, assembled in a shell-and-tube arrangement with selective membranes inside (Goulas and Grandison, 2008). The tubular module provides a large volume per unit surface area for feed streams, and can be readily cleaned by mechanical or chemical treatments.

The hollow fibre module consists of 50-3,000 individual hollow fibres bundled and sealed together inside ceramic tubes (Cui et al., 2010). Compared to other modules, the hollow fibre module has the greatest effective membrane area with low hold-up volume. Moreover, the asymmetric structures with self-supported membranes normally used in this module result in good backwash capacity and is easy to clean.

The plate-frame is a traditional module comprised of one selective flat sheet membrane on top and a flat plate at bottom (Goulas and Grandison, 2008). It is easy to operate, but the limitations are leakage and contamination of feed and permeate streams.

The spiral-wound module is similar in principle to the plate-frame module, but configured of two selective flat-sheet membranes separated by a spacer with the active membrane sides facing away each other (Hausmann et al., 2013). This module offers a large surface area but is easily blocked by suspended substances. Therefore pre-treatment e.g. enzymatic degradation to remove relatively macromolecules in feed streams is required.

A summary comparison of these four membrane modules is presented in Table 2-2.

Table 2-2: A summary comparison of four (4) membrane modules widely used in foods and chemicals engineering (Cui et al., 2010; Echavarria et al., 2011; Goulas and Grandison, 2008)

Parameter	**Membrane module**			
	Tubular	**Hollow fibre**	**Plate-frame**	**Spiral-wound**
Surface area / volume (m^2 m^{-3})	300	15000	600	1200
Internal diameters (mm)	5-25	0.2-3	2-10	4-20
Module length (cm)	0.6-600	18-120	10-60	10-60
Feed flow condition (Re)	10000	500-3000	2100	2100
Driving pressure (bar)	2-4	0.5-2.5	4-20	4-20
Production (m^3 m^{-3} day^{-1})	1000	450-1500	150-500	300-1000
Manufacturing cost (\$ m^{-2})	50-200	2-10	50-200	5-50
Membrane fouling control	Good	Moderate	Poor	Poor
Replacement	Easy	Impossible	Difficult	Difficult
Cleaning				
Mechanical	Yes	No	No	No
Chemical	Yes	Yes	Yes	Yes
Pre-treatment	No	Yes	Yes	Yes

2.5 Membrane unit-operations

The membrane operation can be described as a classical filtration with thin membranes as a filter and pressure as the driving force. Separation of a mixture is achieved by rejection of at least one component by the membrane and passing of other components through the filter (Cui et al., 2010).

The typical configuration of membrane operation for juices contains a membrane module (e.g. tubular and hollow fibre, module), feed tank, pump, control valves and flow rate, temperature and pressure monitoring equipment (Goulas and Grandison, 2008).

This is shown schematically in Fig. 2-1.

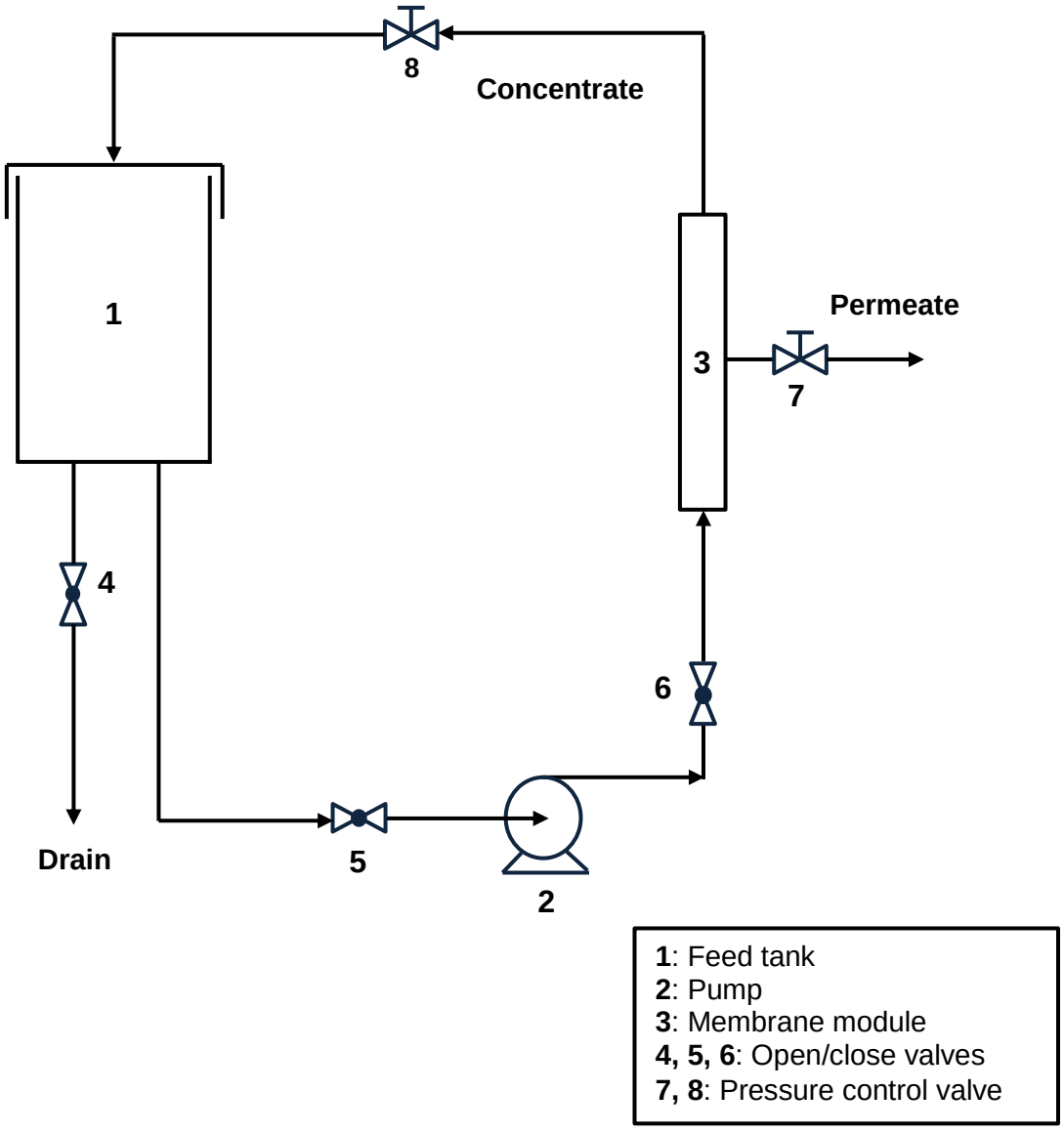

Fig. 2-1: A simplified schematic of a typical membrane unit-operation for juices (adapted from Domingues et al., 2014)

2.5.1 Classification of membrane unit-operations

Based on the different physical properties of membranes and applied driving pressure, there are four (4) classifications of membrane unit-operations that pre-dominantly used for juices, namely microfiltration (MF), ultrafiltration (UF), nanofiltration (NF) and reverse osmosis (RO) (Cassano, 2013).

Table 2-3 presents a summary of these classifications of membrane unit-operations, and the respective separation characteristics. It should be noted that there are no boundaries between unit-operation, and the classifications are conceptually similar.

Table 2-3: Classification of membrane unit-operations and separation characteristics

Process	**Separation characteristics**		
	Pore size range	**ΔP**	**Retained molecules**
MF	0.1-5 µm	1-10 bar	proteins, fat globules, micron particles, macromolecules, casein micelles, suspended particles
UF	1-100 nm	1-10 bar	
NF	0.5-10 nm	10-30 bar	Water, salts, amino acids, simple sugars, organic molecules, bacteria, monovalent electrolytes
RO	< 0.5 nm	35-100 bar	

As shown in Table 2-3, MF and UF are closely matched to remove suspended particles and macromolecules in juices and milk. NF and RO are applicable for the desalination and sterilization of waste and sea, water.

2.5.2 Advantages and disadvantages of membrane processing

Traditional processing of juices is based on thermal treatments with fining agents, such as gelatin, silicasol and bentonite, which results in loss of nutritional compounds and energy wastage (Domingues et al., 2014). Presently, non-thermal membrane processing e.g. MF, UF and OD, is more widely applied in juice and beverage and dairy industries as an alternative emerging technology.

The advantages of membrane processing over traditional thermal treatments include (Cassano, 2013):

1. Reduction of energy requirement and cost
2. Reduction of operational temperature
3. Reduction of waste productions
4. Reduction in enzyme utilization (usage of enzyme reduced from 50 to 75, %)
5. Decreased processing time (traditional ~ 12 to 36 h; cross-flow MF/UF ~ 2 to 4 h)
6. Increased product (juice) quality with rich nutrient compounds
7. Increased juice yield (juice recovery of 96 to 98, %)
8. Possible avoidance of chemical agents, gelatins and other filtration aids
9. Easier replacement and cleaning of equipment.

A major limitation of membrane applications however is fouling which results in a reduction in the transmembrane flux, or blockage of filter. Basically, this is caused by the deposition of suspended or dissolved substances at the membranes interface. Fouled membranes can reduce process efficiency, and potentially plant safety, and disrupt processing. Therefore, cleaning or replacement of membranes is necessary when fouling (failure) occurs – with attendant costs and downtime (Cassano et al., 2006; Cassano et al., 2011; Nandi et al., 2012).

2.5.3 Dead-end and cross-flow filtration

Based on the feed stream flow direction, there are two relatively straightforward models of pressure-driven steady-state membrane filtration, namely dead-end and cross-flow, and each is presented schematically in Fig. 2-2.

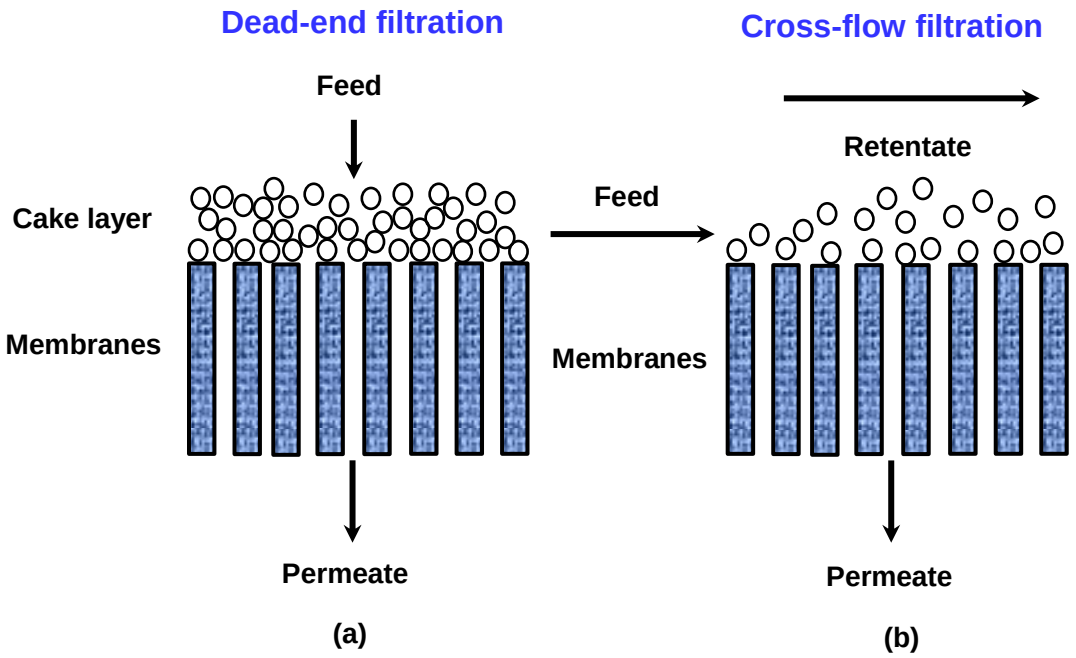

Fig. 2-2: Schematic diagrams of steady-state, dead-end filtration mode (a) and cross-flow filtration mode (b) (adapted from Echavarria et al., 2011)

In dead-end filtration, Fig. 2-2 (a), feed streams flow perpendicularly onto the membrane interface and only permeate stream separates from the membrane. In the build-up of a barrier, titled *cake layer*[5], filtration is the main restriction to *permeate flux* (Saxena et al., 2009). Whereas, in the cross-flow filtration, Fig. 2-2 (b), the feed stream flows tangentially over the membrane interface, and the resulting two streams, the retentate and permeate, are separated by the membranes filter (Goulas and Grandison, 2008).

Compared to dead-end filtration, the tangential flow in cross-flow filtration can help to sweep accumulated solutes away from the membrane interface, limiting the maximum thickness of cake layer, and therefore maintaining permeate flux and increasing the service-life of membranes (Saxena et al., 2009; Cui et al., 2010).

Some membrane researchers have proposed the optimal operating conditions for steady-state dead-end (MF) and cross-flow (UF), filtration of juices to be employed for various types of fruit. Some typical studies are summarized in Table 2-4.

[5] *see* Appendix A for a definition of some important terms used in this research.

Table 2-4: Optimal process conditions reported for steady-state dead-end (MF) and cross-flow (UF) filtration for various types of fruit juices

Fruit juice	Process conditions				Flux ($L\ m^{-2}\ h^{-1}$)	Reference(s)
	T (^{O}C)	A (m^2)	ΔP (kPa)	Q ($L\ h^{-1}$)		
Apple	nd*	0.74	150-400	720	82.5	De Bruijn et al. (2003)
Apple	50	nd	73	1200	55	Constela and Lozano (1997)
Blood orange	25	0.23	85	800	12	Cassano et al. (2007)
Kiwi fruit	20	0.56	1375	nd	15	Wilson and Burns (1983)
Kiwi fruit	25	0.23	85	500	7	Cassano et al. (2004)
Lemon	20	0.0069	60	24.84	20	Espamer et al. (2006)
Orange	20	0.0022	344.74	108	15.12	Nandi et al. (2012)
Orange	19	0.046	50	972	11.8	Todisco et al. (1996)
Passion fruit	25	0.056	100	648	10.8	Domingues et al. (2014)
Passion fruit	36	0.48	150	1500	50	Vaillant et al. (1999)
Pineapple	25	0.98	150-300	nd	103	De Carvalho et al. (2008)
Pomegranate	25	0.0046	96	69.84	25.13	Cassano et al. (2011)
Pomegranate	nd*	nd*	50	nd*	6	Mirsaeedghazi et al. (2010)

nd*: not determined

Cassano et al. (2007) for example investigated the effects of process conditions (ΔP, Q and T) on the performance of cross-flow UF and tested with blood-orange juice (Table 2-4). Optimal operating conditions proposed were ΔP = 85 kPa; Q = 800 L h^{-1} and T = 25 ^{O}C. The quality of clarified blood orange juice was found similar to initial raw juice in terms of total soluble solids (TSS), suspended solids (SS), total antioxidant activity (TAA) and flavones.

Domingues et al. (2014) applied the cross-flow UF to produce clarified Yellow passion fruit (*Passiflora edulis var. flavicarpa*) juice. Hollow fibre membranes with pore diameter of 0.4 µm and surface area of 0.056 m^2 were used (Table 2-4). Permeate flux varied between 12.5 and 20 L m^{-2} h^{-1}. The clarified passion fruit juice was almost free of turbidity. Further, the effects of some pre-treatments (i.e. enzymatic, centrifugation and chitosan coagulation) on permeate flux were studied. and optimal operating conditions were selected as ΔP = 100 kPa; Q = 648 L h^{-1}; A = 0.056 m^2 and T = 25 ^{O}C.

Nandi et al. (2012) used low-cost ceramic membranes with a Molecular Weight Cut-Off (MWCO)[6] of 52.5 Da and thickness of 4.55 mm to test dead-end MF of orange juice (Table 2-4). The optimal condition for enzyme-treated centrifuged (ETCJ) orange juice was found to be at ΔP = 344.74 kPa; Q= 106.2 L h^{-1}, t = 720 s and T = 25 ^{O}C.

In summary, due to the ready scalability and advantage of low-cost, cross-flow filtration proved to be more extensively used for clarification of raw fruit juices, compared with dead-end filtration (Saxena et al., 2009; Cassano, 2013).

2.5.4 Osmotic distillation

Osmotic distillation (OD) is an emerging technique for the concentration of thermal sensitive liquid foods, such as milk, fruit juices and natural colors. The aim of OD is to produce the concentrated liquid products, while preserving nutritional and organoleptic properties (Ravindra Babu et al., 2006).

The OD concentration is based on application of porous hydrophobic membranes designed to separate two liquid phases (feed and stripping solutions) with different solute concentrations. The membrane functions as a vapour gap between two solutions. Any volatile component (i.e. pure water) is free to migrate by diffusion or convection (Hogan et al., 1998). The driving force of such transportation is vapour pressure across membrane, induced by different water activity between feed and stripping (osmotic agent) solutions. This is schematically presented as Fig. 2-3.

[6] MWCO refers to the lowest molecular weight solute (in Da or kDa) in which 90% of the solute is retained by the membrane, or the molecular weight of the molecule that is 90% retained by the membrane.

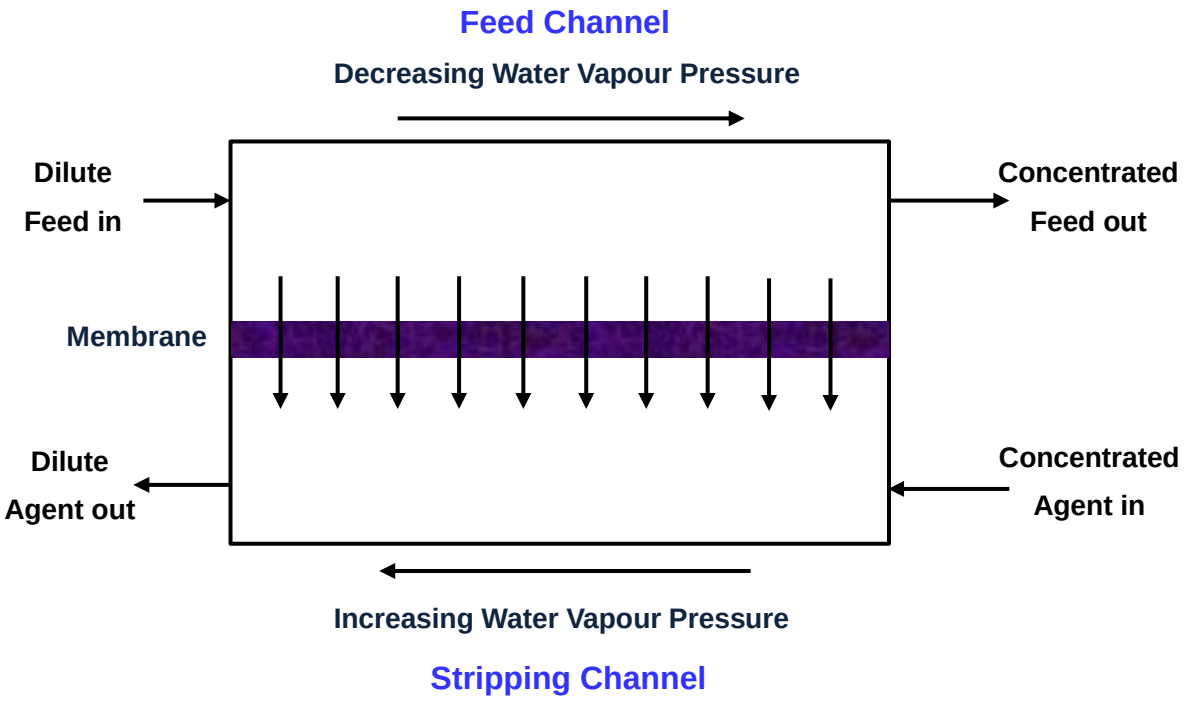

Fig. 2-3: Mechanism of OD through a porous hydrophobic membrane with different water vapour of feed and stripping solutions (adapted from Hogan et al., 1998)

In the mechanism of OD, a dilute solution is on one side of the membrane and a hypertonic stripping solution is on the opposite side. Water evaporates from the feed solution with high vapour pressure, passing through the membrane pores, and condensing on surface of stripping solution of low vapour pressure. This migration leads to a concentration of feed solution, and dilution of stripping solution (osmotic agent) without thermal damage of liquid products (Fig. 2-3) (Ravindra Babu et al., 2008; Cassano and Drioli, 2007).

OD concentration has been of interest to beverage industries for the past decade. The major advantage of OD concentration is that low and stable processing temperature limits the loss of organic and nutrient compounds of liquid products.

For example, Cassano and Drioli (2007) used OD to concentrate kiwi fruit juice in the laboratory. The experiment was conducted at ΔP = 413.7 kPa; A = 1.4 m^2 and T = 25 to 40, ^{O}C, using four (4) different types of stripping solutions. The juice was successfully

concentrated from 9.4 to 66.6 ^{O}Brix[7]. Results indicated that OD concentrated juice has the advantage of maintaining ascorbic acid content and total antioxidant activity (TAA), as compared to a 50 % reduction of TAA was detected in samples undergoing traditional thermal treatment.

Cranberry juice was concentrated by Zambra et al. (2015) with the objective to increase juice concentration from 8.6 to 40 ^{o}Brix. Optimal conditions were selected at T = 30 to 40, ^{O}C; Q = 90 L h^{-1}; A = 0.58 m^{2} and $CaCl_2$ solution as osmotic agent. The permeate flux of water vapour varied from 0.25 to 1.21 L m^{-2} h^{-1}. Results revealed that OD concentration did not affect nutrient compounds of raw cranberry juice (e.g. phenolic contents and anthocyanin), and the process could be widely applied to other berry juices.

2.6 Membrane failure as fouling

In membrane processing of fruit juices, fouling failure is a dominant limitation of membrane behaviour that reduce processes efficiency and potentially, plant safety.

Membrane fouling is a consequence of reduced permeate flux over processing time caused by accumulation of suspended or dissolved substances on the membrane interface or inside pores (Cui et al., 2010). Chemical interaction between materials, solutes and microorganisms growth on the interface of membranes can also lead to fouling failures (Echavarria et al., 2011). Therefore, fouling of membranes cannot be simply eliminated by just stopping the process.

Four (4) pre-dominant fouling mechanisms for porous membranes are complete blocking, internal pore blocking, partial pore blocking and cake layer formation (Fig. 2-4).

[7] ^{O}Brix is the dissolved solid content of an aqueous solution. One degree ^{O}Brix equals 1 gram of sucrose in 100 grams of solution and represents the strength of the solution as percentage by mass.

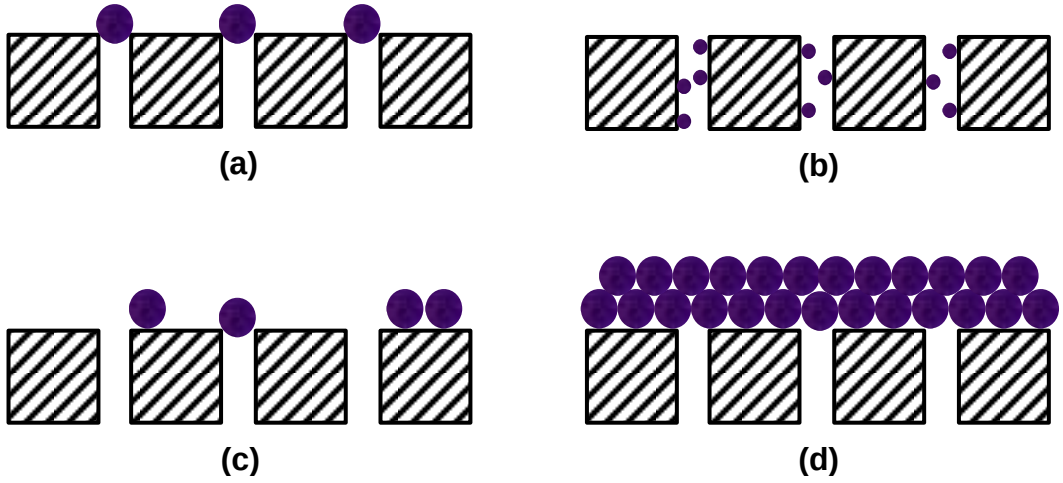

Fig. 2-4: Schematic representation of fouling mechanisms for porous membranes: (a) Complete pore blocking; (b) Internal pore blocking; (c) Partial pore blocking; (d) Cake layer formation (reproduced from Cui et al., 2010)

For complete blocking (Fig. 2-4 a), the size of rejected molecules is larger than pores diameter of membrane, which leads to complete pore obstruction over the membrane interface. In internal pore blocking (Fig. 2-4 b) the occlusion of particles smaller than pore size inside membrane pores reduces internal volume and increases membrane resistance. In partial pore blocking (Fig. 2-4 c), large particles may bridge a pore by obstructing membrane surface but not completely block it.

In these three (3) fouling modes (Fig. 2-4 a, b, c), cross-flow velocity has no effects on fouling mechanism and no limited permeate flux is observed.

However, for the cake layer formation (Fig. 2-4 d), solid particles form a '*cake layer*' on the membrane interface and the thickness of 'cake' increases over processing time. The overall resistance is linked to resistance of membranes plus resistance of the cake layer.

Based on membrane studies of various types of fruit juices, for example apple, pineapple, orange, passion fruit, kiwi fruit and pomegranate, juices, some researchers report that cake layer formation is the prominent fouling mode which controls membrane processing of fruit juices (Nandi et al. 2012; Domingues et al., 2014; De Carvalho et al., 2008; Cassano et al., 2004; Cassano et al., 2006; Cassano et al., 2011; Razi et al., 2012).

In general, fouling failure of membranes can be addressed using cleaning treatments which can efficiently remove fouling deposit and recover membrane permeability (Echavarria et al., 2011). The methods are reported in three categories (Cassano, 2013; Echavarria et al., 2011).

1. Chemical cleaning.
2. Mechanical cleaning.
3. Hydraulic cleaning.

Chemical cleaning is the most common method for fouling control by using different chemical detergents separately or in combination. The frequency that membranes require to be cleaned and chemical concentration used depends on the membrane resistance and specific process conditions.

Mechanical cleaning is used only for tubular membranes. The idea is using oversized sponge balls to remove foulant from membranes interface.

Hydraulic cleaning, such as back-flushing reverses transmembrane flows to remove the cake layer through permeate liquid or gas as a back-flushing medium (Cassano, 2013).

In general, membrane resistance, module configuration and membrane foulant are three (3) important factors that need to consider when selecting an appropriate cleaning method.

2.7 Membrane unit-operations models

Membrane fouling in juice processing has been discussed in the literature for over 30 years. In principle, membrane fouling result in reduction of permeate flux which is below original membrane permeability (Field et al., 1995). Process models developed to date have a conjoint origin and are a function of system thermo-hydraulics, e.g. temperature, transmembrane pressure, filtration time and volumetric feed flow rate.

The overall characteristics of flux reduction during steady-state membrane filtration can be described through the following equation (Aimar and Howell, 1989):

$$J' = \frac{\Delta P}{\mu_T \cdot R_T} = \frac{\Delta P}{\mu_T \cdot (R_m + R_{ir} + R_r)} \qquad (2.1)$$

where J' = instantaneous value of permeate flux; ΔP = transmembrane pressure; μ_T = viscosity of liquid product; R_m = hydraulic resistance of clean membrane; R_{ir} and R_r = hydraulic resistance of irreversible and reversible fouling effects on flux, respectively.

Hermia (1982) was the first to develop a physical model for dead-end filtration based on intermediate blocking law (empirical) for pressure-driven membranes.

The result was presented in the form of:

$$-\frac{1}{A^2 \cdot J'^3} \cdot \frac{dJ'}{dt} = K_n \cdot \left(\frac{1}{A \cdot J'}\right)^n \tag{2.2}$$

where A = average surface area of membranes, and K_n and n are phenomenological coefficients depending upon the fouling mechanism involved.

Eq. (2.2) is the fundamental mathematical expression for dead-end membrane model in the absence of any cross-flow effect.

Cui et al. (2010) and Field and Wu (2011) modified Eq. (2.2) as:

$$J' = J_0 \cdot \left(1 + K_n \cdot (2-n) \cdot (A \cdot J_0)^{(2-n)} \cdot t\right)^{\frac{1}{n-2}} \tag{2.3}$$

According to the fouling mechanism outlined in section 2.6, the value of n and relevant model equations for steady-state dead-end membrane filtration are summarized in Table 2-5 and labelled Eqs. (2.4) to (2.7).

Field et al. (1995) was the first to synthesize a unifying model for cross-flow membrane filtration, hypothesizing that, the transmembrane flux tends to a steady-state value over a long processing time. The flux equation is given as:

$$-\frac{dJ'}{dt} = k_n \left(J' - J^*\right) \cdot J'^{(2-n)} \tag{2.8}$$

The value of k_n and n are determined by different fouling mechanisms. J^* is the 'steady flux' measured at completion of filtration, assuming a single fouling mechanism is operating. The modified flux equations for steady-state cross-flow membrane filtration are summarized in Table 2-6 and labelled Eqs. (2.9) to (2.11).

Table 2-5: Phenomenological background and flux equations of four (4) different fouling modes in dead-end membrane filtration (adapted from Cui et al., 2010)

Fouling mechanism	***n***	**Phenomenological background**	**Flux equation**
Complete pore blocking	2	Pore blocked due to the particles larger than the pore size	$J = J_0 \cdot e^{-K_n \cdot t}$ (2.4)
Internal pore blocking	1.5	Instruction of particles (smaller than pore size) into the membrane pores. Reduction in pore volume leads to blinding pores	$J = J_0 \cdot (1 + 0.5 \cdot K_n \cdot (A \cdot J_0)^{0.5} \cdot t)^{-2}$ (2.5)
Partial pore blocking	1	Large particles might bridge a pore by obstructing membrane surface but not block it completely	$J = J_0 \cdot (1 + K_n \cdot (A \cdot J_0) \cdot t)^{-1}$ (2.6)
Cake layer formation	0	Formation of a cake layer on the membrane surface but do not instruction into the pores	$J = J_0 \cdot (1 + 2 \cdot K_c \cdot (A \cdot J_0)^2 \cdot t)^{-0.5}$ (2.7)

Table 2-6: Flux equations of four (4) different fouling modes in cross-flow membrane filtration (adapted from Field and Wu, 2011)

Fouling mechanism	***n***	**Flux equation** (Field and Wu, 2011)
Complete pore blocking	2	$J' = (J_0 - J^*) \cdot e^{-k_n \cdot t} + J^*$ (2.9)
Internal pore blocking	1.5	As for dead-end filtration i.e. Eq. (2.3)
Partial pore blocking	1	$J' = \frac{J^*}{\left[1 - \left(\frac{J_0 - J^*}{J_0}\right) \cdot e^{(-J^* \cdot k_n \cdot t)}\right]}$ (2.10)
Cake layer formation	0	$k_0 \cdot t = \frac{1}{J^{*2}} \cdot \left[\ln\left(\frac{J'}{J_o} \cdot \frac{(J_0 - J^*)}{(J' - J^*)}\right) - J^* \cdot \left(\frac{1}{J'} - \frac{1}{J_0}\right)\right]$ (2.11)

At present, there is no established mathematical model to meaningfully predict fouling risk of membrane processes. Further, published unit-operations models do not involve a stochastic element that might impact low permeate flux and failure of operation. The flux equations Eq. (2.7) and (2.11) from Table 2-5 and 2-6 were therefore selected for further *Fr 13* investigation of juice processing, discussed in detail in the following chapters.

2.8 *Fr 13* framework for membranes

Based on review of the *Fr 13* framework and membranes, the *Fr 13* framework applied to membrane processes of juices can be outlined as:

1. Structure membrane processing as an identifiable steady-state unit-operation and establish a clear definition (s) of fouling failure
2. Identify key membrane parameters (e.g. transmembrane pressure and processing time) on fouling failure using a traditional engineering solution (SVA)
3. Derive, investigate and test plausible probability distributions for key parameters
4. Simulate the established membrane process models and failure(s) using *Fr 13* with r-MC (Latin Hypercube) samplings
5. Distil insights, i.e. *Fr 13* second-tier study into intervention strategies, for minimizing vulnerability to fouling failure and improve membrane unit-operations and processes.

2.9 Chapter summary and conclusions

Based on critical review of the literature, the following important factors emerge as relevant to this research:

1. The *Fr 13* risk framework has been successfully developed from and applied to steady-state, single-step foods and engineering unit-operations to gain new insight into how naturally occurring, random fluctuations within process parameters can lead to unexpected (surprise) failures in a well-operated steady-state plant

2. A major advantage claimed for *Fr 13* is that, because it provides quantitative insight into underlying unit-operations behaviour and plant outcomes, it can be used to devise process intervention strategies and re-design of physical plant i.e. second-tier studies to reduce risk, and it can be applied at both analysis and synthesis stages. An important limitation of the *Fr 13* framework to date however is that it is has been applied to one-step (single) unit-operations

3. Membrane processing MF, UF and OD is widely used in juice and dairy industries as an alternative to traditional thermal treatments. Fouling of membranes caused by deposition of rejected macromolecules above the interface of membranes is the major process limitation, resulting in low permeate flux, will significantly reducing process efficiency and disputing processing

4. The membrane models developed and synthesized by Field and Wu (2011) are particularly well-suited for *Fr 13* assessment of failure vulnerability in a well-operated membrane plant. Failure (fouling) is defined as an unwanted permeate flux which is below the design criteria

5. Despite apparent utility of failure vulnerability for gaining greater insight into practical operations of membranes, none has been reported

6. The *Fr 13* framework appears applicable for a novel risk analysis of one- and two-step steady-state membrane processing of juices.

In the next chapter a preliminary one-step, dead-end membrane model is synthesized and tested with independent data for clarification of orange juice. A comparison is made between SVA and *Fr 13* solutions. The important effect of random fluctuations of transmembrane pressure, filtration time and volumetric flow rate on fouling (failure) is quantitatively highlighted.

CHAPTER 3

A PRELIMINARY ONE-STEP *FR 13* MEMBRANE MODEL FOR STEADY-STATE DEAD-END FILTRATION OF ORANGE JUICE

Parts of this chapter have been published as:

Zou, W., Davey, K.R., 2014. A novel Friday 13th stochastic assessment of failure of membrane filtration in juice clarification. In Proc. 44th Australasian Chemical Engineering Conference (Processing Excellence, Powering our Future)-CHEMECA 2014. Sept. 27 – Oct. 1, Perth, Australia, paper No. 1259. ISBN/ISSN: 1922107387

3.1 Introduction

The literature reviewed in Chapter 2 disclosed that *Fr 13* has been successfully applied in a number of batch-continuous, single-step unit-operations. In this chapter, *Fr 13* is applied for the first time to a steady-state, single-step, dead-end membrane model. The model is illustrated with independent experimental data for orange juice.

The aim was to gain insight and new knowledge about the impact of random fluctuation that could lead to surprise failures as unexpected fouling of steady-state dead-end filtration.

An unambiguous definition of membrane fouling failure is developed based on the introduction of a risk factor (p) such that for all $p > 0$ filtration failed because of lower operational permeate flux than the design criterion.

3.2 Dead-end membrane model with independent data for orange juice

In the following synthesis, all symbols used for parameters are carefully defined in the relevant Nomenclature at the end of this thesis.

3.2.1 Synthesis of a unit-operations model

An underlying unit-operations model for steady-state, dead-end filtration necessitates integration and synthesis of mathematical equations for transmembrane pressure (ΔP), filtration time (t), membrane surface area (A), kinetic constant for fouling mode (K_n) and an adjustment parameter (n) for cake layer formation.

The fundamental equation for permeate flux (J') of steady-state dead-end filtration (Field et al., 1995) is given as:

$$-\frac{dJ'}{dt} = K_n \cdot A^{2-n} \cdot J'^{\,3-n} \tag{3.1}$$

In membrane processing of juices, cake layer formation with $n = 0$ has been indicated as the best controlling mode of fouling for a number of different fruit types e.g. apple, pineapple, orange, blood orange, passion fruit and pomegranate.

Based on extensive experimental data, Field and Wu (2011) modified Eq. (3.1) to give:

$$J' = J_0 \cdot \left[1 + K_c \cdot (2 - n)\,(A \cdot J_0)^{(2-n)} \cdot t\right]^{1/(n-2)} \tag{3.2}$$

where K_c = kinetic constant for cake layer formation, and J_0 = permeate flux of deionized water, an important parameter to measure the membrane permeability carefully defined as (Schafer et al., 2005; Boerlage et al., 2002; Echavarria et al., 2011)[8]:

$$J_0 = \frac{\mu_T}{\mu_{T,20^\circ C}} \cdot \frac{Q}{A \cdot \Delta P} \tag{3.3}$$

where Q = volumetric feed flow rate at the auto-set temperature, and μ_T and $\mu_{T,\,20^{o}C}$ are, respectively, viscosity of clean water at operational and reference temperature of 20 ^{O}C (Roorda and Graaf, 2001).

Substitution for J_0 from Eq. (3.3) and $n = 0$ into Eq. (3.2) and simplifying gives:

$$J' = \frac{\mu_T}{\mu_{T,20^\circ C}} \cdot \frac{Q}{A \cdot \Delta P} \cdot \left[1 + 2K_c \cdot \left(\frac{\mu_T}{\mu_{T,20^\circ C}} \cdot \frac{Q}{\Delta P}\right)^2 \cdot t\right]^{-0.5} \tag{3.4}$$

Eq. (3.1) through Eq. (3.4) composes the mathematical equations for dead-end membrane filtration for all types of fruit juice.

[8] This equation was later revealed as widely incorrectly reported in the literature. This is being addressed *see* Davey and Zou (2015) and *also* Appendix C. Here the affect is to overestimate *Fr 13* vulnerability. Importantly, this form is corrected in Chapter 5 for the integrated two-step UF-OD synthesis and testing.

3.2.2 Required (design) operational flux for orange juice

In steady-state dead-end filtration, there exists a required (design), operational flux below which reversible fouling (failure) occurs. For successful operation, actual operational flux (J') needs to be equal to or greater than required operational flux ($J_{required}$), otherwise the membrane will become fouled.

Experimental data for dead-end filtration of enzyme-treated centrifuged (ETCJ) orange juice has been independently reported by Nandi et al. (2012). Ceramic membranes with an average pore diameter of 52.55 mm and A = 0.00166 m^2, ΔP = 344.74 kPa and 28.2 x 10^{-6} m^3 m^{-2} s^{-1} < J < 102.5 x 10^{-6} m^3 m^{-2} s^{-1} were used. These data are conveniently re-plotted in Fig. 3-1.

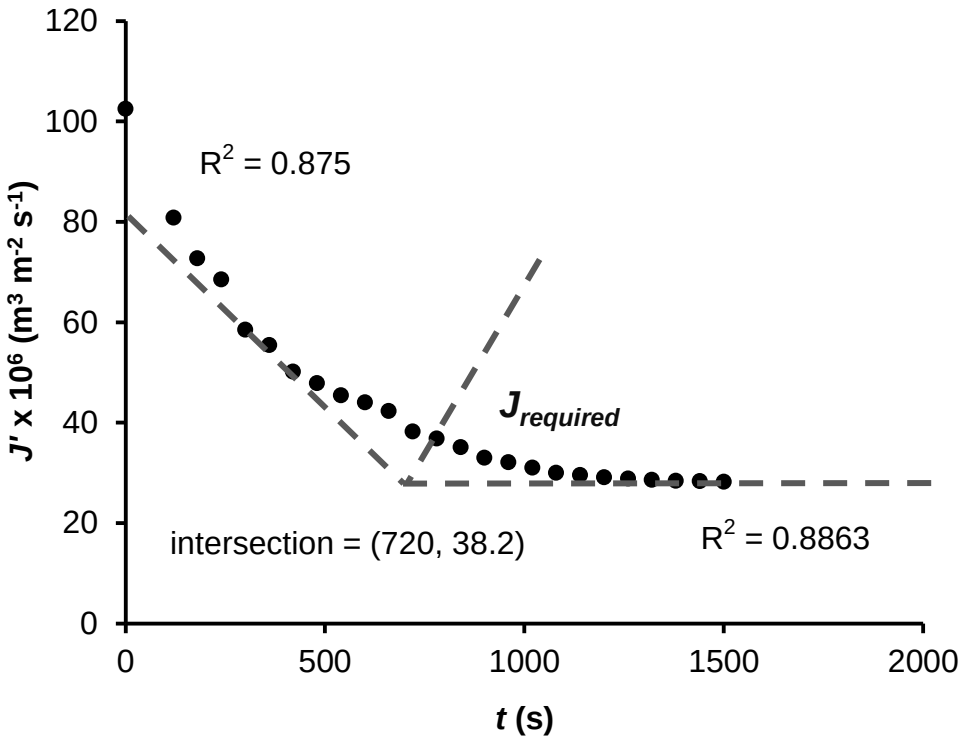

Fig. 3-1: Experimental data for permeate flux (n = 25) in steady-state dead-end filtration of orange juice at ΔP = 344.74 kPa and T = 25 ^oC (adapted from Nandi et al., 2012) showing determination of $J_{required}$ = 38.2 x 10^{-6} m^3 m^{-2} s^{-1}

From the figure, the *required flux*, $J_{required}$ = 38.2 x 10^{-6} m^3 m^{-2} s^{-1} was determined (in Microsoft Excel) by intersection of trend lines 0-720, s (n = 1-13), with R^2 = 0.875 (Snedecor and Cochran, 1989) and 720-1500, s (n = 14-25), with R^2 = 0.8863, parts of the curve, as highlighted on the figure. $J_{required}$ for steady-state dead-end filtration of orange juice is determined at t = 720 s (Fig. 3-1). All $J' < J_{required}$ indicates membrane fouling (failure) where cleaning or replacement of membranes is needed.

The unit-operations model for dead-end filtration of orange juice is defined by Eq. (3.1) through (3.4), together with the value of required (design), operational flux, $J_{required}$.

3.3 Traditional single value assessment (SVA)

The traditional, deterministic solution is the point or single value assessment (SVA) which can be undertaken with or without sensitivity analyses (Sinnott, 2005)

For the steady-state dead-end model of orange juice, auto-set process conditions include T = 25 ^oC, ΔP = 344.74 kPa, A = 0.00166 m^2, Q = 2 .95 x 10^{-5} m^3 s^{-1}, t = 720 s and K_c = 4 x 10^7 s m^{-2} (Nandi et al., 2012). Substitution of these values into Eq. (3.4), gives the permeate flux, J' = 41.8 x 10^{-6} m^3 m^{-2} s^{-1}.

3.4 *Fr 13* risk assessment

In *Fr 13* risk assessment, the single values of input parameters are replaced by a probability distribution of values, the mean of which generally agrees with SVA. A r-MC with Latin Hypercube sampling of distributions is used because pure MC can over–and under- sample from the distribution. This refinement ensures samples cover the entire distribution (Vose, 2008). The method uses a random number generator.

3.4.1 Defining dead-end membrane failure (risk factor)

A fundamental step in *Fr 13* framework is to derive a practical and unambiguous definition of failure.

For the steady-state one-step dead-end filtration, a risk factor (p) for vulnerability to failure can be conveniently defined in terms of J' and $J_{required}$, together with an assumed process tolerance (Zou and Davey, 2015; Davey et al., 2016) such that:

$$p = \%tolerance + 100 \cdot (1 - \frac{J'}{J_{required}}) \quad (3.5)$$

where J' = instantaneous value of permeate flux (or more strictly one membrane operation scenario). In the absence of hard (unconditional) data it is assumed that a practical mid-range tolerance = 2 %, so that Eq. (3.5) gives:

$$p = 2 + 100 \cdot (1 - \frac{J'}{J_{required}}) \quad (3.6)$$

The practical result is that if the value of permeate flux is less than 1.02 times the critical flux ($J' < 1.02 \times J_{required}$), the dead-end membrane has fouled (failed).

This risk equation is computationally convenient because all $p > 0$ ($J' < 1.02 \times J_{required}$) are recognized as membrane fouling failure. Additionally, these can be readily identified in standard spread sheeting tools (Davey, 2015 a; Davey et al., 2015).

The one-step *Fr 13* membrane model for the steady-state, dead-end filtration of orange juice is defined by Eq. (3.1) through (3.6) together with the independent value of $J_{required}$.

3.4.2 *Fr 13* simulation

The *Fr 13 simulation* is used to identify each practical scenario that may produce a process failure. To guarantee the output mean is normally distributed, a sufficiently large number of r-MC samples, of 10,000 to 100,000 is needed. It is a simple matter to check output distribution is normal in commercial software.

Simulations here were carried out in Microsoft Excel with a commercial add-on *@Risk* version 5.5. As spread-sheet tools are widely used, results can be communicated streamlined to a range of users of varying sophistication.

3.5 Results

For the steady-state dead-end membrane model, a comparative summary of results from both the SVA and *Fr 13* simulation are presented in Table 3-1. 100,000 r-MC samples of distributions were used. Each simulation can be properly considered as a (daily) dead-end filtration. Key parameters are given in column 1 of Table 3-1. Column 2 gives the traditional SVA where permeate flux $J' = 41.8 \times 10^{-6}$ m^3 m^{-2} s^{-1} is shown. The *Fr 13* simulation is summarized in columns 3 and 4. The values given in column 3 are for one only of 100,000 scenarios. Column 4 sets out distributions used for key parameters ΔP, t and Q, defined as: **RiskNormal** (mean, stdev, **RiskTruncate** (minimum, maximum)). Column 3 shows that at ΔP = 376.57 kPa, t = 703.59 s and $Q = 2.97 \times 10^{-5}$ m^3 s^{-1}, the permeate flux $J' = 38.5 \times 10^{-6}$ m^3 m^{-2} s^{-1}; the value of risk factor, p = 1.104 (> 0), emphasizing a membrane fouling failure, plus a practical tolerance = 2 %.

Table 3-1: Summary comparison of deterministic SVA with probabilistic *Fr 13* simulation of steady-state dead-end filtration of orange juice with a 2 % tolerance. Failure is defined for all $p > 0$

Parameter	**SVA**[1]		***Fr 13* simulation**[2]
ΔP (kPa)	**344.74**	**376.57**	**RiskNormal**(344.74,17.237,**RiskTruncate**(310.266,379.214))
t (s)	**720**	**703.59**	**RiskNormal**(720,36,**RiskTruncate**(648,792))
Q (m^3 s^{-1})	**0.0000295**	**0.0000297**	**RiskNormal**(0.0000295,0.0000018,**RiskTruncate**(0.0000259,0.0000331))
T (^{o}C)	25	25	constant
$\mu_{T,\,20\,^oC}$ (pa s)	0.00102	0.00102	constant
μ_T (pa s)	0.00089	0.00089	constant
A (m^2)	0.00166	0.00166	constant
K_c (s m^{-2})	40000000	40000000	constant
$J_{required}$ (m^3 m^{-2} s^{-1})	0.0000382	0.0000382	constant
J' (m^3 m^{-2} s^{-1})	0.0000418	0.0000385	Eq. (3.4)
p (risk factor)	-	**1.104**	Eq. (3.6)

[1] Traditional, deterministic Single Value Assessment
[2] *Fr 13* simulation with Latin Hypercube sampling

Importantly however, the values in column 3 of Table 3-1 are only one of the 100,000 scenarios. A graphical summary of all 100,000 iterations are presented in Fig. 3-2.

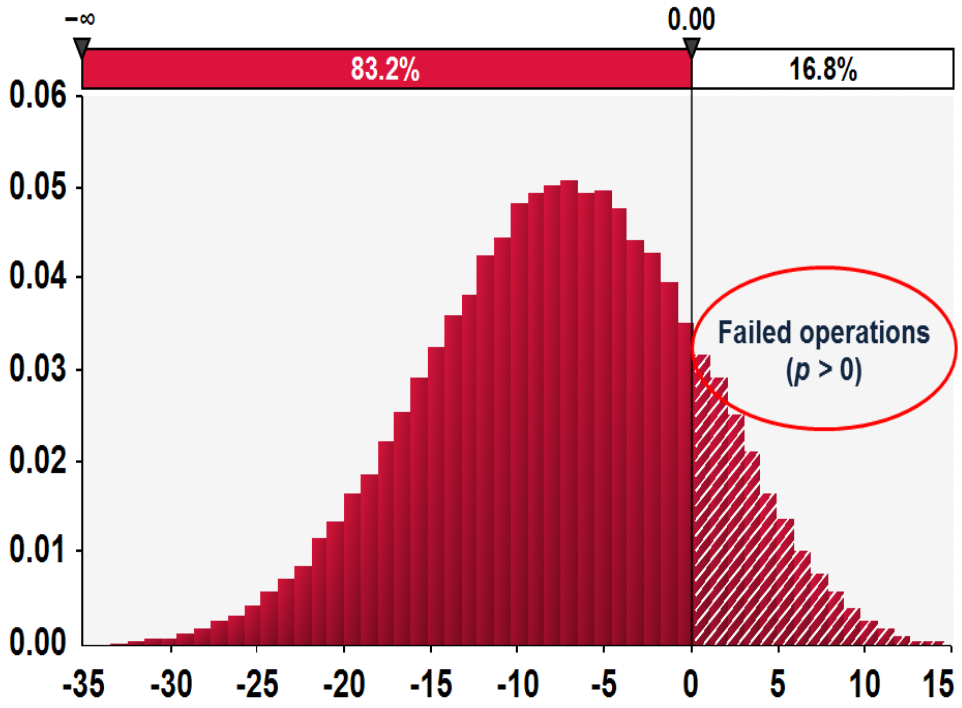

Fig. 3-2: Summary of *Fr 13* simulation of 100,000 scenarios of risk factor (p) for steady-state dead-end filtration of orange juice with a tolerance = 2 %. The 16,843 failed scenarios are seen on the right side of the figure where $p > 0$

It can be seen from the figure that a total of 16,843 (16.8 %) of all dead-end filtrations resulted in $p > 0$ i.e. $J' < J_{required}$ (with a tolerance = 2 %), a membrane fouling failure, over a prolonged period of time.

3.6 Discussion

3.6.1 Dead-end membrane failures

If each scenario is thought as a batch-continuous processing day there would be (16,843 / (100,000 days) x 365.25 days / year =) 62 surprise failures per year plus a tolerance = 2 %,

over an extended time i.e. approximately five (5) failure per month despite good operations and maintenance. These failures would not be expected to be equally spaced in time.

Ten (10) of the 16,483 failures (as failed dead-end filtration) are presented in Table 3-2. An advantage of the table is that the instantaneous value of key parameters that combined to produce a failure can be clearly identified. For example, row 10 of Table 3-2, scenario 8, shows that with ΔP = 376.57 kPa, t = 703.59 s and Q = 2.97 x 10^{-5} m^3 s^{-1} gave rise to a permeate flux of J' = 38.5 x 10^{-6} m^3 m^{-2} s^{-1} with p = 1.104, indicating membrane fouling (failure). This is the practical scenario presented in Table 3-1.

Table 3-2: Ten (10) selected *Fr 13* failures of the 16,483 in 100,000 scenarios of steady-state dead-end filtration of orange juice with a practical tolerance = 2 %

Scenario	**ΔP (kPa)**	***t* (s)**	**Q x 10^5 (m^3 s^{-1})**	***p***
1	361.86	685.33	2.60	10.128
2	367.71	652.09	2.78	5.402
3	349.86	702.83	2.79	0.066
4	344.89	757.38	2.75	0.195
5	353.81	733.80	2.71	4.039
6	370.49	694.86	2.96	0.022
7	360.81	715.56	2.76	4.221
8	**376.57**	**703.59**	**2.97**	**1.104**
9	362.61	726.00	2.83	2.294
10	350.02	715.17	2.63	5.957

In all cases shown in Table 3-2 permeate flux (J') is found to be less than the $J_{required}$ plus a 2 % tolerance, i.e. evidenced by $p > 0$.

From Table 3-1, 3-2 and Fig. 3-2, it can be concluded that the batch-continuous steady-state, dead-end filtration of orange juice should be more correctly considered as a combination of successful and failed operations. These failed operations cannot be attributed to ‘faulty fittings’ or ‘human error’, but are due to naturally occurring random fluctuations within the membrane plant itself (Zou and Davey, 2014 a, b).

Significantly, these findings are not available from traditional risk (SVA) and hazard analyses; this is because the random element is not explicit in these risk and hazard methods.

3.6.2 Visualizing *Fr 13* risk failures

The adequate presentation and depiction of risk data is an acknowledged challenge (Anon., 2012; Abdul-Halim and Davey, 2015 a; Davey, 2015 a). Although the tabulated presentation (Table 3-1, Table 3-2 and Fig. 3-2) provided a good summary of *Fr 13* simulation of dead-end filtration, a difficulty however is to visually depict the plant outcome behaviour.

Abdul-Halim and Davey (2015 a) introduced a three-dimensional (3D) graphical treatment in an attempt to present *Fr 13* failures in UV irradiation for potable water. They acknowledged this was practically limited to a three-parameter model, but did demonstrate a useful visualization of the *Fr 13* risk and random nature with time in continuous steady-state unit-operations.

In an attempt to investigate this, here a 3D plot of 40 selected failures ($p > 0$) from 100,000 scenarios is presented as Fig. 3-3. The figure was produced using Statistica™ (version 10) software.

Part (a) of Fig. 3-3 presents a scatter plot for three key membrane parameters, ΔP, t and Q, respectively. Part (b) shows the surface plot for 40 values with $p > 0$. The purpose is to visually illustrate the random nature of p values for steady-state dead-end filtration and show the plot cannot be extrapolated in any reliable way.

Nonetheless, Fig. 3-3 does serve to show that p values increase with longer filtration time and greater volumetric feed flow rate, i.e. with increasing t, filtration is more likely to fail due to reduced permeate flux. This underscores decreased vulnerability to unexpected failures in steady-state, dead-end filtration with less processing time (t).

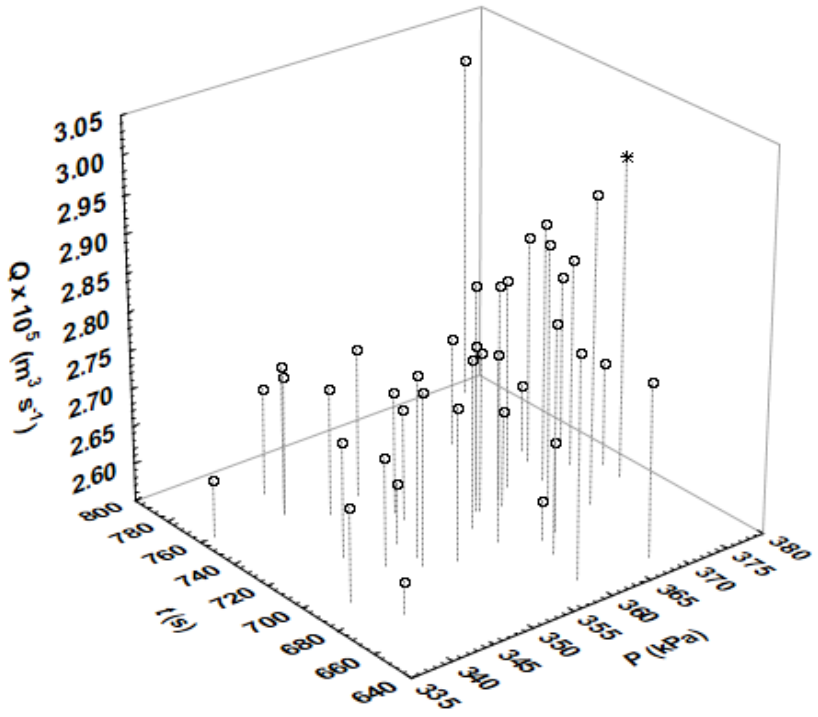

(a)

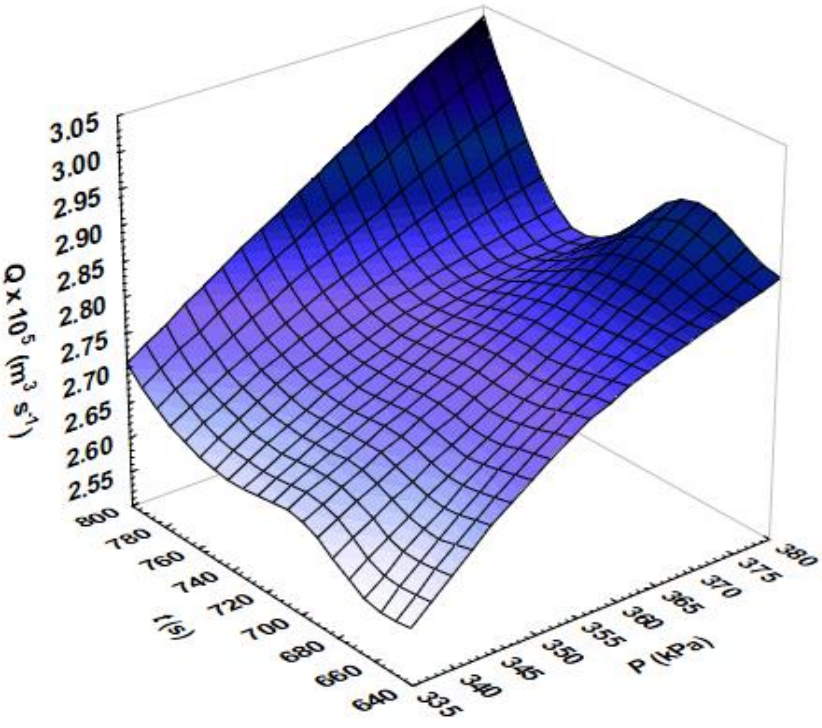

(b)

Fig. 3-3: 3D plot of 40 selected *Fr 13* failures ($p > 0$) in steady-state, dead-end filtration of orange juice with tolerance = 2 %: 3D scatter plot (a) and 3D surface plot (b). The highlighted failure of Table 3-1 is indicated by the data marker **x**

However, with an increased number of input parameters to describe more complex global model e.g. there are 20 input parameters defined by distributions in the study of Davey (2015 a) and six in the study of Chandrakash et al. (2015). A radar-type plot as an alternative to aid visualization of *Fr 13* failures was recommended by Abdul-Halim and Davey (2015 a). This is carried out theoretically in Chapter 5.

3.7 Chapter summary and conclusions

1. A preliminary one-step *Fr 13* membrane model for steady-state, dead-end membrane filtration was synthesized and developed based on the model of Field and Wu (2011), together with independent experimental data for orange juice from Nandi et al. (2012). A drawback with this dead-end membrane model is that it is mathematically simple and rarely applied on an industrial scale.

2. Results show that with processing temperature of 25 ^{O}C and a practical tolerance of 2 % as a design margin of safety membrane fouling failure can occur in 16.8 % of all batch-continuous operations in otherwise well-operated membrane plant. This translates to vulnerability to 62 surprise failures each year averaged over the long term.

3. Steady-state, dead-end filtration of orange juice can be considered a mix of successful and failed operations. All possible elements that combined to result in a failure can be identified by the *Fr 13* framework. This is not available from traditional risk and hazard analyses, with or without sensitivity analysis.

4. The random nature of *Fr 13* failures of steady-state, dead-end filtration can be visualized using 3D graphical methods. However, the significant limitation of the 3D plot is the restricted number of input parameters.

Compared to the dead-end filtration, the alternated cross-flow filtration is reported to be more extensively used in juice clarification, due to improved process efficiency and reduced energy cost (Echavarria et al., 2011).

In the following chapter, a preliminary one-step *Fr 13* membrane model is synthesized for a batch-continuous steady-state, cross-flow filtration and is tested with independent data for blood orange juice.

CHAPTER 4

A PRELIMINARY ONE-STEP *FR 13* MEMBRANE MODEL FOR STEADY-STATE CROSS-FLOW FILTRATION OF BLOOD ORANGE JUICE

Parts of this chapter have been published as:

Zou, W., Davey, K.R., 2014. A Friday 13th risk model for failure in cross-flow membrane filtration of passion fruit juice. In: Proc. 26th European Modelling and Simulation Symposium-EMSS 2014. Sept. 10-12, Bordeaux, France, paper 106.
ISBN: 9788897999447

4.1 Introduction

Findings from Chapter 3 highlighted that the dead-end membrane model of Field and Wu (2011), together with independent data for orange juice of Nandi et al. (2012), could be synthesized and generalized as a one-step *Fr 13* membrane model steady-state filtration. A significant drawback of the model was that it is mathematically simple and dead-end filtration is now rarely used in juice processing because of low process efficiency and high operational cost. A familiarization with techniques and methods was gained however.

In this chapter, a one-step *Fr 13* analysis is applied for the first time to a more widely applied steady-state, cross-flow membrane model, and tested with independent experimental data for blood orange juice. The aim was to gain new insight(s) into unexpected fouling failure of batch-continuous, cross-flow filtration and to explore intervention strategies to improve process efficiency and possible plant safety.

A risk factor (p) is defined as an operational flux less than the design value.

4.2 Cross-flow membrane model with independent data of blood orange juice

Symbols used in the following for parameters are defined in the relevant Nomenclature at the end of this thesis.

4.2.1 Synthesis of a unit-operations model

Based on studies of critical flux and fouling mechanism of cross-flow membranes (Field et al., 1995; Field and Wu, 2011), the original mathematical expression for permeate flux (J') in cross-flow filtration can be expressed as:

$$-\frac{dJ'}{dt} = k_n \cdot (J' - J^*) \cdot J^{2-n} \tag{4.1}$$

where J^* = steady-state flux at completion of filtration, t = filtration time, k_n = kinetic constant for fouling mode in cross-flow membranes, and an adjustment parameter (n) for different fouling modes.

In cross-flow membranes for juice processing, $n = 0$ (cake layer formation) has been shown to be the 'best' controlling mode of fouling. Based on the extensive experimental data, Field and Wu (2011) modified Eq. (4.1) to give:

$$k_0 \cdot t = \frac{1}{J^{*2}} \cdot \left[\ln\left(\frac{J'}{J_O} \cdot \frac{(J_0 - J^*)}{(J' - J^*)}\right) - J^* \cdot \left(\frac{1}{J'} - \frac{1}{J_0}\right)\right] \tag{4.2}$$

where k_0 = kinetic constant for cake layer formation and, J_0 = initial permeate flux of deionized water, a significant parameter for original permeability of new membranes. J_0 is defined as (Schafer et al., 2005; Boerlage et al., 2002; Echavarria et al., 2011)[9]:

$$J_0 = \frac{\mu_T}{\mu_{T,20^\circ C}} \cdot \frac{Q}{A \cdot \Delta P} \tag{4.3}$$

where Q = volumetric flow rate of feed stream (juices), at the operational temperature, and μ_T and $\mu_{T,\,20^oC}$ are, respectively, the viscosity of clean water at operation, and a reference temperature of 20 ^oC (Roorda and Graaf, 2001).

Substitution for J_0 from Eq. (4.3) into Eq. (4.2) and simplifying gives:

$$k_0 \cdot t = \frac{1}{J^{*2}} \cdot \left[\ln\left(\frac{J' \cdot \mu_{T,20^\circ C} \cdot A \cdot \Delta P}{\mu_T \cdot Q} \cdot \frac{\left(\left(\frac{\mu_T}{\mu_{T,20^\circ C}} \cdot \frac{Q}{A \cdot \Delta P}\right) - J^*\right)}{(J' - J^*)}\right) - J^* \cdot \left(\frac{1}{J'} - \frac{\mu_{T,20^\circ C} \cdot A \cdot \Delta P}{\mu_T \cdot Q}\right)\right] \tag{4.4}$$

Eq. (4.1) through (4.4) is therefore synthesized as the physical flux equations for a steady-state batch-continuous cross-flow filtration of juices.

[9] ibid N. 7 p. 37.

4.2.2 Required (design) operational flux for blood orange juice

In steady-state cross-flow filtration, actual operational flux, J' must meet the required operational flux, $J_{required}$, for successful processing without reversible fouling. This value can be determined from practical experimental data only, for a specific juice and membranes.

Experimental data for cross-flow UF of blood orange juice had been independently reported at 25 ^{o}C (Cassano et al., 2007). PVDF membranes with A = 0.23 m^2, ΔP = 85 kPa, μ_T = 0.89 x 10^{-3} pa s, $\mu_{T,\,20^{o}C}$ = 1.02 x 10^{-3} pa s, Q = 2.2 x 10^{-4} m^3 s^{-1}, k_0 = 2.4 x 10^6 s m^{-2} and 3.05 x 10^{-6} m^3 m^{-2} s^{-1} < J < 5.28 x 10^{-6} m^3 m^{-2} s^{-1} were used. These data are conveniently re-plotted as Fig. 4-1.

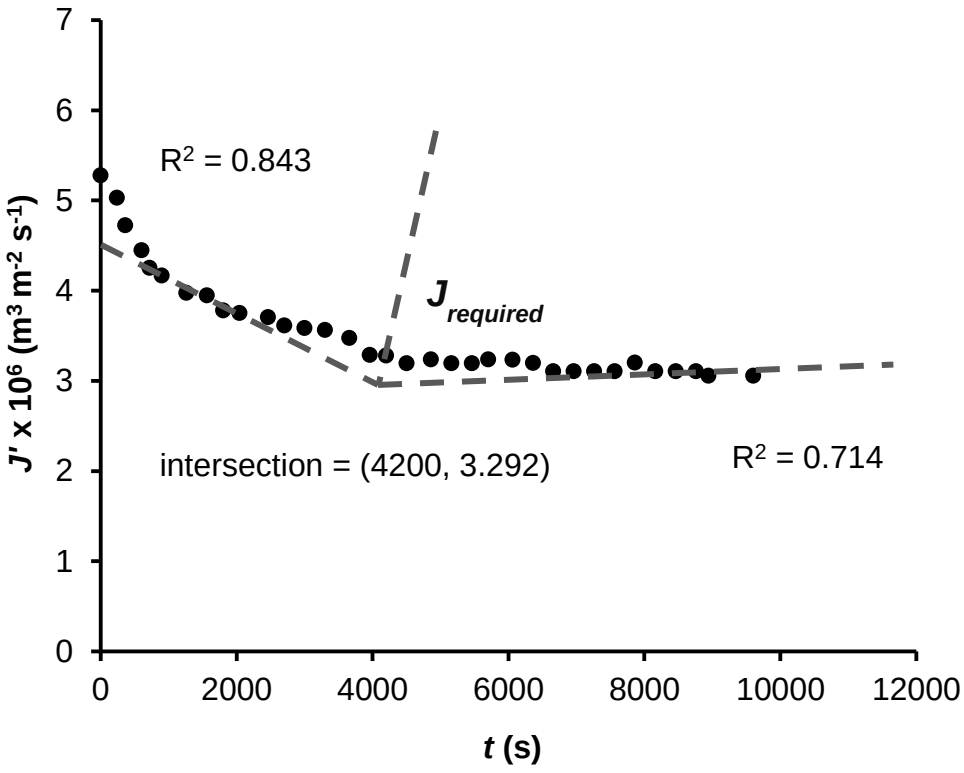

Fig. 4-1: Independent experimental data (n = 34) for permeate flux in steady-state cross-flow filtration of blood orange juice at ΔP = 85 kPa (Cassano et al., 2007) showing determination of $J_{required}$ = 3.292 x 10^{-6} m^3 m^{-2} s^{-1}

Required flux, $J_{required}$ = 3.278 x 10^{-6} m^3 m^{-2} s^{-1}, is determined by intersection of trend lines to the initial 0-4,200, s (n = 1-17), with R^2 = 0.843 and 6,360-9,600 s (n = 18-34), with R^2 = 0.714 (Snedecor and Cochran, 1989), parts of the curve, as highlighted in Fig. 4-1. It is seen that $J_{required}$ for steady-state, cross-flow filtration of blood orange juice is determined at t = 4,200 s.

Eq. (4.1) through (4.4) plus the determined required flux, $J_{required}$ defines the steady-state cross-flow filtration model of blood orange juice.

4.3 Traditional single value assessment (SVA)

For the cross-flow filtration of blood orange juice, the SVA is computed as follows: with T = 25 ^{O}C, ΔP = 85kPa, A = 0.23m^2, Q = 2.2 x 10^{-4} m^3 s^{-1}, J^* = 3.06 x 10^{-6} m^3 m^{-2} s^{-1}, k_0 = 2.4 x 10^6 s m^{-2} and t = 4,200 s substituted into Eq. (4.4) to give the permeate flux, J' = 3.37 x 10^{-6} m^3 m^{-2} s^{-1}. All $J' < J_{required}$ indicate fouling (failure) occurs.

Here permeate flux is computationally greater than the required, operational flux ($J' > J_{required}$), the process is therefore assessed as successful without the reversible fouling.

4.4 *Fr 13* risk assessment

Fr 13 risk assessment for the cross-flow membrane model is conducted in a similar way as for the dead-end membrane model discussed in Chapter 3.

For steady-state, cross-flow filtration, a risk factor is defined in terms of J' and $J_{required}$ (Zou and Davey, 2015), such that $P_1 = J_{required} - J'$. This can be rearranged as a more convenient, dimensionless fouling risk factor (Davey et al., 2015; Davey, 2015 a) as:

$$p = \left(1 - \frac{J'}{J_{required}}\right) \cdot 100\ \% \qquad (4.5)$$

In general, membrane processing would include a practical tolerance such that J' needs to be equal to the minimum design value, plus an additional tolerant flux such that:

$$p = \%\ tolerance + \left(1 - \frac{J'}{J_{required}}\right) \cdot 100\ \% \tag{4.6}$$

In the absence of hard (unconditional) data practical mid-range tolerance = 2 % is assumed, so that:

$$p = 2 + 100 \cdot \left(1 - \frac{J'}{J_{required}}\right) \tag{4.7}$$

Practically, if actual operational (permeate) flux is less than 1.02 times the required flux i.e. $J' < 1.02 \times J_{required}$, the cross-flow membrane will fouled.

Thus, Eq. (4.7) is convenient because it is dimensionless, but importantly, all $p > 0$ are intuitively recognized as fouling failures, and can be easily shown in spread-sheet tools.

Eq. (4.1) through (4.7), together with the independent $J_{required}$, constitutes the one-step *Fr 13* membrane model for steady-state, cross-flow filtration of blood orange juice.

Simulations were conducted in Microsoft Excel with the add-on *@Risk* version 5.5. 100,000 r-MC samples of key input parameters ΔP and t were simulated to provide sufficiently number of normal output distributions.

4.5 Results

A summary comparison of results from SVA and *Fr 13* is presented in Table 4-1where all calculations can be logically read down the columns. Process parameters are given in column 1 and traditional SVA is presented in column 2. Computations can be readily read down column 2 where a permeate flux $J' = 3.370 \times 10^{-6}$ m^3 m^{-2} s^{-1} is shown. Defined distributions used for ΔP and t are set out in column 4. Column 3 presents only one of 100,000 scenarios. It can be seen that at a randomly sampled process condition of ΔP = 92.54 kPa and t = 4,535.7 s, the value of risk factor, p = 0.12 (> 0), highlighting a fouling failure with a practical tolerance = 2 %.

Table 4-1: A summary comparison of SVA and *Fr 13* simulation of steady-state, cross-flow filtration of blood orange juice at 25 ^{O}C with a process tolerance = 2 %

Parameter	**SVA**		***Fr 13* simulation**
ΔP (kPa)	**85**	**92.54**	**RiskNormal**(85,4.25,**RiskTruncate**(76.5,93.5))
t (s)	**4200**	**4535.71**	**RiskNormal**(4200,210,**RiskTruncate**(3780,4620))
T (^{o}C)	25	25	constant
$\mu_{T,\ 20\ ^{o}C}$ (pa s)	0.00102	0.00102	constant
μ_T (pa s)	0.00089	0.00089	constant
Q (m^3 s^{-1})	0.00022	0.00022	constant
A (m^2)	0.23	0.23	constant
k_0 (s m^{-2})	2400000	2400000	constant
J^* (m^3 m^{-2} s^{-1})	0.00000306	0.00000306	constant
$J_{required}$ (m^3 m^{-2} s^{-1})	0.000003292	0.000003292	constant
J' (m^3 m^{-2} s^{-1})	0.000003370	0.000003354	Eq. (4.4)
p (risk factor)	-	**0.120**	Eq. (4.7)

Furthermore, the overall simulation result of 100,000 scenarios can be conveniently summarized as Fig. 4-2. The y-axis is the probability of p actually taking place in the simulation and the x-axis is calculated value of p from Eq. (4.7) (Vose, 2008). The right side of Fig.4.2 shows that a total of 4.0 % (4,000) of all scenarios over a prolonged period would have $p > 0$, i.e. $J' < J_{required}$ (with a practical tolerance = 2 %).

Ten (10) of the failed scenarios were selected for further analysis as presented in Table 4-2. Row 11 of Table 4-2 (**bold-text**) is the particular scenario given in column 3 of Table 4-1. In this scenario, at ΔP = 92.54 kPa together with t = 4,531.71 s, would result in a permeate flux J' = 3.354 x 10^{-6} m^3 m^{-2} s^{-1} with p = 0.120, highlighting a membrane fouling failure. Other process combinations that lead to surprise membrane failures include Row 5 of the table where ΔP = 92.85 kPa and t = 4,494.87 s.

In all the cases of Table 4-2, permeate flux is less than required flux plus a 2 % tolerance ($J' < 1.02 \times J_{required}$), as evidenced by $p > 0$. The advantage of Table 4-2 is that the individual combination of key parameters that can give rise to process failure can be easily identified (Abdul-Halim and Davey, 2015 a, b; Zou and Davey, 2015).

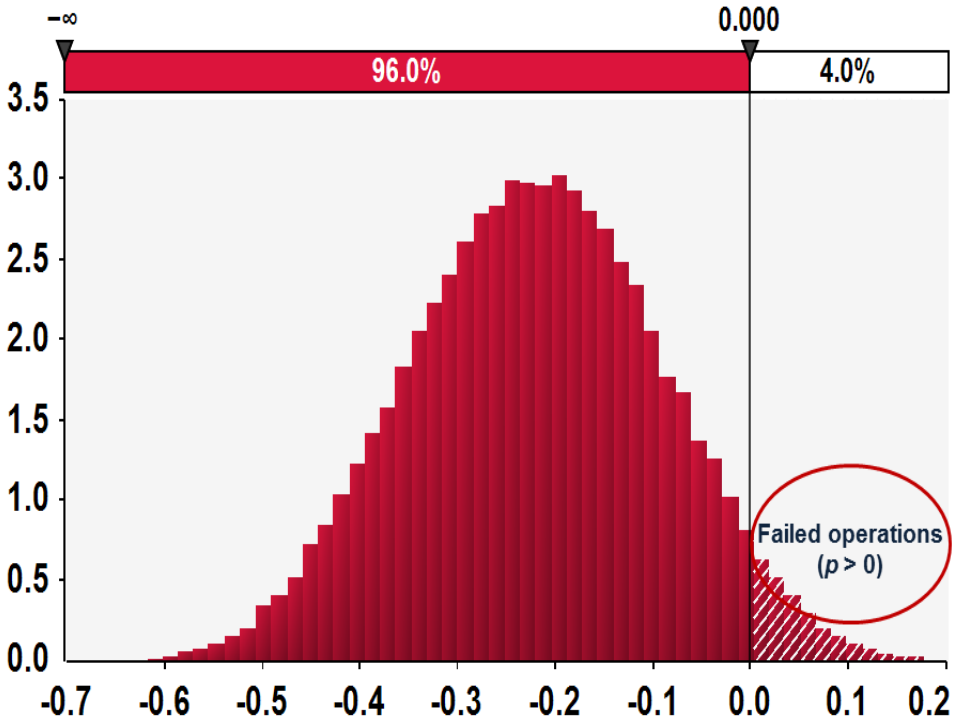

Fig. 4-2: An overall summary of *Fr 13* simulation of 100,000 scenarios of risk *p* for the steady-state cross-flow filtration of blood orange juice with a tolerance = 2 %. The 4,000 failures are seen in the right side of the figure, evidenced by $p > 0$

Table 4-2: Ten (10) selected *Fr 13* failures from 4,000 in 100,000 scenarios of steady-state cross-flow filtration of blood orange juice with a practical tolerance = 2 %

Scenario	**ΔP (kPa)**	***t*** **(s)**	***J'*** **x 10^6 (m^3 m^{-2} s^{-1})**	***p***
1	90.95	4450.57	3.357	0.040
2	92.18	4518.93	3.354	0.103
3	90.93	4565.61	3.355	0.010
4	89.37	4456.04	3.358	0.008
5	92.85	4494.87	3.354	0.105
6	86.95	4549.61	3.358	0.006
7	89.11	4457.77	3.358	0.003
8	87.96	4555.33	3.357	0.030
9	89.76	4440.86	3.358	0.008
10	**92.54**	**4535.71**	**3.354**	**0.120**

Parameter values reported in Table 4-2 are computed from r-MC sampling. Therefore, it is not implied they need to be measured to this order.

As a result, the overall failure rate of the steady-state, cross-flow filtration of blood orange juice is 4.0 % (= 4,000 / 100,000) of daily operations, plus a 2 % tolerance.

4.6 Discussion

4.6.1 Cross-flow membrane failures

It is evident that batch-continuous, steady-state, cross-flow filtration has a within system unexpected tendency to fail. If each scenario is considered a processing day, then an occurrence of surprise membrane fouling failure would result every (100,000 / 365.25 / 4,000 =) 0.07 years (25 days) on average with a 2 % tolerance. Alternatively, this can be translated to (4,000 / (100,000 days) x 365.25 days/year =) 15 failures per year over a prolonged period of operations. However, this result cannot be expected to be equally spaced in time.

Fig. 4-2 together, with ten (10) selected *Fr 13* failures from Table 4-2, underscore that the batch-continuous, steady-state, cross-flow filtration of blood orange juice is more correctly thought of as a combination of successful and failed operations. Surprise failures are almost certainly attributed to naturally occurring random (stochastic) changes within the membrane plant itself (Zou and Davey, 2015).

4.6.2 *Fr 13* second-tier simulation

Because *Fr 13* failures are due solely to random fluctuations within the system, further study or measurement or knowledge of the one-step cross-flow filtration cannot be used to reduce vulnerability to these failures (Davey et al., 2015).

However, a practical advantage of the *Fr 13* framework is that once adequately established, second-tier simulations can be used to test proposed changes to the physical process and their impact on vulnerability to surprise failure (Abdul-Halim and Davey,

2015 a, b; Zou and Davey, 2015). This is because physical changes to the system are mimicked by changes to input distributions describing parameters.

For the steady-state, cross-flow filtration, the impact of naturally occurring fluctuations in key parameters on fouling failure was re-simulated through a change of stdev in distributions for both ΔP and t with the range $2 \leq \text{stdev} \leq 20$, % about the mean. Results are summarized in Fig. 4-3.

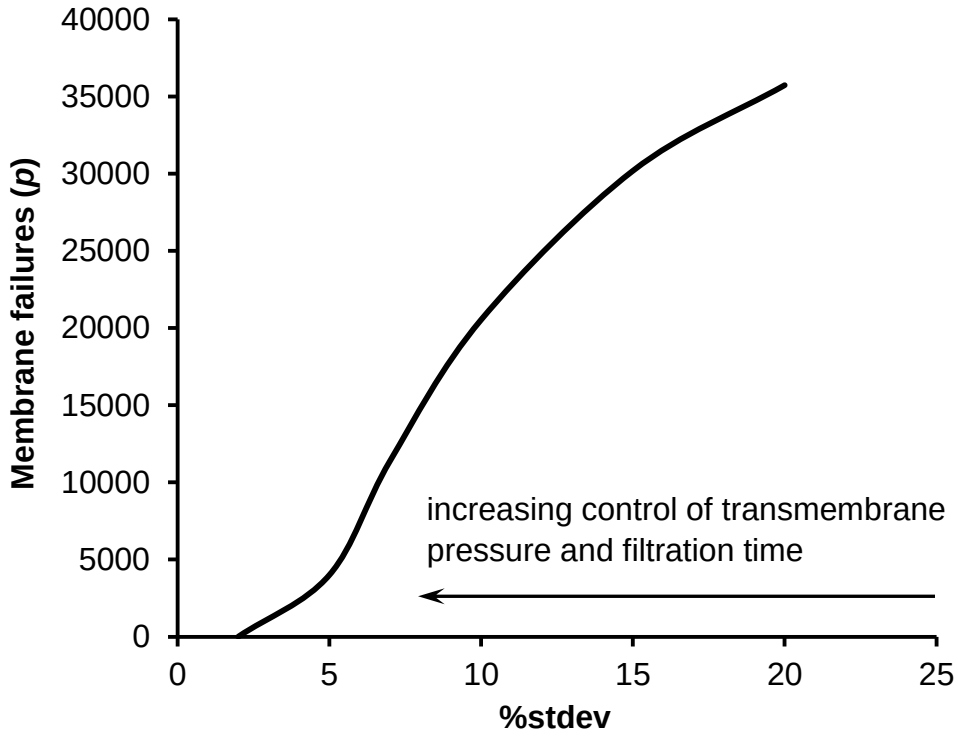

Fig. 4-3: Impact of process control as %stdev in distribution of ΔP and t on failures (p) numbers in steady-state, cross-flow filtration of blood orange juice

Fig. 4-3 shows an apparent exponential rise in the number of membrane failures with increasing %stdev and fall away as %stdev decreases. At a %stdev = 2, the predicted number of *Fr 13* failures is close to zero.

Because the value of %stdev used in probability distribution is practically a quantitative measure of the quality, cost and accuracy of relevant process control, the results from Fig. 4-3 underscore that increasing precision control of membrane physical

system (e.g. ΔP and t) will meaningfully reduce the number of unexpected fouling failures in steady-state, cross-flow filtration, but will probably have disadvantage of energy waste and increased costs.

It is therefore glimpsed that the *Fr 13* could be used in second-tier simulations to investigate the effect of improved control and design decisions to produce a balance of process benefits and increased cost.

4.6.3 Comparison of dead-end and cross-flow membrane models

In Chapters 3 and 4, an underlying, one-step *Fr 13* membrane model was successfully synthesized for steady-state, dead-end and cross-flow filtration (clarification) of orange and blood orange juices. A summary comparison of those two (2) membrane models is presented in Table 4-3.

Table 4-3: A summary comparison of the one-step *Fr 13* membrane models for steady-state dead-end and cross-flow filtration of orange and blood orange juice

Parameter	***Fr 13* membrane model**	
	Dead-end	**Cross-flow**
Input(s)		
Juice type	Orange juice	Blood orange juice
Temperature (T, ^{o}C)	25	25
Transmembrane pressure (ΔP, kPa)	**RiskNormal** (344.74,17.237, **RiskTruncate** (310.266,379.214))	**RiskNormal** (85,4.25, **RiskTruncate** (76.5,93.5))
Filtration time (t, s)	**RiskNormal** (720,36, **RiskTruncate** (648,792))	**RiskNormal** (4200,210, **RiskTruncate** (3780,4620))
Feed flow rate (Q, $m^3\ s^{-1}$)	**RiskNormal** (0.0000295,0.0000018, **RiskTruncate** (0.0000259,0.0000331))	0.00022
Membrane area (A, m^2)	0.00166	0.23
Required flux ($J_{required}$, $m^3\ m^{-2}\ s^{-1}$)	0.0000382	0.000003292
Output(s)		
Permeate flux (J', $m^3\ m^{-2}\ s^{-1}$)	0.0000418	0.00000337
Failures per 100,000 scenarios	16843	4000
Failure rate	16.8 %	4.0 %

Table 4-3 shows that predicted *Fr 13* failure numbers is apparently different with 16,843 for dead-end, and 4,000 for cross-flow filtration model. This outcome cannot result in the assumption that cross-flow is better in any aspect than dead-end, membrane model, because failures are sensitive to the inherent structure of the unit-operations model itself.

It is important to note that, in contrast to the dead-end membrane model, the widely used cross-flow filtration model is considered less vulnerable to surprise fouling failure. This is because in cross-flow filtration, tangential feed flow can help to wash away accumulated substances on the interface of membranes, leading to a slow decay of permeate flux with longer service (filtration) time and reduced risk of fouling.

4.7 Chapter summary and conclusions

1. A preliminary one-step *Fr 13* membrane model of steady-state, cross-flow filtration of blood orange juice revealed that surprise fouling can occur in 4.0 % of all operations with a 2 % tolerance as a margin of safety, in otherwise well-operated and well-maintained plant. This is equal to a vulnerability of some 15 unexpected failures per year on average over an extended time.

2. Steady-state, cross-flow filtration should be more correctly considered a mix of successful and failed operations.

3. *Fr 13* second-tier studies highlighted that reduction in vulnerability to fouling in could be achieved by reducing the (stochastic) fluctuations in transmembrane pressure and filtration time. Practically, this suggests an increase in precision control of the membrane physical system might be warranted.

4. Compared to dead-end, the cross-flow membrane model was less vulnerable to surprise fouling (failure).

Based on findings and experience gained from these preliminary studies, a two-step *Fr 13* membrane global model is synthesized in the following chapter for an integrated UF-OD membrane process. It is the first *Fr 13* analysis of integrated foods processing with two inter-connected unit-operations.

The principle aim is to advance and test the *Fr 13* framework to gain unique insight(s) into how random fluctuations in apparent steady-state plant parameters can be transmitted and impact in progressively integrated complex, global processes.

CHAPTER 5

A NOVEL TWO-STEP *FR 13* MEMBRANE GLOBAL MODEL FOR INTEGRATED ULTRAFILTRATION - OSMOTIC DISTILLATION (UF-OD) OF CONCENTRATED JUICES

Parts of this chapter have been published as:

Davey, K.R., Zou, W., 2015. Fruit juice processing and membrane technology application (*sic*) – A response. Food Eng. Rev. – submitted Oct.

Zou, W., Davey, K.R., 2015. An integrated two-step *Fr 13* synthesis - demonstrated with membrane fouling in combined ultrafiltration-osmotic distillation (UF-OD) for concentrated juice. Chem. Eng. Sci. – submitted Nov.

5.1 Introduction

In Chapters 3 and 4, a preliminary *Fr 13* risk assessment was successfully applied to the single-step, steady-state, dead-end and cross-flow filtration for clarified juices, and; a familiarization with the *Fr 13* framework and methodology was gained.

A current drawback identified in Chapter 2 with overall development of the *Fr 13* framework however is that the work has been largely limited to single, i.e. one-step, unit-operations. It is not known if there is benefit in applying the approach or developing the framework as a useful tool in integrated multi-step foods and chemicals engineering unit-operations.

A research study was undertaken to advance the *Fr 13* framework to gain insight into how the naturally occurring fluctuations in apparent steady-state plant parameters might be transmitted and impact in progressively complex[10] processes.

In this chapter the development and demonstration of a *Fr 13* risk assessment of an integrated two-step, steady-state process is addressed. Two or more integrated unit-operation steps have been defined as a 'global' process by Davey and co-workers (e.g. Chandrakash et al., 2015).

5.1.1 Two-step membrane processing of juices

The processing of concentrated fruit juices is an important integrated two-step process. Pomegranate (*Punica granatum*) juice is particularly valued over other juices as it is thought to reduce blood pressure and promote low density lipoprotein oxidation (Aviram and Dornfeld, 2001). Consequently, production and demand of pomegranate juice has increased in the past five years, and significant independent data are available (Cassano et al., 2011). A typical integrated two-step membranes process for a concentrated juice is shown schematically in Fig. 5-1where two integrated unit-operations, cross-flow ultrafiltration (UF) and osmotic distillation (OD), are used.

[10] In the context of 'integrated' not 'complicated'.

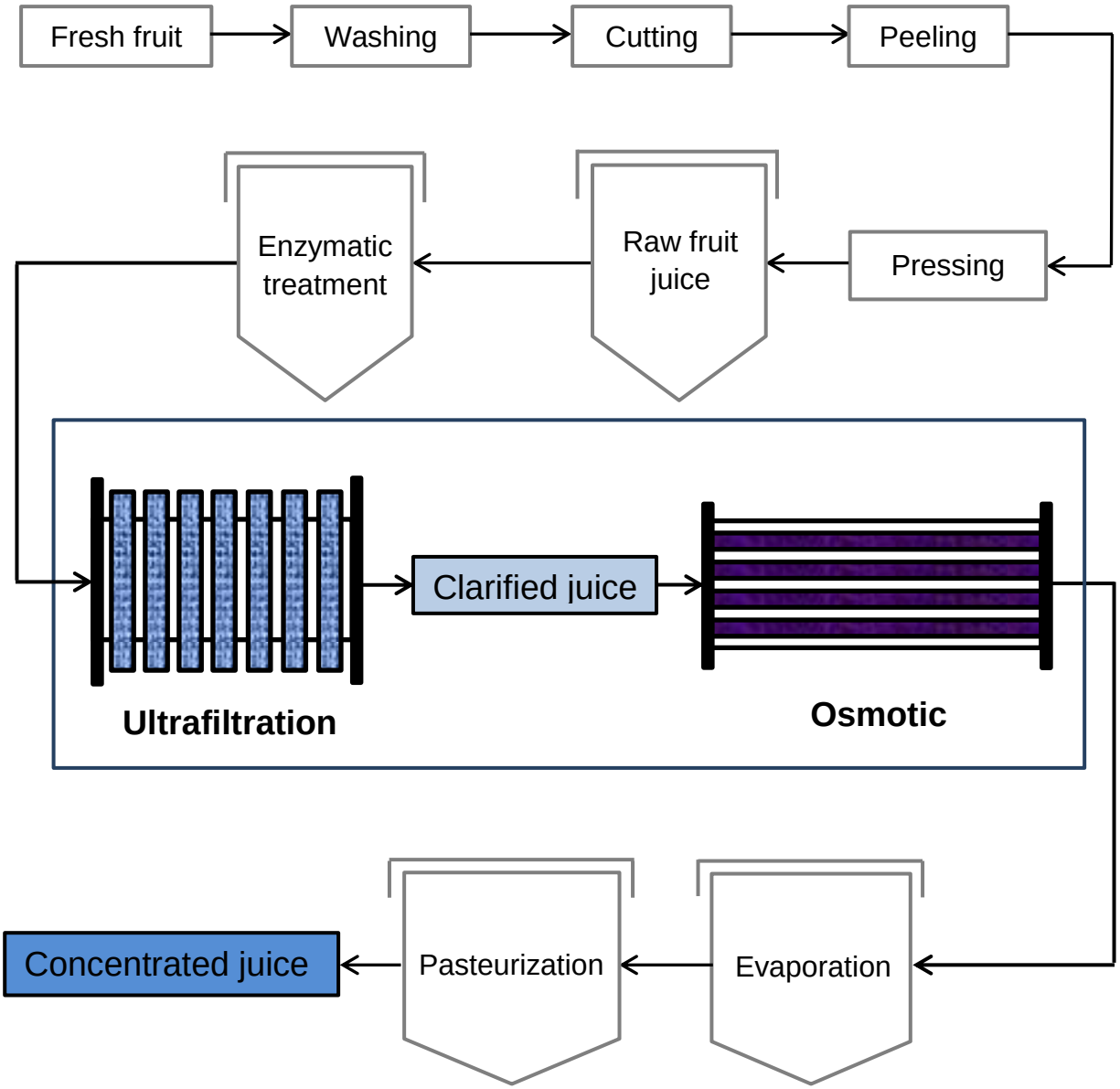

Fig 5-1: Schematic for integrated UF-OD membrane processing of juice (adapted from Cassano et al., 2011)

Chapter 3 and 4 demonstrated a *Fr 13* assessment of (a simplified) MF of fruit juices in a dead-end (and a UF cross-flow) membrane. However, the integrated UF-OD is more widely used to achieve both clarification and concentration. This combined mechanism of integrated UF-OD is becoming a widely substituted technology for thermal treatments (Nandi et al., 2012). It presents a sufficiently stringent and practical test therefore for the

purpose of investigation of the *Fr 13* risk thesis to a two-step, steady-state process.

In integrated UF-OD, output permeate flux from UF is the input feed flow to OD. Fouling of either membrane is a significant process limitation.

In the following, a *Fr 13* assessment is carried out for each of UF and OD separately. These are then synthesized into the integrated global two-step model for membrane operations. A membrane fouling risk factor (p) is defined in terms of a required (design) flux for membrane operations, plus a practical tolerance.

The global model is demonstrated with independent, published data for pomegranate juice and is used to re-assess design to limit vulnerability to surprise failure in second-tier studies.

Results will be of interest to risk analysts, and more generally, processors and manufacturers of membrane equipment.

5.2 A two-step membrane global model of integrated UF-OD concentration

All symbols used are carefully defined in the Nomenclature at the end of this thesis. Additionally, the numeric subscript used for parameters follows that established by Chandrakash et al. (2015) and is explained as follows: the first subscript is to identity the specific unit-operation item of equipment, and, the second is the order in which it is connected in the global model. For example $UF_{1\text{-}1}$ is the first UF, which is also the first unit-operation of the global model. It follows $A_{OD\,1\text{-}2}$ is the surface area of the membrane used in the first OD, which is the second unit-operation in the global model.

5.2.1 Cross-flow UF clarification

An adequate unit-operations model for steady-state simple, cross-flow membrane filtration necessitates integration of equations for transmembrane pressure ($\Delta P_{UF\,1\text{-}1}$), processing time ($t_{UF\,1\text{-}1}$), kinetic constant for fouling mode ($k_{UF\,1\text{-}1}$), and an adjustment parameter (n) for differing fouling mechanisms (Domingues et al., 2014; Field and Wu, 2011).

The mathematical expression for permeate flux ($J'_{UF\ 1\text{-}1}$) for steady-state simple cross-flow membrane filtration (Field et al., 1995) is:

$$-\frac{dJ'_{UF\ 1-1}}{dt_{UF\ 1-1}}\ J'^{(n-2)}_{UF\ 1-1} = k_{UF\ 1-1}\ (J'_{UF\ 1-1} - J^*) \tag{5.1}$$

where J^* is steady-state flux at completion of filtration.

In cross-flow UF, cake layer formation with $n = 0$ has been shown to be the principle controlling mode of fouling in juice clarification, and covers a number of different fruit types.

Based on extensive experimental data, Field and Wu (2011) modified Eq. (5.1) for cross-flow membrane filtration to give:

$$k_{0,UF\ 1-1}\ t_{UF\ 1-1} = \frac{1}{J^{*2}}\left[\ln\left(\frac{J'_{UF\ 1-1}}{J_0}\ \frac{(J_0 - J^*)}{(J'_{UF\ 1-1} - J^*)}\right) - J^*\left(\frac{1}{J'_{UF\ 1-1}} - \frac{1}{J_0}\right)\right] \tag{5.2}$$

where $k_{0,\ UF\ 1\text{-}1}$ = a kinetic constant for cake layer formation, and J_0 = the initial permeate flux of deionized water, a significant parameter for measuring membrane permeability[11]. For pomegranate juice this can be derived directly from the extensive graphical data of Cassano et al. (2011) as:

$$J_0 = L \cdot \Delta P_{UF\ 1-1} \tag{5.3}$$

where[12] $L = 1.821 \times 10^{-6}$ m^3 m^{-2} s^{-1} kPa^{-1} and is applicable for $0 \leq \Delta P_{UF\ 1\text{-}1} \leq 96$ kPa. Substitution for J_0 from Eq. (5.3) into Eq. (5.2) and simplifying gives:

$$k_{0,UF\ 1-1}\ t_{UF\ 1-1} = \frac{1}{J^{*2}}\left[\ln\left(\frac{J'_{UF\ 1-1}}{\Delta P_{UF\ 1-1} \cdot L}\ \frac{(\Delta P_{UF\ 1-1} \cdot L - J^*)}{(J'_{UF\ 1-1} - J^*)}\right) - J^*\left(\frac{1}{J'_{UF\ 1-1}} - \frac{1}{\Delta P_{UF\ 1-1} \cdot L}\right)\right] \tag{5.4}$$

Eqs. (5.1) through (5.4) define the steady-state unit-operations model for cross-flow UF clarification of juices.

---

[11] This is the correct form required. The reader should note that J_0 is currently widely incorrectly defined e.g. by Schafer et al. (2005), Boerlage et al. (2002) and Echavarria et al. (2011) as:

$J_0 = \frac{\mu_{T,UF\ 1-1}}{\mu_{T,20°C}}\ \frac{Q_{UF\ 1-1}}{A_{UF\ 1-1}\ \Delta P_{UF\ 1-1}}$ in which it is not possible to reconcile the form or units in engineering science. This is being addressed by Davey and Zou (2015) (Appendix C).

[12] i.e. $L = 655.6\ \frac{\text{L}}{\text{m}^2\ \text{h bar}} \cdot \frac{\text{m}^3}{1000\ \text{L}} \cdot \frac{\text{h}}{3600\ \text{s}} \cdot \frac{\text{bar}}{100\ \text{kPa}} = 1.821 \times 10^{-6}$ m^3 m^{-2} s^{-1} kPa^{-1}.

The permeate flux, $J'_{UF\ 1\text{-}1}$, must exceed the required, operational flux, $J_{UF\ 1\text{-}1,\ required}$ for successful membrane processing without (reversible) fouling. This value can be determined from practical experimental data only, for a specific juice and membrane(s).

Extensive experimental data (n = 19) for clarification of pomegranate juice with cross-flow UF have been independently reported at a temperature of 25 ^{O}C (Cassano et al., 2011). These data are re-plotted as Fig. 5-2. Hollow fibre membranes ($A_{UF\ 1\text{-}1}$ = 0.0046 m^2) with transmembrane pressure $\Delta P_{UF\ 1\text{-}1}$ = 96 kPa ($Q_{UF\ 1\text{-}1}$ = 1.94 x 10^{-5} m^3 s^{-1}) , $k_{0,\ UF\ 1\text{-}1}$ = 5.7 x 10^6 s m^{-2} and 5.62 x 10^{-6} < $J_{UF\ 1\text{-}1}$ < 7.92 x 10^{-6}, m^3 m^{-2} s^{-1} were used.

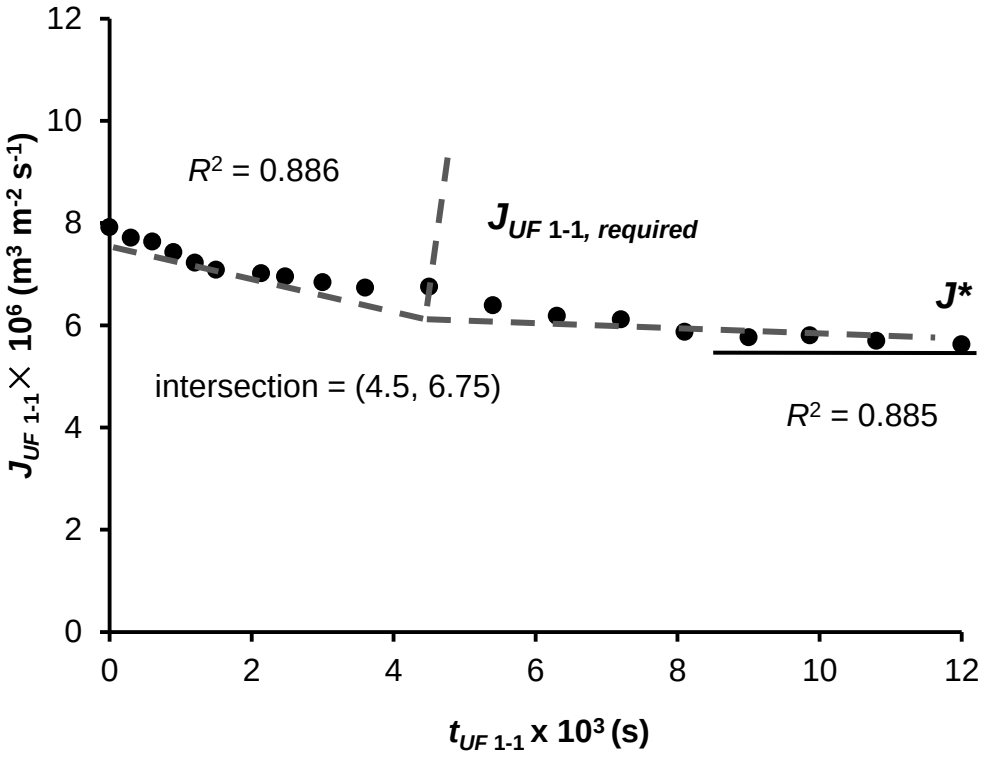

Fig. 5-2: Independent experimental data (n = 19) for permeate flux in cross-flow UF in clarification of pomegranate juice at $\Delta P_{UF\ 1\text{-}1}$ = 96 kPa (adapted from Cassano et al., 2011) showing determination $J_{UF\ 1\text{-}1,\ required}$ = 6.75 x 10^{-6} m^3 m^{-2} s^{-1} and J^* = 5.62 × 10^{-6} m^3 m^{-2} s^{-1}

From the figure, the required flux, $J_{UF\ 1\text{-}1,\ required}$ = 6.75 x 10^{-6} m^3 m^{-2} s^{-1} is determined (in Microsoft Excel) by intersection of trend lines 0 to 4,500, s (n = 1 to 11), with R^2 = 0.886 (Snedecor and Cochran, 1989) and 6,100 to 12,000, s (n = 12 to 19), with R^2 = 0.885, parts of the curve. Fig. 5-2 shows that $J_{UF\ 1\text{-}1,\ required}$ for cross-flow UF clarification of pomegranate juice is determined at $t_{UF\ 1\text{-}1}$= 4,500 s, and that J^* = 5.62 x 10^{-6} m^3 m^{-2} s^{-1}.

5.2.2 OD concentration

Clarified pomegranate juice from the cross-flow UF is then concentrated by integrated OD. The general steady-state design equation of permeate flux, or evaporation flux ($J'_{OD\ 1\text{-}2}$), in the case of OD concentration is given as (Ravindra Babu et al., 2006):

$$J'_{OD\ 1-2} = K_{OD\ 1-2}\ (a_1 - a_2) \tag{5.5}$$

where a_1 and a_2 = water activities of feed and stripping solutions and, $K_{OD\ 1\text{-}2}$ = overall mass transfer coefficient, assumed to take the following standard form:

$$K_{OD\ 1-2} = \left(\frac{1}{k_{1,OD\ 1-2}} + \frac{1}{k_{m,OD\ 1-2}} + \frac{1}{k_{2,OD\ 1-2}}\right)^{-1} \tag{5.6}$$

where $k_{1,OD\ 1\text{-}2}$ and $k_{2,OD\ 1\text{-}2}$ = mass transfer coefficient of feed and stripping solutions, respectively. These can be computed (adapted from Ravindra Babu et al., 2008) from:

$$k_{1,OD\ 1-2} = (5.16 \times 10^5\ Q_{OD\ 1-2} + 0.47) \times 10^{-5} \tag{5.7}$$

with

$$Q_{OD\ 1-2} = J'_{UF\ 1-1}\ A_{OD\ 1-2} \tag{5.7 a}$$

and

$$k_{2,OD\ 1-2} = 16.46\ e^{(-0.203\ C)} \times 10^{-5} \tag{5.8}$$

where C = concentration of osmotic agent (stripping solution).

The mass transfer coefficient, $k_{m,\,OD\,1\text{-}2}$ is expressed as (Alves and Coelhoso, 2004; Ravindra Babu et al., 2008):

$$k_{m,OD\,1-2} = \frac{P^{*}\,(1.8\times10^{-5})}{RT_{OD\,1-2}\,\delta}\left(\frac{3\tau}{\varepsilon d_p\sqrt{8RT_{OD\,1-2}/3.14M_w}} + \frac{\Delta P_{OD\,1-2}\,\tau}{\varepsilon\left(4.46\times10^{-6}\,{T_{OD\,1-2}}^{2.334}\right)}\right)^{-1} \quad (5.9)$$

where P^* = vapour pressure of pure water, R = gas constant, $T_{OD\,1\text{-}2}$ = processing temperature, δ = membrane thickness, τ = tortuosity of membrane, d_p = average membrane pore diameter, ε = membrane porosity, M_w = molar mass of pure water, and; $\Delta P_{OD\,1\text{-}2}$ = process driving pressure.

Substituting Eq. (5.6), (5.7), (5.7 a), (5.8) and (5.9) into Eq. (5.5), and simplifying gives:

$$J'_{OD\,1-2} = \left[\left((5.16\times10^{5}\,J'_{UF\,1-1}\,A_{OD\,1-2} + 0.47)\times10^{-5}\right)^{-1} + \frac{\left(\frac{3\tau}{\varepsilon d_p\sqrt{\frac{8RT_{OD\,1-2}}{3.14M_w}}} + \frac{\Delta P_{OD\,1-2}\,\tau}{\varepsilon\left(4.46\times10^{-6}\,{T_{OD\,1-2}}^{2.334}\right)}\right)}{\frac{1.8\times10^{-5}}{RT_{OD\,1-2}\,\delta}\,P^{*}} + (16.46\,e^{-0.203\,C})^{-1}\right]^{-1}(a_1 - a_2) \quad (5.10)$$

The steady-state unit-operations model for OD concentration is defined by Eqs. (5.5) through (5.10).

During OD concentration, a required value of flux exists below which fouling is observed. The permeate flux ($J'_{OD\,1\text{-}2}$) must be equal to or greater than the required flux ($J_{OD\,1\text{-}2,\,required}$); otherwise, the membrane has fouled (failed).

OD concentration of pomegranate juice was conducted by Cassano et al. (2011) at 25 ^{O}C with a driving pressure of 40,000 Pa. Micro-porous polypropylene, hollow fibers with pore diameter of 0.2 µm and a total surface area $A_{OD\,1\text{-}2}$ = 1.4 m^2 were used together with a stripping solution ($CaCl_2{\cdot}2H_2O$) with C = 9.02 mol kg^{-1}. Experimental data (n = 27) for these OD permeate flux are re-plotted as Fig. 5-3.

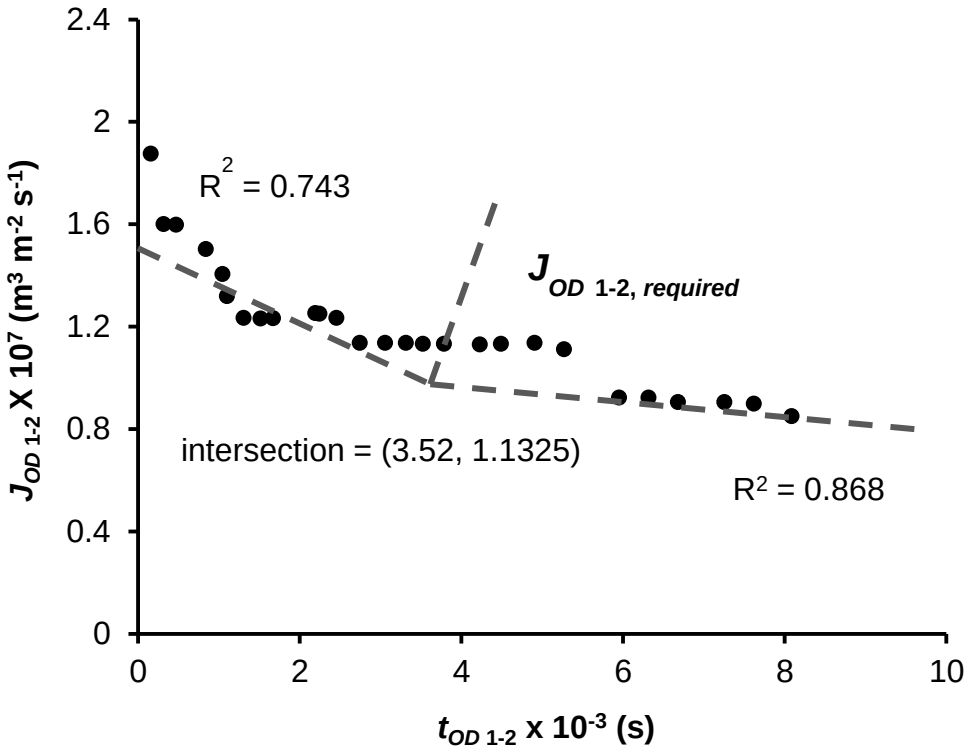

Fig. 5-3: Experimental data for evaporation flux (n = 27) in OD for concentration of pomegranate juice at $\Delta P_{OD\ 1\text{-}2}$ = 40,000 Pa (adapted from Cassano et al., 2011) showing determination $J_{OD\ 1\text{-}2,\ required}$ = 1.1325 x 10^{-7} m^3 m^{-2} s^{-1}

From Fig. 5-3, $J_{OD\ 1\text{-}2,\ required}$ is determined (using the Excel method of intersecting trend lines) 0 to 3,520, s (n = 1 to 17) (R^2 = 0.743) and 4,000 to 8,000, s (n = 18 to 27) (R^2 = 0.868) (Snedecor and Cochran, 1989), to be = 1.1325 x 10^{-7} m^3 m^{-2} s^{-1} for the concentrated pomegranate juice. This occurs at $t_{OD\ 1\text{-}2}$ = 3,520 s.

5.2.3 UF-OD membrane global model

Eqs. (5.1) through (5.10), define the integrated global model for continuous integrated UF-OD membrane processing of fruit juices.

These equations plus the values determined for the required fluxes, $J_{UF\ 1\text{-}1,\ required}$ and J^* and $J_{OD\ 1\text{-}2,\ required}$ specify the integrated two-step steady-state, membrane global model for the concentration of pomegranate juice.

5.3 Deterministic single value assessment (SVA)

The traditional, deterministic model simulation is point, or single value, assessment (SVA) which can be undertaken with or without sensitivity analyses (Sinnott, 2005).

For cross-flow UF clarification of pomegranate juice, SVA is computed as follows: from Eq. (5.3) with $\Delta P_{UF\ 1\text{-}1} = 96$ kPa, $L = 1.821 \times 10^{-6}$ m^3 m^{-2} s^{-1} kPa^{-1} gives $J_0 = 174.8 \times 10^{-6}$ m^3 m^{-2} s^{-1}. Substitution for J_0 into Eq. (5.2) with $k_{0,\ UF\ 1\text{-}1} = 5.7 \times 10^6$ s m^{-2}, $t_{UF\ 1\text{-}1} = 4{,}500$ s and $J^* = 5.62 \times 10^{-6}$ m^3 m^{-2} s^{-1} (Fig. 5.2) and rearranging gives for permeate flux, $J'_{UF\ 1\text{-}1} = 7.02 \times 10^{-6}$ m^3 m^{-2} s^{-1}. All $J'_{UF\ 1\text{-}1} < J_{UF\ 1\text{-}1,\ required}$ indicates membrane fouling (failure) (*see* calculation in Appendix E).

Similarly, SVA for OD concentration of pomegranate juice is computed as follows: from Eq. (5.7) and (5.7 a) $k_{1,\ OD\ 1\text{-}2} = 5.54 \times 10^{-5}$ m s^{-1} and from Eq. (5.8), $k_{2,\ OD\ 1\text{-}2} = 2.638 \times 10^{-5}$ m s^{-1}. Using Eq. (5.9), $k_{m,\ OD\ 1\text{-}2} = 1.22 \times 10^{-6}$ m s^{-1}. Since the values of $k_{1,\ OD\ 1\text{-}2}$, $k_{2,\ OD\ 1\text{-}2}$ and $k_{m,\ OD\ 1\text{-}2}$ are now known, the value of overall mass transfer coefficient, $K_{OD\ 1\text{-}2} = 1.142 \times 10^{-6}$ m s^{-1} is obtained from Eq. (5.6). Substitution for $K_{OD\ 1\text{-}2}$ and water activities, $a_1 = 0.95$, $a_2 = 0.85$ (Cassano et al., 2011), into Eq. (5.5), gives the permeate flux, $J'_{OD\ 1\text{-}2} = 1.167 \times 10^{-7}$ m^3 m^{-2} s^{-1} (*see* calculation in Appendix E).

A summary of SVA for each UF and OD unit-operations is presented in Table 5-1. The bold text (column 2, row 22 and column 5, row 18) is used to highlight that the output flux from the UF clarification is actually the input flux to the subsequent OD concentration.

5.4 *Fr 13* model and simulations

Fundamental to the *Fr 13* framework is a practical and unambiguous definition of failure (Davey et al., 2015; Abdul-Halim and Davey, 2015 a, b; Davey, 2015 a). For UF clarification, a risk factor for vulnerability to failure can be mathematically defined in terms of $J'_{UF\ 1\text{-}1}$ and $J_{UF\ 1\text{-}1,\ required}$ such that $P_1 = J_{UF\ 1\text{-}1,\ required} - J'_{UF\ 1\text{-}1}$.

This can be rearranged as a more convenient, dimensionless fouling risk factor (Davey et al., 2015; Abdul-Halim and Davey, 2015 a, b) as:

$$p_1 = \left(1 - \frac{J'_{UF\ 1-1}}{J_{UF\ 1-1,\ required}}\right) \times 100\ \% \tag{5.11}$$

where $J'_{UF\ 1\text{-}1}$ is the instantaneous value of permeate flux (or more strictly one membrane process scenario). However, generally membrane processing would include a practical tolerance such that $J'_{UF\ 1\text{-}1}$ needs to be equal to the minimum required value, plus an additional flux (or tolerance) such that:

$$p_1 = \%tolerance_{\ UF\ 1-1} + 100\ (1 - \frac{J'_{UF\ 1-1}}{J_{UF\ 1-1,\ required}}) \tag{5.12}$$

In the absence of unconditional data that a practical mid-range tolerance = 3 % is assumed, so that:

$$p_1 = 3 + 100\ (1 - \frac{J'_{UF\ 1-1}}{J_{UF\ 1-1,\ required}}) \tag{5.13}$$

That is if the value of UF permeate flux is less than 1.03 times the required flux ($J'_{UF\ 1\text{-}1} < 1.03 \times J_{UF\ 1\text{-}1,\ required}$), cross-flow UF has failed. It is seen that Eq. (5.13) is convenient because it is dimensionless, but importantly all $p_1 > 0$ are recognized as UF failures. Additionally, these can be readily identified in standard spread sheeting tools (Davey et al., 2015).

Eqs. (5.1) through (5.4) and Eqs. (5.11) through (5.13), together with the independent values of $J_{UF\ 1\text{-}1,\ required}$ and J^* constitute the *Fr 13* model for cross-flow UF clarification of pomegranate juice.

Similarly, for the OD concentration, a membrane fouling risk factor, p_2, is defined in terms of the $J'_{OD\ 1\text{-}2}$ and $J_{OD\ 1\text{-}2,\ required}$ with assumed tolerance = 3 % such that:

$$p_2 = 3 + 100\ (\ 1 - \frac{J'_{OD\ 1-2}}{J_{OD\ 1-2,\ required}}) \tag{5.14}$$

The *Fr 13* model for the steady-state OD concentration of pomegranate juice is defined by Eq. (5.5) through (5.10) and Eq. (5.14), together with the experimental value of $J_{OD\ 1\text{-}2,\ required}$.

Table 5-1: SVA for UF and OD unit-operations for concentration of pomegranate juice. The bolded text (column 2, row 21 and column 5, row 17) highlights that the output from UF clarification is the input for OD concentration

Unit-operation					
UF clarification			**OD concentration**		
Parameter	**SVA**		**Parameter**	**SVA**	
$T_{UF\ 1\text{-}1}$ (^{O}C)	25	constant	a_1 (water activity)	0.95	constant
$k_{0,\ UF\ 1\text{-}1}$ (s m^{-2})	5700000	constant	a_2 (water activity)	0.85	constant
L (m^3 m^{-2} s^{-1} kPa^{-1})	0.000001821	constant	R (J mol^{-1} K^{-1})	8.314	constant
$J_{UF\ 1\text{-}1,\ required}$ (m^3 m^{-2} s^{-1})	0.00000675	constant	$T_{OD\ 1\text{-}2}$ (K)	298	constant
J^* (m^3 m^{-2} s^{-1})	0.00000562	constant	M_w (kg mol^{-1})	0.018	constant
			$\Delta P_{OD\ 1\text{-}2}$ (Pa)	40000	constant
			P^* (Pa)	3169	constant
			$J_{OD\ 1\text{-}2,required}$ (m^3 m^{-2} s^{-1})	0.000000113	constant
			C (mol kg^{-1})	9.02	constant
			$A_{OD\ 1\text{-}2}$ (m^2)	1.4	constant
			δ (m)	0.000175	constant
			τ (tortuosity factor)	2	constant
			ε (porosity)	0.75	constant
			d_p (m)	0.0000002	constant
$\Delta P_{UF\ 1\text{-}1}$ (kPa)	96	input	$J'_{UF\ 1\text{-}1}$ (m^3 m^{-2} s^{-1})	**0.00000702**	input
$t_{UF\ 1\text{-}1}$ (s)	4500	input	$Q_{OD\ 1\text{-}2}$ (m^3 s^{-1})	0.000009662	input
Calculations					
J_0 (m^3 m^{-2} s^{-1})	0.0001748	Eq. (5.3)	$K_{OD\ 1\text{-}2}$ (m s^{-1})	0.000001142	Eq. (5.6)
$J'_{UF\ 1\text{-}1}$ (m^3 m^{-2} s^{-1})	**0.00000702**	Eq. (5.4)	$J'_{OD\ 1\text{-}2}$ (m^3 m^{-2} s^{-1})	0.0000001167	Eq. (5.10)

Importantly however, overall global failure of the integrated two-step UF-OD is defined by an unwanted flux $J_{OD\ 1\text{-}2}$ < ($J_{OD\ 1\text{-}2,\ required}$ plus 3 %) i.e. $p_2 \geq 0$.

This is because even though $p_1 > 0$ for the UF, this membrane can continue to practically operate at the steady-state value, J^*. Therefore juice concentration will continue until $p_2 > 0$ i.e. the OD would need to be stopped.

In *Fr 13* simulations the single value for model parameters is replaced by a probability distribution of values, the mean of which generally agrees with SVA. In the absence of specific data, input probability distributions to mimic naturally occurring fluctuations in values of key parameters of transmembrane pressure and process time are assumed to be normal and truncated. Truncation is used to obviate nonsensical values (e.g. Davey, 2015 a). In contrast, equipment parameters are assumed as constants to underscore that these do not naturally fluctuate with time.

The resulting *Fr 13* integrated UF-OD membrane global model for pomegranate juice is shown schematically as Fig. 5-4, showing the two-step UF-OD unit-operations and the truncated probability distributions used to define naturally occurring fluctuations in global key parameters, $\Delta P_{UF\ 1\text{-}1}$ and $t_{UF\ 1\text{-}1}$.

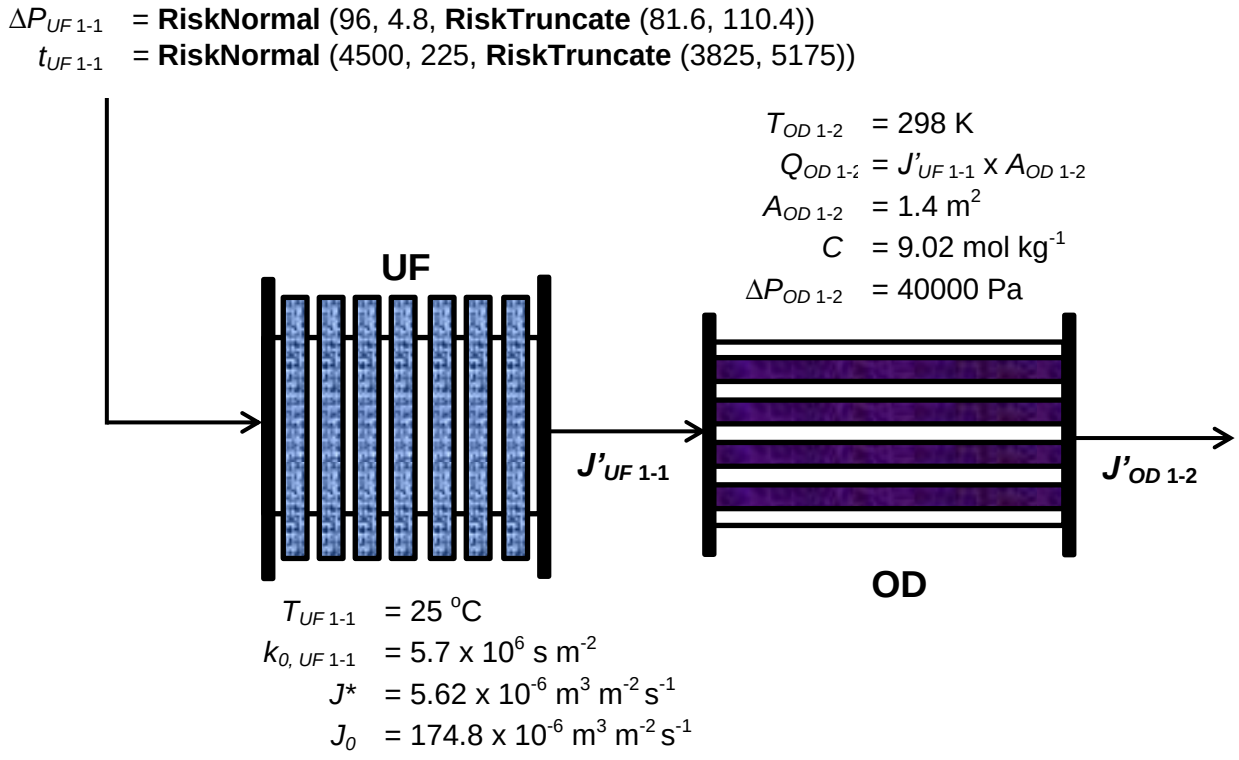

Fig. 5-4: *Fr 13* global model for membrane clarification (UF) and concentration (OD) of pomegranate juice (*Punica granatum*)

An alternative schematic of the *Fr 13* global model for UF-OD concentration of pomegranate juice can be shown as a flow sheet using a fish bone (Ishikawa) diagram Fig. B-1 (Appendix B) in which the figure is read from left to right.

From the figure, the bones represent input factors that lead to the process output. This clearly identifies the relationship between output result and possible related causes. A benefit of this type of presentation is that the combination of key factors is underscored. The format of the diagram is easy-to-read and for increasing levels of model sophistication puts the focus on the inputs and possible output effects and behaviour.

5.5 Results

Simulations were conducted in Microsoft Excel using a commercial add-on *@Risk* version 5.5 (Palisade Corporation). A comparative summary of results for deterministic SVA and probabilistic *Fr 13* simulation for cross-flow UF clarification are presented in Table 5-2.

Table 5-2: Summary comparison of traditional deterministic SVA with probabilistic *Fr 13* simulation of cross-flow UF clarification of pomegranate juice (*Punica granatum*) with a 3 % tolerance. Failure is defined for all $p_1 > 0$

Parameter	**SVA**[1]	***Fr 13* simulation**[2]	
$\Delta P_{UF\ 1\text{-}1}$ (kPa)	96	**97.42**[†]	**RiskNormal** (96,4.8, **RiskTruncate** (81.6,110.4))
$t_{UF\ 1\text{-}1}$ (s)	4500	**4904.10**[†]	**RiskNormal** (4500, 225, **RiskTruncate** (3825,5175))
$T_{UF\ 1\text{-}1}$ (^{O}C)	25	25	constant
L ($m^3\ m^{-2}\ s^{-1}\ kPa^{-1}$)	0.000001821	0.000001821	constant
$k_{0,\ UF\ 1\text{-}1}$ ($s\ m^{-2}$)	5700000	5700000	constant
J^* ($m^3\ m^{-2}\ s^{-1}$)	0.00000562	0.00000562	constant
$J_{UF\ 1\text{-}1,\ required}$ ($m^3\ m^{-2}\ s^{-1}$)	0.00000675	0.00000675	constant
$J'_{UF\ 1\text{-}1}$ ($m^3\ m^{-2}\ s^{-1}$)	0.00000702	0.000006902[†]	Eq. (5.4)
p_1	-	**0.754**[†]	Eq. (5.13)

[1] Traditional, deterministic SVA.
[2] *Fr 13* simulation with Latin Hypercube sampling.
[†] Values reproduced exactly from r-MC; it is not implied they need to be measured to this order.

One hundred thousand (100,000) random samples of distributions were sufficient. Each simulation can be considered a daily UF process of pomegranate juice. Key parameters are given in column 1 of Table 5-2. Traditional SVA is read down column 2 where permeate flux $J'_{UF\ 1\text{-}1} = 7.02 \times 10^{-6}$ m^3 m^{-2} s^{-1} is shown. The *Fr 13* simulation is summarized in columns 3 and 4. Column 4 sets out the distributions used for key parameters $\Delta P_{UF\ 1\text{-}1}$ and $t_{UF\ 1\text{-}1}$ (Fig. 5-4). It can be seen in the column that at $\Delta P_{UF\ 1\text{-}1} = 97.42$ kPa and corresponding $t_{UF\ 1\text{-}1} = 4{,}904.10$ s, permeate flux, $J'_{UF\ 1\text{-}1} = 6.902 \times 10^{-6}$ m^3 m^{-2} s^{-1}; the value of risk factor, $p_1 = 0.754$ (> 0), emphasizing a membrane fouling failure with the assumed tolerance = 3 %.

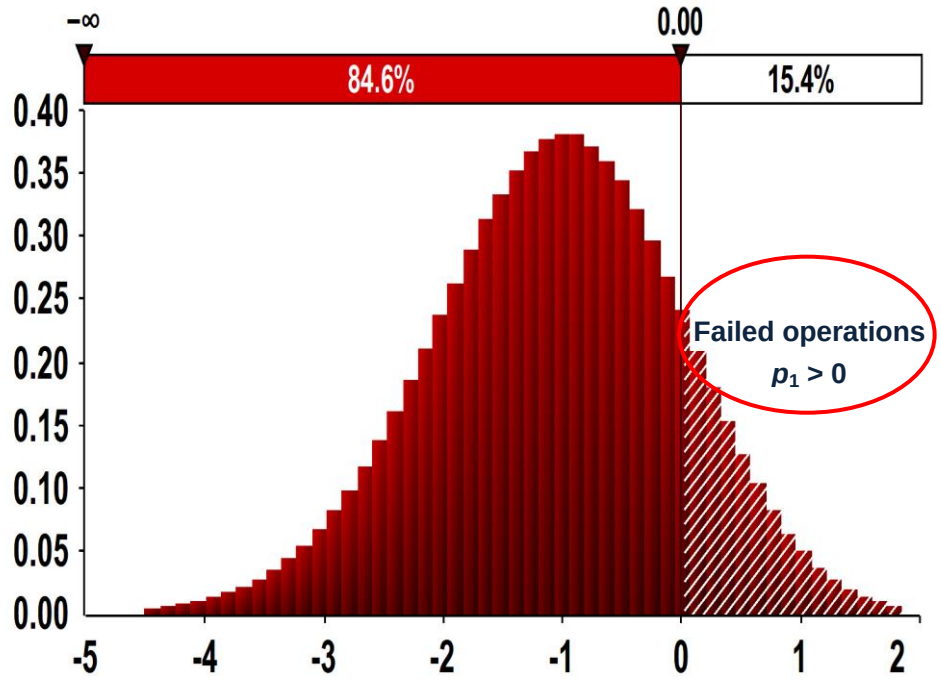

Fig. 5-5: Summary of *Fr 13* simulation of 100,000 scenarios of the risk actor (p_1) for cross-flow UF clarification of pomegranate juice (*Punica granatum*) with 3 % tolerance. The 15,407 failure scenarios are shown on the right of the figure where $p_1 > 0$

Importantly, the values in columns 3 of Table 5-2 represent only one of the 100,000 scenarios. A graphical summary of all 100,000 scenarios for UF clarification is presented in Fig. 5-5. The *x*-axis is the computed value of p_1 from Eq. (5.13) and the *y*-axis is the probability of p_1 actually occurring (Vose, 2008). From the figure, it can be seen the area

under the curve (~ 6.5 x 0.16) = one (1). A total of 15,407 failures with $p_1 > 0$ were identified. Therefore, failure rate is therefore (15,407 / 100,000 =) 15.4 %, over an extended period as shown on the right side of the Fig. 5-5.

Ten (10) of the 15,407 failures from UF clarification were selected and are presented in Table 5-3. An advantage of Table 5-3 is that the value of each key parameter that combined to produce a failure can be identified. For example in column 5, failure 4 (bolded text), shows that with input transmembrane pressure of $\Delta P_{UF\ 1\text{-}1}$ = 97.42 kPa in combination with filtration time of $t_{UF\ 1\text{-}1}$= 4,904.10 s gave rise to permeate flux of $J'_{UF\ 1\text{-}1}$ = 6.902 x 10^{-6} m^3 m^{-2} s^{-1} with p_1 = 0.754, highlighting membrane fouling (failure). This is the particular scenario reported in Table 5-2. In all cases shown in Table 5-3 the permeate flux is less than $J_{UF\ 1\text{-}1,\ required}$ plus a 3 % tolerance and resulting $p_1 > 0$.

With these 15,407 failures in cross-flow UF as the input volumetric flow rate to the OD concentration, there were 10,468 failures identified with $J'_{OD\ 1\text{-}2} < J_{OD\ 1\text{-}2,\ required}$ plus a 3 % tolerance. Table 5-4 presents the corresponding results in OD concentration from the ten (10) failure scenarios in UF clarification from Table 5-3 as inputs. These tabulated data reveal that six (6) of the ten (10) corresponding scenarios failed to meet the design criteria ($J_{OD\ 1\text{-}2,\ required}$) in OD concentration, plus a 3 % tolerance, as is evidenced by $p_2 > 0$, columns 2, 4, 5, 8, 9 and 11, respectively, failure numbers 1, 3, 4, 7, 8 and 10.

As a result, overall failure rate of the apparent steady-state integrated UF-OD membrane global process with pomegranate juice (p_2) is 10.5 % (= 10,468/100 000) of all membrane processes, averaged over the long term, of daily operations.

Table 5-3: Ten (10) selected *Fr 13* failures from 15,407 in 100,000 scenarios in UF clarification of pomegranate juice with a 3 % tolerance. (The bolded text of column 5, failure 4, is the particular scenario reported in Table 5-2)

Parameter†	**10 selected UF *Fr 13* failures**									
	1	**2**	**3**	**4**	**5**	**6**	**7**	**8**	**9**	**10**
$\Delta P_{UF\ 1\text{-}1}$ (kPa)	105.34	94.83	100.58	**97.42**	97.59	99.46	96.90	98.26	95.64	105.67
$t_{UF\ 1\text{-}1}$ (s)	4815.50	4742.29	4823.59	**4904.10**	4752.85	4774.07	4865.80	5030.01	4728.58	4889.76
$J'_{UF\ 1\text{-}1}$ x 10^6 ($m^3\ m^{-2}\ s^{-1}$)	6.927	6.948	6.925	**6.902**	6.945	6.939	6.912	6.867	6.952	6.906
p_1	0.376	0.061	0.412	**0.754**	0.107	0.199	0.593	1.274	0.001	0.692

† The parameter values tabulated are computed from our r-MC sampling; it is not implied they need to be measured to this order.

Table 5-4: Corresponding output scenarios in OD concentration with the ten (10) failures in UF of Table 5-3 as inputs

Parameter†	**10 corresponding OD *Fr 13* scenarios**									
	1	**2**	**3**	**4**	**5**	**6**	**7**	**8**	**9**	**10**
$J'_{UF\ 1\text{-}1}$ x 10^6 ($m^3\ m^{-2}\ s^{-1}$)	6.927	6.948	6.925	**6.902**	6.945	6.939	6.912	6.867	6.952	6.906
$Q_{OD\ 1\text{-}2}$ x 10^6 ($m^3\ s^{-1}$)	9.698	9.728	9.695	**9.662**	9.723	9.715	9.677	9.613	9.733	9.668
$J'_{OD\ 1\text{-}2}$ x 10^7 ($m^3\ m^{-2}\ s^{-1}$)	1.16644	1.16651	1.16645	**1.16636**	1.16650	1.16648	1.16640	1.16625	1.16652	1.16637
p_2	0.0028	-0.0032	0.0035	**0.0100**	-0.0024	-0.0006	0.0069	0.0201	-0.0044	0.0089

† The values tabulated are computed from r-MC sampling; it is not implied they need to be measured to this order.

5.6 Discussion

5.6.1 UF-OD global simulations

The *Fr 13* simulations proved to be stable. An advantage of spread sheeting was that the distributions could be entered, copied and pasted and viewed as Excel formulae.

Most importantly, it is not implied that numerical values given in Tables 5-2 through 5-5 for parameter values e.g. Table 5-2, $\Delta P_{UF\ 1\text{-}1}$ = 97.42 kPa and $t_{UF\ 1\text{-}1}$ = 4,904.10 s would need to be measured (or achieved) to these exactly; these values are reproduced as the exact value sampled randomly in r-MC simulations.

A careful check showed mean simulation outputs agreed with SVA values. Therefore, it was concluded that *Fr 13* simulations and results were free of computation and programming errors.

A detailed simulation data of *Fr 13* risk assessment of integrated UF-OD is presented in Appendix F.

5.6.2 UF-OD membrane failures

It is evident from Table 5-4 that not all ten (10) failed scenarios in UF clarification automatically led to a failure in the connected OD concentration. This outcome might not have been anticipated. To underscore this finding, the ten (10) selected scenarios are presented in Table 5-5 for the integrated UF-OD membrane global model. For example, column 6, scenario 5 (bolded text), illustrates that for UF with an input $\Delta P_{UF\ 1\text{-}1}$ = 97.59 kPa in combination with $t_{UF\ 1\text{-}1}$ = 4,752.85 s gave rise to a permeate flux, $J'_{UF\ 1\text{-}1}$ = 6.945 x 10^{-6} m^3 m^{-2} s^{-1} which is less than $J_{UF\ 1\text{-}1,\ required}$ plus a 3 % tolerance, resulting in p_1 = 0.107, highlighting a failure in cross-flow UF. With $J'_{UF\ 1\text{-}1}$ = 6.945 x 10^{-6} m^3 m^{-2} s^{-1} as the input feed flow to OD, the volumetric flow rate becomes $Q_{OD\ 1\text{-}2}$ = 9.723 × 10^{-6} m^3 s^{-1} (Eq. 5.7 a). This gave rise to $J'_{OD\ 1\text{-}2}$ = 1.16650 × 10^{-7} m^3 m^{-2} s^{-1} which is actually greater than 1.03 times the required flux ($J_{OD\ 1\text{-}2,\ required}$ x 1.03 = 1.16648 × 10^{-7} m^3 m^{-2} s^{-1}), and p_2 = - 0.0024.

Table 5-5: Ten (10) selected *Fr 13* scenarios of integrated UF-OD membrane global model demonstrated with pomegranate juice (*Punica granatum*) with a 3 % tolerance. These include six (6) failure scenarios 1, 3, 4, 7, 8 and 10 (all with $p_2 > 0$)

Parameter[†]	***Fr 13* scenario**									
	1	**2**	**3**	**4**	**5**	**6**	**7**	**8**	**9**	**10**
Cross-flow UF clarification										
$\Delta P_{UF\ 1\text{-}1}$ (kPa)	105.34	94.83	100.58	97.42	**97.59**	99.46	96.90	98.26	95.64	105.67
$t_{UF\ 1\text{-}1}$ (s)	4815.50	4742.29	4823.59	4904.10	**4752.85**	4774.07	4865.80	5030.01	4728.58	4889.76
$J^* \times 10^6$ ($m^3\ m^{-2}\ s^{-1}$)	5.62	5.62	5.62	5.62	**5.62**	5.62	5.62	5.62	5.62	5.62
$J_0 \times 10^6$($m^3\ m^{-2}\ s^{-1}$)	174.8	174.8	174.8	174.8	**174.8**	174.8	174.8	174.8	174.8	174.8
$J'_{UF\ 1\text{-}1} \times 10^6$ ($m^3\ m^{-2}\ s^{-1}$)	6.927	6.948	6.925	6.902	**6.945**	6.939	6.912	6.867	6.952	6.906
$J_{UF\ 1\text{-}1,\ required} \times 10^6$ ($m^3\ m^{-2}\ s^{-1}$)	6.75	6.75	6.75	6.75	**6.75**	6.75	6.75	6.75	6.75	6.75
p_1	0.376	0.061	0.412	0.754	**0.107**	0.199	0.593	1.274	0.001	0.692
OD concentration										
$J'_{UF\ 1\text{-}1} \times 10^6$ ($m^3\ m^{-2}\ s^{-1}$)	6.927	6.948	6.925	6.902	**6.945**	6.939	6.912	6.867	6.952	6.906
$Q_{OD\ 1\text{-}2} \times 10^6$ ($m^3\ s^{-1}$)	9.698	9.728	9.695	9.662	**9.723**	9.715	9.677	9.613	9.733	9.668
a_1	0.95	0.95	0.95	0.95	**0.95**	0.95	0.95	0.95	0.95	0.95
a_2	0.85	0.85	0.85	0.85	**0.85**	0.85	0.85	0.85	0.85	0.85
$T_{OD\ 1\text{-}2}$ (K)	298	298	298	298	**298**	298	298	298	298	298
$\Delta P_{OD\ 1\text{-}2}$ (Pa)	40000	40000	40000	40000	**40000**	40000	40000	40000	40000	40000
$A_{OD\ 1\text{-}2}$ (m^2)	1.4	1.4	1.4	1.4	**1.4**	1.4	1.4	1.4	1.4	1.4
$k_{OD\ 1\text{-}2} \times 10^6$ (m s^{-1})	1.142	1.142	1.142	1.142	**1.142**	1.142	1.142	1.142	1.142	1.142
C (mol kg^{-1})	9.02	9.02	9.02	9.02	**9.02**	9.02	9.02	9.02	9.02	9.02
$J'_{OD\ 1\text{-}2} \times 10^7$ ($m^3\ m^{-2}\ s^{-1}$)	1.16644	1.16651	1.16645	1.16636	**1.16650**	1.16648	1.16640	1.16625	1.16652	1.16637
$J_{OD\ 1\text{-}2,\ required} \times 10^7$ ($m^3\ m^{-2}\ s^{-1}$)	1.1325	1.1325	1.1325	1.1325	**1.1325**	1.1325	1.1325	1.1325	1.1325	1.1325
p_2	0.0028	-0.0032	0.0035	0.0100	**-0.0024**	-0.0006	0.0069	0.0201	-0.0044	0.0089

[†] The values tabulated are computed from r-MC sampling; it is not implied they need to be measured to this order.

A failure in UF membrane flux is shown not to be automatically a failure in the overall integrated UF-OD membrane global model. That is scenario 5, is reasonably considered a successful integrated two-step UF-OD membrane global process for concentration of pomegranate juice. Other examples of similar overall successful membrane operations include scenarios 2, 6 and 9 of Table 5-5. These can be considered overall successes because the integrated UF-OD process would not need to be stopped.

However failure scenarios 1, 3, 4, 7, 8 and 10 in UF resulted in corresponding overall failure in the flux in the integrated two-step UF-OD membrane global process (all $p_2 > 0$). Therefore processing would need to stop to clean or replace the UF-OD membranes.

Detailed data shown in Table 5-5 can be conveniently presented visually as, **F** = Fail, NF = Not Fail, to give an overall immediate summary, presented in Table 5-6. This table shows directly the six (6) of ten (10) selected UF failed scenarios as failures of integrated UF-OD membrane global process of pomegranate juice (row 4).

Table 5-6: Visual summary of the ten (10) selected *Fr 13* scenarios of Table 5-5 for integrated UF-OD membrane global model demonstrated with pomegranate juice (*Punica granatum*) with a 3 % tolerance

Operation	***Fr 13* scenario**									
	1	**2**	**3**	**4**	**5**	**6**	**7**	**8**	**9**	**10**
UF clarification	**F**	**F***	**F**	**F**	**F**	**F**	**F**	**F**	**F**	**F**
UF-OD integrated	**F**	NF*****	**F**	**F**	NF	NF	**F**	**F**	NF	**F**

***F** = Failure
*NF = Not Failure

Table 5-6 provides an immediate visual and unassuming way to display the random nature of *Fr 13* failures, and importantly illustrates the potential for counter-intuitive accumulation of the impact of naturally occurring random fluctuations in key parameters in an overall steady-state global plant.

An extension to all 100,000 scenarios would show 10,468 failures (**F**) in the juice global model which equals 10.5 % of all UF-OD processes, averaged over the long term.

Fr 13 findings are most usefully interpreted in terms of daily operations. With batch-continuous processes, for example, daily pasteurisation of raw milk with Clean-in-Place (CIP) (Davey et al., 2015), each day can be reasonably thought of as ‘one’ event. However, membranes processing is designed to be largely continuous. To achieve this in industrial application, banks of parallel UF-OD would be needed to cover shutdowns and maintenance to give a continuous flow of juice. A rationale therefore is to assume a daily basis with a fixed-time for maintenance – say a possible replacement of particular UF-OD membrane bank (there are essentially no moving parts) at say 1.25 h (i.e. 4,500 s *see* Table 5-2, column 2). Practically, all fouled membrane banks are required to be

cleaned at the end of a processing day. Another period however might be used, depending on what maintenance is required. For example, on a monthly basis the plant might need to be shut down for significant maintenance.

However, if each scenario is considered one bank of membranes, there would therefore be (10,468 / (100,000 days) x 365.25 days / year =) 39 surprise failures per year with a tolerance = 3 % i.e. approximately three (3) per month despite good operations and maintenance. Nonetheless membrane failures would not be expected to be equally distributed in time.

Given that large-scale UF-OD plant is most likely housed inside a controlled environment, it is not considered there will be any significant variations caused to operational parameters by seasonal change. The impact of seasonal variations with the pomegranate juice, or the processing of different types of juice e.g. orange, passion, can be readily accounted for by a range of values routinely determined experimentally for $J_{UF\ 1\text{-}1,\ required}$.

Overall, a more unequivocal statement is that 10.5 % of all operations over the long term would be vulnerable to surprise fouling.

Importantly, this new insight is not available from traditional risk and hazard analyses such as HACCP, HAZOP or Reliability Engineering. As pointed out recently by Davey et al. (2015), and others including Abdul-Halim and Davey (2015 a, b), Davey (2011) and Davey (2015 a), the random element is not explicit in these risk and hazard methods.

Fig. 5-5 together, with ten (10) *Fr 13* scenarios from Table 5-5 and 5-6, underscore that the integrated UF-OD membrane global processing of juices is to be more correctly understood as a combination of successful and failed operations. These failure operations cannot be blamed on faulty fittings or human error (Cerf and Davey, 2001; Davey and Cerf, 2003) but are due to uncontrolled naturally occurring random, small fluctuations within the apparent steady-state membrane global plant.

Significantly, the failure is defined in terms of failed fluxes (p_1 and overall p_2). However, an alternative could be to define failure of the concentrated product juice in (measurable and) suitable terms involving, for example, clarity, colour and so on. Unless there is an instantaneous delivery required, the concentrated juice could then be held in

storage where ‘off-spec’ product could be carefully blended with a ‘super on-spec’ commercial product. The final product juice will then be ‘on-spec’ and product failures minimized. (The CFB of Davey (2015 a) is a (reverse) example of this in which a consistent feed stock is obtained by the blending of a range of stocks to control significant fluctuation and outcome plant behaviour).

5.6.3 Input probability distributions

How the probability distributions for the key parameters are arrived at, and how these might impact on the value of the risk factor *p*, are important to *Fr 13* simulation. There is a need is to find a sufficiently accurate approximation to mimic the naturally occurring fluctuations in parameter values so that results can be realistically applied. It is clear that the qualified rigidity of the distributions for $\Delta P_{UF\ 1\text{-}1}$ and $t_{UF\ 1\text{-}1}$, together with %*tolerance*, will govern the probabilistic failure and success rates. These rates could of course therefore be greater or lower than shown (e.g. Fig. 5-5).

Historical data could be used to define a refined empirical input distribution (Davey, 2010). However, a drawback is that simulations would then reproduce only what has happened historically, and it is seldom likely there will be enough historical data to be able to simulate all possible practical operations. Indeed, historical failure data are generally difficult to obtain because commercial industries do not commonly disclose ‘failures’, but rather ‘successes’. This presents immediate difficulties in ‘closing the loop’ on the present UF-OD simulations and comparison with direct data. For the present purpose, a theoretical distribution, limited to the range of values covering published parameters, is a better prospect (Vose, 2008; Law, 2011).

In the absence of contrary data, and for the purpose of investigating the integrated two-step *Fr 13* global model, probability distributions are defined theoretically as normal and truncated. Truncation has been used to limit values to those that can practically occur (Chandrakash et al., 2015; Davey, 2015 a; Davey et al., 2015). For example for the transmembrane pressure $\Delta P_{UF\ 1\text{-}1}$ = **RiskNormal** (96, 4.8, **RiskTruncate** (81.6, 110.4)); this is a normal distribution with a mean of 96 kPa, stdev = 4.8 kPa (5 % about the mean)

and, truncated at a minimum = 81.6 kPa and maximum = 110.4 kPa. As shown in Fig. 5-4 and Table 5-2 this same truncated distribution is used to define $t_{UF\ 1\text{-}1}$.

Distributions are defined with a 3 x stdev about the mean to establish the minimum and maximum. The result is that 99.73 % of all r-MC samples will fall in this interval (Sullivan, 2004; Vose, 2008). Thus, distribution of values sampled to mimic the naturally occurring fluctuations in these key parameters covers a realistically wide range.

Repeat simulations were conducted to investigate the impact of the minimum and maximum obtained with 2 x stdev (95.45 % of all samples) for both key parameters on the number of *Fr 13* failures. Results were not meaningfully changed as the failure rate of cross-flow UF clarification decreased from 15.4 to 14.2, %.

Generally, there are some 40 theoretical probability distributions that could be used including Triangle, Beta-subjective and Normal. For example Davey and Cerf (2003) used Beta-subjective as a distribution for residence time in UHT milk processing. Evidently, the more realistic the probability distributions used for model inputs, the better the *Fr 13* simulations. However, some experimenting (Davey et al., 2015; Davey, 2015 a; Abdul-Halim and Davey, 2015 a, b) has revealed that the number of *Fr 13* failures is not sensitive to a range of distributions. This might not always be the case however (Law, 2011). A development could be the defining of distributions using expert experience or even opinion (Davey, 2010; Law, 2011).

Regardless of how distributions are defined, it is important for *Fr 13* that each scenario simulated can be observed in practical daily operation.

5.6.4 Process tolerance

A practical tolerance (*%tolerance*) was used in defining the risk factor (Eq. (5.12) and (5.14)) to ensure the process permeate flux is greater than the required, operational flux.

Overall the number of integrated UF-OD *Fr 13* failures (p_2) would be expected to be sensitive to the process tolerance. Repeated simulations were therefore carried out for a range of values $1 \leq$ *%tolerance* ≤ 5 on the UF fouling risk factor in Eq. (5.12).

These overall failures are summarized graphically in Fig. 5-6, which shows an apparent exponential dependence of the number of failures on tolerance. With decreasing *%tolerance* these failures fall away to zero at a value of 1. With increasing values the number of predicted failures increases rapidly, especially at *%tolerance* ≥ 3. This result is interpreted as the lower the permitted design tolerance the greater the loss of flexibility and the greater the precision needed for process control of the UF membrane. This suggests that precision control of UF, whilst expensive, could provide benefits in minimizing vulnerability to surprise failures.

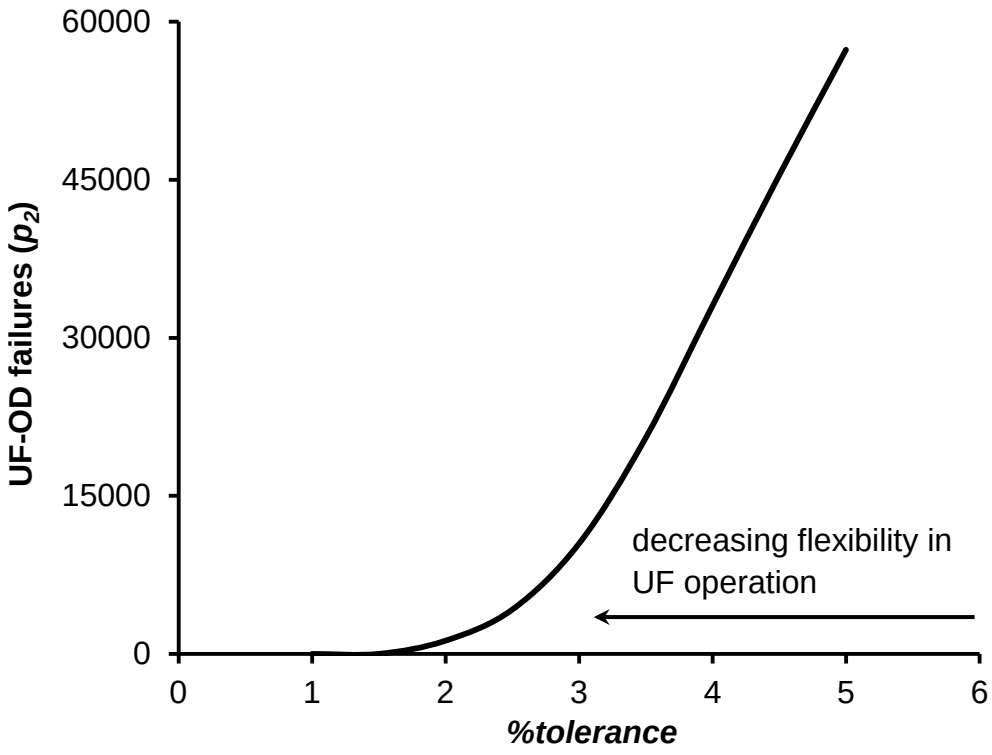

Fig. 5-6: Effect of *%tolerance* (in Eq. (5.12)) on the number of overall *Fr 13* failures (p_2) per 100,000 scenarios in integrated two-step UF-OD membrane concentration of pomegranate juice (*Punica granatum*)

Clearly, for the integrated two-step UF-OD the criteria for %*tolerance* will be a balance where decreasing %*tolerance* means reducing vulnerability to risk and therefore the result is ‘safer’.

5.6.5 Impact of filtration time

Practically, the key parameters of an integrated two-step UF-OD membrane global model are transmembrane pressure ($\Delta P_{UF\ 1\text{-}1}$) and filtration time ($t_{UF\ 1\text{-}1}$). To highlight this, the Spearman Rank correlation coefficient (available in *@Risk*) (Snedecor and Cochran, 1989) for these two parameters is provided in Table 5-7 which shows a very strong positive correlation (0.96) between $t_{UF\ 1\text{-}1}$ and p_1.

This discloses that naturally occurring random fluctuations in filtration time will have a highly significant impact on permeate flux of cross-flow UF clarification and in consequence, on the integrated UF-OD membrane global process.

Table 5-7: Spearman rank correlation coefficient (Snedecor and Cochran, 1989) for key input parameters on fouling (p_2) in integrated UF-OD membrane global model

Input parameter	Coefficient
$t_{UF\ 1\text{-}1}$	+ 0.96
$\Delta P_{UF\ 1\text{-}1}$	- 0.04

5.6.6 Depicting membrane failure in the integrated two-step *Fr 13* synthesis

Although the tabulated presentation (Tables 5-3, 5-4, 5-5, and 5-6) provides a good summary of the integrated UF-OD membrane global process, the difficulty is how to depict the outcome of the plant behaviour.

Abdul-Halim and Davey (2015 a) introduced a 3D graphical treatment in an attempt to present *Fr 13* failures in UV irradiation for potable water. They acknowledged this was practically limited to a three-parameter model, but did demonstrate a useful visualization of the *Fr 13* risk and its random nature with time in the apparent steady-state flow unit-operation.

Fig. 5-7 is an adaption of that work using a 3D scatter plot of 14 selected *Fr 13* failures ($p_2 > 0$) from the steady-state integrated UF-OD membrane global model for pomegranate juice (produced with Statisitica™ version 12, StatSoft Inc.).

Six (6) of the 14 failures, marked as triangle (▲) in the figure, are the failed scenarios from Tables 5-5 and 5-6, scenarios 1, 3, 4, 7, 8 and 10. The purpose is to visually illustrate the random nature of p_2 values for the integrated UF-OD membrane global process and to show the plot cannot be extrapolated in any reliable way. However, the figure shows that p_2 values increase with longer processing time and lower transmembrane pressure i.e. with increasing $t_{UF\ 1\text{-}1}$ or decreasing $\Delta P_{UF\ 1\text{-}1}$ the integrated UF-OD membrane global process is more likely to fail due to decreased permeate flux. This highlights that there will be reduced vulnerability to failures in the integrated UF-OD membrane global model with lower filtration time and higher transmembrane pressures.

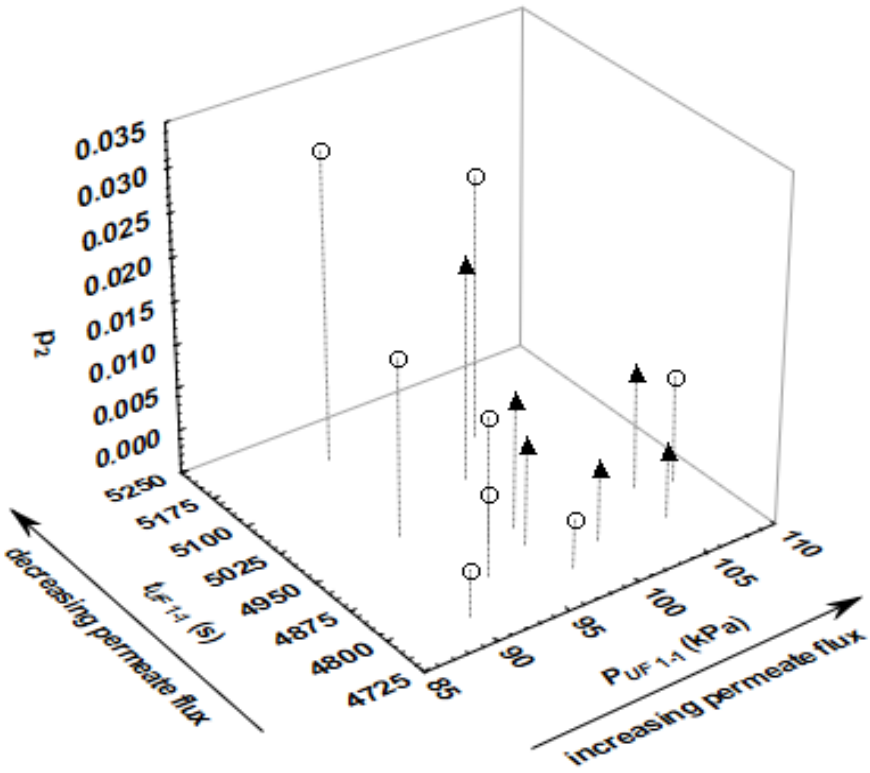

Fig. 5-7: 3D scatter plot of 14 selected *Fr 13* failures ($p_2 > 0$) in integrated UF-OD membrane global model for pomegranate juice (*Punica granatum*) with 3 % tolerance. The six failures of Tables 5-5 and 5-6 are indicated by the data marker ▲

With an increasing number of input parameters to describe more complex global models, Abdul-Halim and Davey (2015 a) and Davey (2015 a) suggested a radar-type plot as an alternative to aid visualization. (There were 20 input parameters defined by distributions in the study of Davey (2015 a) and three in the study of Abdul-Halim and Davey (2015 a)).

Fig. 5-8 is a radar plot of the six (6) failed scenarios from Fig. 5-7 indicated by the marker ▲ (and produced in Excel with the commercial add-on *TM Custom Radar*). The figure shows two input values for $t_{UF\ 1\text{-}1}$ and $\Delta P_{UF\ 1\text{-}1}$ from distributions for the particular scenario, and the corresponding three key outputs values for $Q_{OD\ 1\text{-}2}$, $J'_{OD\ 1\text{-}2}$ and p_2. In Fig. 5-8, the axes are independent scales for each parameter in the integrated UF-OD membrane global model; the global model is condensed to a polygon.

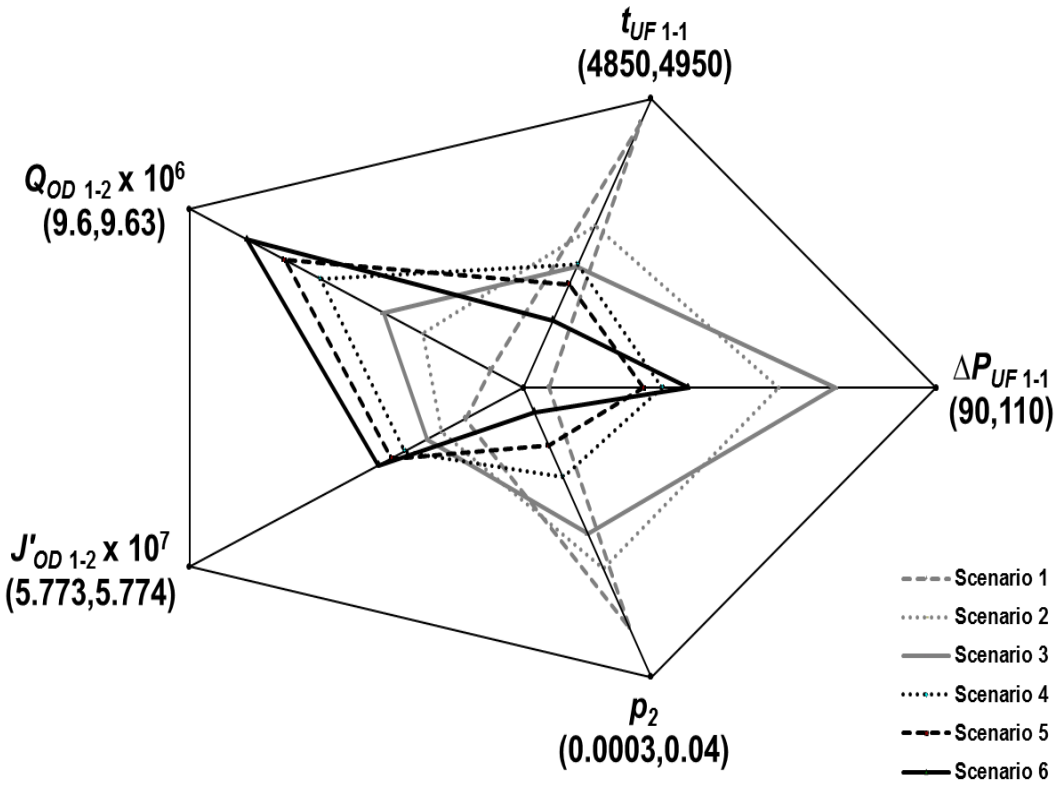

Fig. 5-8: Radar plot of six selected *Fr 13* failures (marked as ▲ in Fig. 5-7) in integrated UF-OD membrane global model for pomegranate juice with a 3 % tolerance

It is concluded however that for 10,468 global model failures ($p_2 > 0$) in 100,000 scenarios this depiction of risk data (Fig. 5-8) is not overall useful in picturing *Fr 13* failure. It is likely to be increasingly less so as the number of input parameters increases with increasingly more complex integrated processes.

In summary, the depiction of risk data as illustrated in Fig 5-5 appears the best overview of *Fr 13* failures. It provides an overview of all scenarios including *Fr 13* failures and rate of occurrence averaged over the long term. Any particular scenario can be readily identified using standard spread sheeting as demonstrated in Tables 5-2 and 5-3.

5.6.7 Reducing process vulnerability through *Fr 13* second-tier simulations

Because *Fr 13* failures are due solely to impact of random fluctuations within the system, further study or measurement or knowledge of the integrated UF-OD membrane global process cannot be used to reduce vulnerability to these. Only changing the physical system can impact vulnerability to failure. Physical changes to the system are mimicked by changes made to the input distributions describing parameters.

For steady-state integrated UF-OD membrane processing, there are two practical options readily apparent. The first is to make use of the insight provided in Table 5-7 and reduce variance in applied filtration time (and transmembrane pressure). Clearly, small changes in filtration time will have a highly significant impact on permeate flux. In practical terms this means an improved process control i.e. control of the stdev. Repeat simulations were therefore carried out on a change in stdev in the input distributions for both $t_{UF\ 1\text{-}1}$ and $\Delta P_{UF\ 1\text{-}1}$ for the range $1 \leq \text{stdev} \leq 20$, % about the mean. 100,000 r-MC samples were used. The results for the overall UF-OD membrane global process are presented as Fig.5-9.

Fig.5-9 shows that the number of overall UF-OD (p_2) failures rise with increasing values of the stdev and fall away as stdev is decreased. At a stdev = 1 % the number of predicted *Fr 13* failures is actually zero. Practically this suggests that a straightforward tradeoff of costs of increased precision control to limit fluctuations in filtration time and transmembrane pressure could be made against gains in reduced vulnerability.

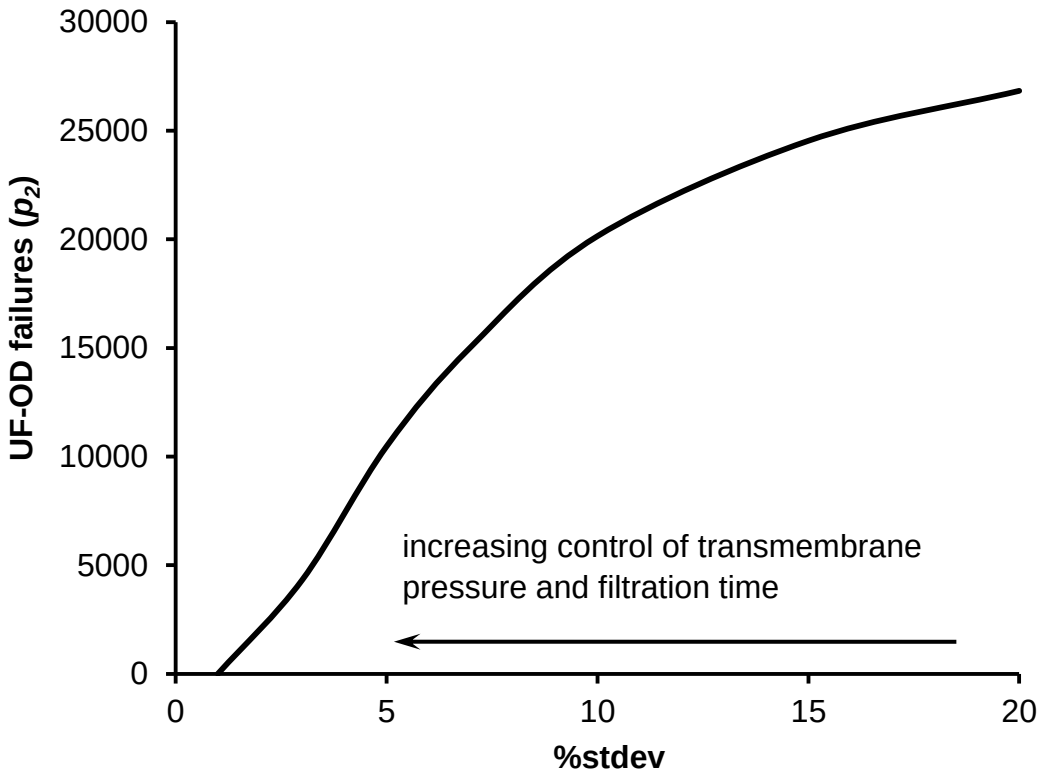

Fig. 5-9: Impact of process control as %stdev in the distributions for both $t_{UF\ 1\text{-}1}$ and $\Delta P_{UF\ 1\text{-}1}$ on the number of *Fr 13* failures (p_2) per 100,000 scenarios in integrated UF-OD membrane global processing of pomegranate juice with a 3 % tolerance

The second option is to change the physical system by reducing $J_{UF\ 1\text{-}1,\ required}$, prior to the juice entering UF membrane unit-operation (Eq. (5.13)).

Thus, repeat simulations were therefore conducted for the range $95 \leq J_{UF\ 1\text{-}1,\ required} \leq 100$, % together with each of stdev = 5, 7, 10 and 15, % in distributions for $t_{UF\ 1\text{-}1}$ and $\Delta P_{UF\ 1\text{-}1}$. One hundred thousand (100,000) r-MC samples were used and the results are visually presented as a 3D surface plot, Fig. 5-10.

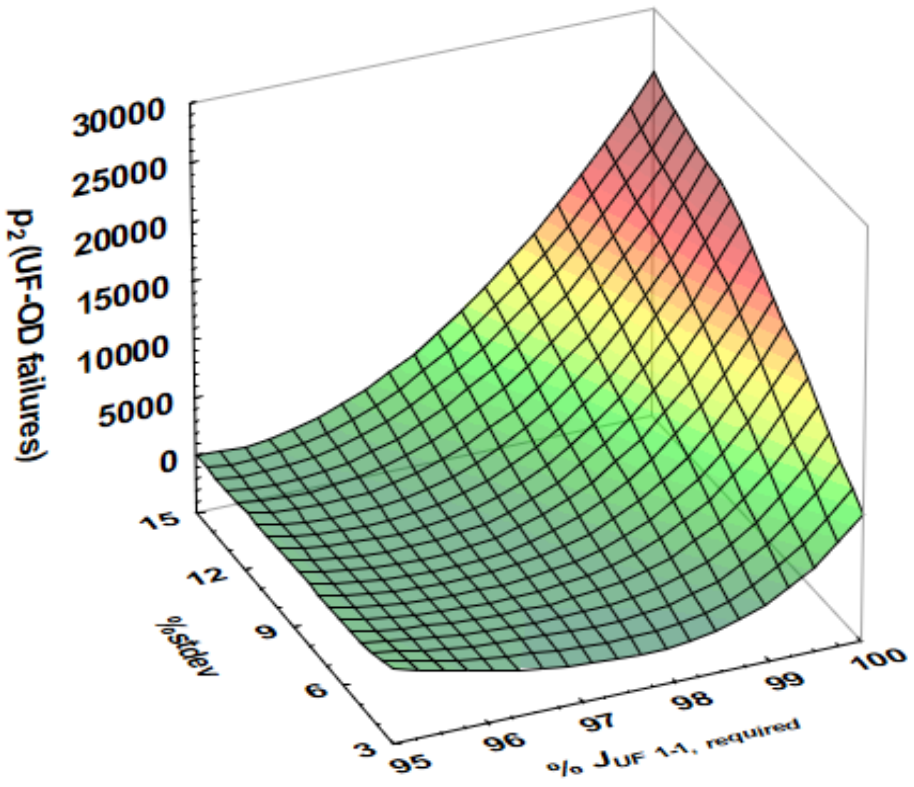

Fig. 5-10: 3D surface plot of the effect of %$J_{UF\ 1\text{-}1,\ required}$ in cross-flow UF clarification on the number of *Fr 13* failures (p_2) per 100,000 scenarios in integrated UF-OD membrane global processing of pomegranate juice with a 3 % tolerance

From the 3D figure it can be seen there is an (apparent) exponential decrease in the number of overall UF-OD failures (p_2) with reduced $J_{UF\ 1\text{-}1,\ required}$ for the pomegranate juice. The figure shows that small reductions in the value of $J_{UF\ 1\text{-}1,\ required}$ (< 3 %) have a highly significant impact. To more quantitatively highlight these impacts, failure data are presented in Table 5-8. From the table, for example, at $J_{UF\ 1\text{-}1,\ required}$ = 6.75 × 10^{-6} m^3 m^{-2} s^{-1} (100 %) and a stdev = 5 % there are 10,461 UF-OD failures, at 98 % $J_{UF\ 1\text{-}1,\ required}$ (6.62 x 10^{-6} m^3 m^{-2} s^{-1}) there would no *Fr 13* failures in the integrated UF-OD membrane global model. Similarly, at 99 % $J_{UF\ 1\text{-}1,\ required}$ (6.68 x 10^{-6} m^3 m^{-2} s^{-1}) and a stdev = 10 %, 8,911 failures would be expected and these would be expected to be reduced to six (6) at 97 % $J_{UF\ 1\text{-}1,\ required}$ (6.55 x 10^{-6} m^3 m^{-2} s^{-1}), per 100,000 scenarios.

Table 5-8: Impact of $\%J_{UF\ 1\text{-}1,\ required}$ and %stdev in UF membrane on the number of failures (p_2) per 100,000 scenarios in the integrated UF-OD membrane global processing of pomegranate juice with a 3 % tolerance

$\%J_{UF\ 1\text{-}1,\ required}$	%stdev			
	5	**7**	**10**	**15**
100	10461	15049	20146	24532
99	0	3198	8911	15677
98	0	10	2134	8362
97	0	0	6	3244
96	0	0	0	295
95	0	0	0	0

Data displayed in Fig. 5-10 and Table 5-8 strongly imply that addition of a process step prior to the UF membrane could be used to significantly reduce vulnerability of the global process and improve process reliability. This reduction in $J_{UF\ 1\text{-}1,\ required}$ could be practically achieved by addition of a carefully selected (and Regulatory acceptable) enzyme to the juice to reduce the number of macromolecules which are more likely to cause fouling of the membrane. Indeed, this has recently been advocated by Domingues et al. (2014) for example. The cost of such a measure is thought to be small for an improved reliability of the integrated UF-OD membrane global treatment of fruit juices.

In fact, this additional step in the schematic is already shown, Fig. 5-1, which otherwise is an adaptation from the literature (Cassano et al., 2011).

To ‘close the loop’ on this two-step *Fr 13* analysis of integrated UF-OD would require significant practical experimental validation studies. These are currently outside the scope of the present work.

However it is contended on the basis of results for the integrated two-step model that the *Fr 13* framework could be successfully developed to include enzymes as an additional step, and iteratively to include all steps shown schematically in Fig. 5-1. A benefit would be an overall, detailed and quantitative new *Fr 13* global risk model for juice processing. This could be used to optimize maintenance of equipment and to act as a counter-balance between capital outlay (capital cost) and maintenance costs.

5.7 Advancing the *Fr 13* framework

5.7.1 Integrated multi-step processes

This integrated two-step application to a mixed membranes process is part of an overall development and investigation of *Fr 13* as a quantitative risk assessment and plant design tool. As neither the impact or accumulation of naturally occurring chance fluctuations in apparent steady-state process parameters is accounted for implicitly in traditional chemical engineering, the *Fr 13* framework advocated here might be further developed to help explain widely acknowledged surprise failures - that otherwise can remain difficult to understand - and be used to minimize these in second-tier studies.

More generally however, unexplained and non-equipment failure data is problematic, as these are not disclosed (publicly at least). Compare this situation for example with the quite vast equipment failure data contained in data bases such as OREDA (2015).

Anecdotal evidence is strong nevertheless (and relatively easy to hear) that surprise failures are very much a part of unremarkable chemicals engineering processing. Due to ever increasing inter-connectedness of product and processing, the impact of such failure outcomes will be compounded, and as acknowledged in the Blackett Review (Anon., 2012) there is a need to develop practical and theoretical tools to anticipate these problems arising.

The demonstration here to quantitatively simulate the possible accumulative effects of chance fluctuations in a steady-state integrated two-step UF-OD membranes operation to identify and minimize potential is therefore a significant step in development of a *Fr 13* framework.

The present research, together with that of Chandrakash et al. (2015) and Chandrakash and Davey (2015) on failure in pasteurization of raw milk, demonstrates the *Fr 13* method can be applied to steady-state global processes. Davey (2010; 2011) proposed such a development - and possible coupling with existing software – although this is yet to be demonstrated.

5.7.2 Time, cost, effort and benefit

Because findings and recommendations of recent work have not been implemented in their respective industries, or if they are implemented the authors are not aware of the outcomes, returns are yet to be confirmed on a large-scale.

However, indications are that the time, cost and effort in applying *Fr 13* is likely to be low, compared with traditional risk assessment methodologies as the latter generally require a large cross-section of stakeholders for a period of at least a full working day.

In contrast, *Fr 13* framework can be conducted in normal design and synthesis stages as it is based on unit-operations, and is likely to be relatively quick and, importantly, widely understandable. It would require minimal man-hours to establish and run as a simulation (a matter of hours). The benefit is a fast turnaround of information regarding key parameters and targeted second-tier process design changes.

In the hierarchy of equipment and facility designs *Fr 13* framework could be used before design is ‘frozen’ in conjunction with traditional risk assessments, and after, with a view to changing the physical system to reduce vulnerability to possible impact of accumulation of fluctuations in parameters.

A major benefit is that it will contribute to a more nuanced understanding of how different outcomes can practically result from apparent steady-state and ‘controlled’ processes.

5.8 Chapter summary and conclusions

1. Results show the *Fr 13* framework is applicable to an integrated, two-step, global process.

2. Application to an integrated two-step UF-OD filtration demonstrated with independent data for pomegranate juice (*Punica granatum*) has shown that membrane fouling can occur in 10.5 % of all operations with a tolerance of 3 %. This translates to a vulnerability to 39 surprise failures each year averaged over the long term. This information cannot be obtained from alternate risk and hazard assessment methods.

3. Most notably, failure in the UF unit-operation does not necessarily lead to a failure in the inter-connected corresponding OD unit-operation.

4. Second-tier simulations highlighted that a reduction in vulnerability to failure could be achieved by 1) an improved process control, to reduce the naturally occurring fluctuations in filtration time, and; 2) the introduction of (Regulatory acceptable) enzymes in an additional process step to limit impact of juice macromolecules on the membrane surface.

CHAPTER 6

CONCLUSIONS AND FUTURE DEVELOPMENT

6.1 Conclusions

The following can be concluded from this research:

1. Because published *Fr 13* applications were (largely) limited to single (i.e. one-step) unit-operations, a research program was undertaken with the aim to advance the *Fr 13* framework to investigate how random fluctuations in apparent steady-state plant parameters can be transmitted and impact in progressively multi-step complex processes. Widely used one- and two-step steady-state membrane processing of fruit juices was selected as a timely and stringent test. Failure of membranes was defined as a permeate flux less than the required (design) operational flux

2. Predictions from a preliminary one-step *Fr 13* analysis, developed for both simplified steady-state dead-end and cross-flow membrane models showed, with independent experimental data for clarification of orange and blood orange juice, 16.8 % of dead-end and 4.0 % of cross-flow filtrations, with an assumed practical tolerance (2 %) will fail unexpectedly, averaged over the long term. If each operation is considered a daily (batch-continuous) filtration then a fouling failure could arise every six (6) and 26 days, respectively. Failures would not be expected to be spaced equally in time however

3. A novel two-step *Fr 13* framework was synthesized for the first time to investigate vulnerability to fouling in a more realistic commercial process of integrated UF-OD for concentration of fruit juice, revealed that integrated UF-OD is expected to be vulnerable to surprise fouling in 10.5 % of all operations, based on extensive independent data for processing pomegranate (*Punica granatum*) juice. This translates to 39 unexpected failures per year with an assumed 3 % tolerance as a design margin of safety

4. In completing this work a significant error in the membrane literature was discovered, corrected and is being addressed

5. To confirm *Fr 13* predictions for the integrated UF-OD, validation trials with new experimentally determined data, are needed. This is outside the scope of the present work however

6. Overall, *Fr 13* simulations of the synthesized models underscored that the three (3) apparent steady-state membrane processes (dead-end, cross-flow and UF-OD) should be more correctly considered a combination of successful and failed operations. This insight is new and cannot be obtained using traditional risk and hazard approaches, with or without sensitivity analyses

7. Second-tier *Fr 13* simulations underscored that reduced vulnerability to membrane fouling could be practically achieved by an improved process control to reduce the random fluctuations in filtration time and addition of an enzymatic treatment step to limit the potential impact of juice macromolecules on the membrane interface

8. It is concluded that the *Fr 13* framework is applicable to an integrated two-step global process. Further, the framework appears generalizable to a range of global steady-state processes of increasing complexity and inter-connectedness. There is no evidence of methodological problems to its advancement. If properly developed, *Fr 13* could provide a new decision tool in both design analysis and synthesis to give new insights and knowledge for understanding of plant process behaviour outcomes

This research is original and not incremental work. Findings will be of immediate interest to researchers in risk analyses and processors and manufacturers of membrane equipment.

6.2 Recommendations for future research

Importantly, the success of this research shows that the *Fr 13* risk framework can, in principle, be applied to assess and be used to minimize risk in a range of global steady-state processes of increasing complexity and inter-connectedness. For example, based on the methodology demonstrated, there is an opportunity to advance and test the *Fr 13* framework for three-step membranes processing i.e. enzymatic pre-treatment, cross-flow ultrafiltration and osmotic distillation.

Further, given the success of this work, it is being planned that *Fr 13* be applied to a generic chemical engineering unit-operations process. A generic unit-operations process can be considered to be one involving each of at least one feed(s) stream, reactor, separator, product, recycle and purge stream. This work is currently in preparation (Davey, 2015 b), where preliminary results indicate a counter-intuitive picture of apparent steady-state processing (and the need for handling increasingly large data sets). It is hoped new insights and knowledge will result that are not available from alternate risk approaches.

The proper and careful advancement of the framework appears to offer real benefits that include an improved knowledge and understanding for practical re-design for a reduced risks processing. The work will continue to be of interest to a range of design engineers and operators of a range of unit-operations.

It is recommended the framework be tested for coupled with existing software (e.g. Aspen Plus® and Batch Process Developer®) to produce a more powerful design and assessment tool for enhanced designs and improved process outcomes in the foods and chemical industries.

APPENDICES

APPENDICES A - F

APPENDIX A – A definition of some important terms used in this research

Cake layer	The particles or macro-molecules formed on membrane interface as a filtration barrier and shaped like a cake layer
Failure	The number of failed scenarios which the actual operational flux do not achieve the required flux for successful membrane processing
Failure modeling	Structured risk technology based on established unit-operations used to estimate and analyze the likelihood of unexpected failures in steady-state unit-operation and process
Friday 13th syndrome	Event defined where adverse outcomes combine to result a failure of plans and opportunities despite all good design and operation as defined by Davey and Cerf, 2003
Fr 13 simulation	Novel, probabilistic simulation for a predicted model output with probability distribution of values as inputs (developed by Davey and Cerf, 2003)
MF	Microfiltration with membrane pore size from 0.1-5 µm; and applied driven pressure ranges from 1-10 bar
Membrane	A filter structured with selective thin layer functioning as a barrier for substances and macromolecules
Membrane fouling	Blockage of membranes, caused by accumulation of rejected materials on the membrane interface or inside pores
OD	Osmotic distillation based on application of porous hydrophobic membranes for concentrated liquid
Probability	A numeric measure of the likelihood of a particular outcome of a stochastic process scenario
Permeate flux	Transmembrane volumetric flux rate during the membrane operations
Iterative Random-impacts Assessment (IRA)	An alternative terminology to *Fr 13* as suggested by Zou and Davey (2015)
Required flux	Required (design) operational flux value for a successful membrane operation, based on the practical industrial data or extensive membrane experiments

Retentate flux	Materials or fluids restricted by membranes during membrane operations
Single Value Assessment	Traditional, deterministic model solution for a predicted model output with single value inputs as defined by Davey and Cerf, 2003; Sinnott, 2005
UF	Ultrafiltration with membrane pore size from 1-100 nm and applied driven pressure ranges from 1-10 bar
Uncertainty	Lack of knowledge, or level of ignorance about parameters that characterize the physical or process system being modelled. Uncertainty is sometimes reducible through further measurement, carefully study, or consulting more experts (Vose, 2008)
Unit-operation	A basic step in process involving physical change or chemical transformation taking place e.g. separation, evaporation, heating, distillation, etc.
Variability	The effect of chance and a function of the system. Variability is not reducible through either further measurement or study, but might be reduced by changing or controlling the physical system (Vose, 2008)

APPENDIX B - Fish bone diagram for *Fr 13* simulation of integrated UF-OD membrane global model for pomegranate juice

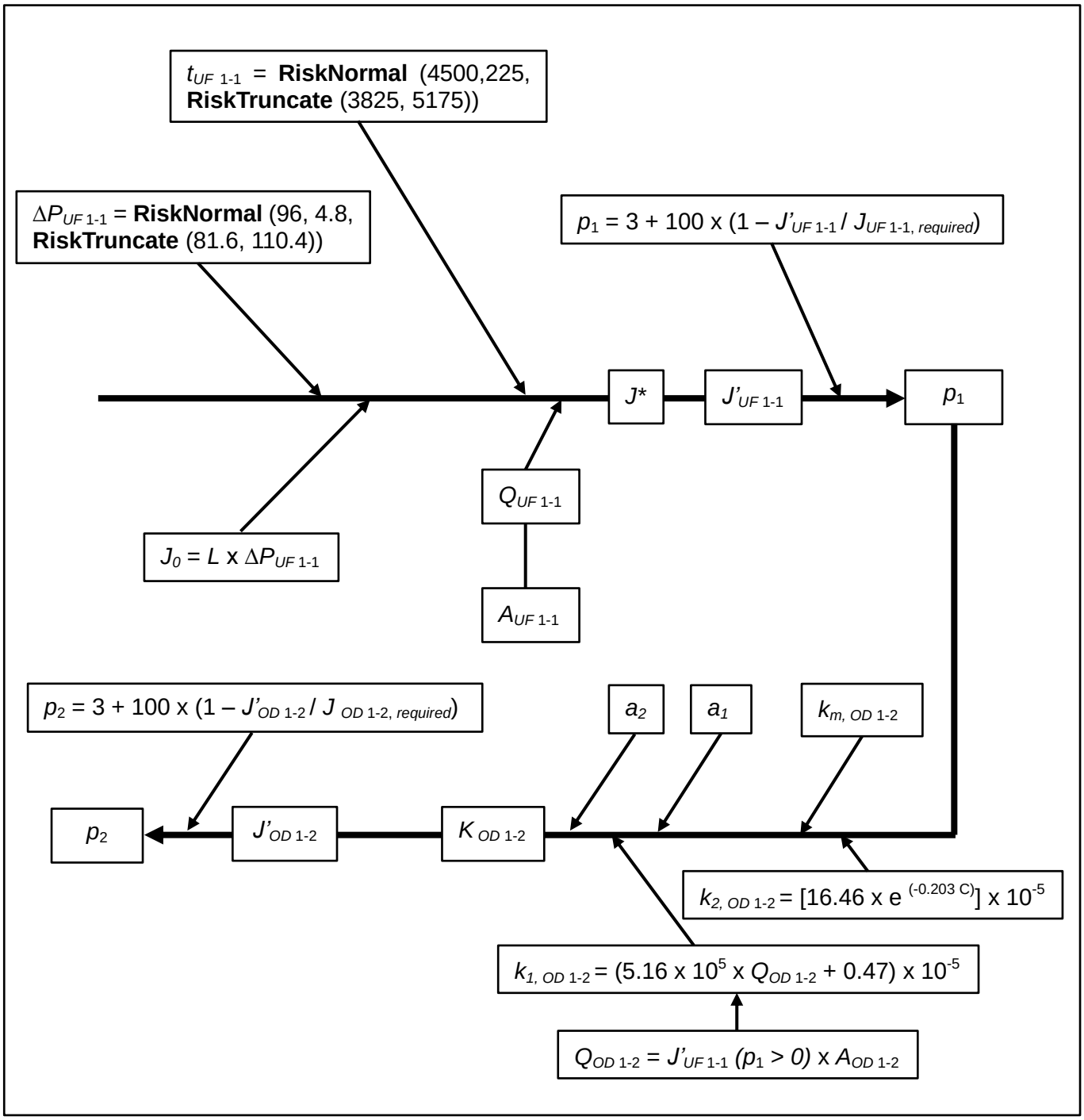

Fig. B-1: Fish bone diagram[13] for the steady-state, integrated two-step membrane global model for concentration of pomegranate juice (*see* discussion in Chapter 5, pp. 74ff)

[13] Also titled an Ishikawa diagram (after Kaoru Ishikawa, 1968).

APPENDIX C - Correcting the literature – Letter to Editor

Dear Sir,

Food Engineering Reviews 3: 136-158 (2011)

http://dx.doi.org/10.1007/s12393-011-9042-8

Fruit juice processing and membrane technology application

20 A P, Torras C, Pagan J, Ibarz A

We are very interested in modelling of unit-operations in foods processing and read with much interest the review paper 'Fruit juice processing and membrane technology application' by Echavarria et al. (2011) in Food Engineering Reviews 3: 136-158 (2011).

The determination of data for application of membrane technology to fruit juice processing is a problem of great practical and theoretical importance.

We have published extensively over > 30 years[1] in engineering foods journals and our work has been widely reviewed and cited e.g. [2,3]. We are particularly interested at present in membranes processing, predominantly fouling failures[4].

---

[1] Davey K R, Chandrakash S, O'Neill, B K (2015) Friday 13th failure assessment of clean-in-place removal of whey protein deposits from metal surfaces with auto-set cleaning times. Chemical Engineering Science 126: 106-115. http://dx.doi.org/10.1016/j.ces.2014.12.013

Davey K R (2015) Development and illustration of a computationally convenient App for simulation of transient cooling of fish in ice slurry at sea. LWT - Food Science and Technology 60: 308-314. http://dx.doi.org/10.1016/j.lwt.2014.08.022

Abdul-Halim N, Davey K R (2015) A Friday 13th risk assessment of failure of ultraviolet irradiation for potable water in turbulent flow. Food Control 50: 770-777. http://dx.doi.org/10.1016/j.foodcont.2014.10.036

Davey K R (2012) Calculating quantities of ice for cooling and maintenance of freshly harvested fish at sea. Journal of Food Science 77 (11): e335-341. http://dx.doi.org/10.1111/j.1750-3841.2012.02963.x

Davey K R, Lin S H, Wood D G (1978) The effect of pH on continuous high-temperature short-time sterilization of liquid. American Institute of Chemical Engineers Journal 24 (3): 537-540. http://dx.doi.org/10.1002/aic.690240322

[2] Pujol L, Albert I, Magras, C, Johnson, N B, Membre J M (2015) Probabilistic exposure assessment model to estimate aseptic-UHT product failure rate. International Journal of Food Microbiology 192: 124–141. http://dx.doi.org/10.1016/j.ijfoodmicro.2014.09.023

Pujol L, Albert I, Johnson N B, Membre J M (2013) Potential application of quantitative microbiological risk assessment techniques to an aseptic-UHT process in the food industry. International Journal of Food Microbiology 162 (3): 283– 96. http://dx.doi.org/10.1016/j.ijfoodmicro.2013.01.021

Daneshmand T N, Beton R, Hill R J, Gehr R, Frigon D (2012) Inactivation mechanisms of bacterial pathogen indicators during electro-dewatering of activated sludge biosolids. Water Research 46 (13): 3999–4008. http://dx.doi.org/10.1016/j.watres.2012.05.009

Munoz-Cuevas M, Metris A, Baranyi J (2012) Predictive modelling of Salmonella: From cell cycle measurements to e-models. Food Research International 45 (2): 852– 62. http://dx.doi.org/10.1016/j.foodres.2011.04.033

Black D G, Ye X P, Harte F, Davidson P M (2010) Thermal inactivation of *Escherichia coli* O157:H7 when grown statically or continuously in a chemostat. Journal of Food Protection 73 (11): 2018–2024.

Kang K A, Kim Y W, Yoon K S (2010) Development of predictive growth models for *Staphylococcus aureus* and *Bacillus cereus* on various food matrices consisting of Ready-to-Eat (RTE) foods. Korean Journal of Food Science and Animal Resources 30 (5): 730–738. ISSN 2234-246X

Huang L, Hwang A, Phillips J (2011) Effect of temperature on microbial growth rate-mathematical analysis: The Arrhenius and Eyring-Polanyi Connections. Journal of Food Science 76 (8): E553–E560. http://dx.doi.org/10.1111/j.1750-3841.2011.02377.x

Chavan R S, Chavan S R, Khedkar C D, Jana A H (2011) UHT milk processing and effect of plasmin activity on shelf life: A review. Comprehensive Reviews in Food Science and Food Safety 10 (5): 251–268. http://dx.doi.org/10.1111/j.1541-4337.2011.00157.x

[3] and also

Deeth H (2010) Improving UHT processing and UHT milk products. In: M. W. Griffiths (ed) Improving the safety and quality of milk, Vol 1: Milk production and processing (pp. 302 – 329). Woodhead Publishing Ltd, Cambridge, UK. ISBN 978-1-85573-676-4

Ross T, Dalgaard P (2004) Secondary models. In: R. C. McKellar & X. Lu (eds) Modeling microbial responses in food (pp. 90 – 91, 138 ff). CRC Press, Florida, USA. ISBN 084931237X

McMeekin T A, Olley J N, Ross T, Ratkowsky D A (1993) Predictive Microbiology – theory and application (pp. 12, 25, 62,106, 108, 130, 134, 166, 172, 174, 179-181, 189, 274). Research Studies Press, Taunton, UK. ISBN 0863801323

We acknowledge review articles are very valuable in the discipline and generate interest not just in coverage and content, but also in critical assessment of the ideas and argument; they are often heavily relied on.

We wish to draw attention therefore to the following:

Eq. (5), p 148, of the Echavarria et al. article where the deionized water flux, J_0, that corresponds to the flux of an un-fouled membrane, is defined as

$$J_0 = \frac{\eta_T}{\eta_{20^oC}} . \frac{Q}{A.\Delta P}$$

It is incorrect. Careful study will show it is not possible to reconcile the form or units in engineering.

Firstly, this flux must of course increase with increasing transmembrane pressure difference (ΔP) not decrease as shown by the equation.

Secondly, the units of flux are quantity per unit area per unit time. Widely used units are L m^{-2} h^{-1} as reviewed (or perhaps more strictly these should be m^3 m^{-2} s^{-1}). The units obtained from Eq. (5) are actually m^3 m^{-2} s^{-1} Pa^{-1} and are not a flux. (Perhaps a quick comparison with Darcy's law – shown as Eq. (8) in the Echavarria et al. article - will help underscore this important point).

Thirdly, Eq. (7) of the article, describing the flux reduction (*FR*) with regard to the clean water flux,

$$FR_{CWF} = \frac{J_{ob} - J_{oa}}{J_{ob}} .100\%$$

cannot not be logically consistent with this defined set of units from Eq. (5). The numerator units for flux must of course be identical for the difference mathematical operation.

Because this equation is widely incorrectly defined elsewhere e.g. Schafer et al. (2005) and Boerlage et al. (2002), both of which are cited in the Echavarria et al. article, we conclude it is not a typographical error.

Lastly, we feel a Nomenclature, together with units and the equation number where the symbol is first used can help the Reader, and act as a natural check for the Writer on the units and consistency of form of important equations.

We write therefore to ask that these points be addressed by the authors in this important food engineering journal.

K R (Ken) Davey

PhD FAIFST FIChemE FIEAust CEng CPEng CSci

W Zou

ME (Chem)

School of Chemical Engineering

The University of Adelaide, SA, 5005

Australia

---

[4] Zou W (2015) Development of a *Fr 13* risk framework - application to one-and two-step steady-state membrane processing of fruit juices. MPhil Research Thesis, The University of Adelaide, Australia - *in prepn*.

Zou W, Davey K R (2015) An integrated two-step *Fr 13* synthesis - demonstrated with membrane fouling in combined ultrafiltration-osmotic distillation (UF-OD) for concentrated juice. *Chemical Engineering Science - in prepn*.

References

Boerlage, S. F. E., Kennedy, M. D., Dickson, M. R., El-Hodali, D. E. Y., Schippers, J. C., 2002. The modified fouling index using ultrafiltration membranes (MFI-UF): Characterisation, filtration mechanisms and proposed reference membrane. Journal of Membrane Science 197: 1-21. http://dx.doi.org/10.1016/S0376-7388(01)00618-4

Echavarria, A.P., Torras, C., Pagan, J., Ibarz, A., 2011. Fruit juice processing and membrane technology application. Food Engineering Reviews 3: 136-158. http://dx.doi.org/10.1007/s12393-011-9042-8

Schafer A. I., Andritsos N., Karabelas A. J., Hoek E. M., Schneider R., Nystrom M., 2005. Fouling in nanofiltration. In: A. I. Schafer, T D Waite A G Fane (eds) Nanofiltration - principles and applications. Elsevier, UK, pp. 169-239. ISBN: 1856174050

END OF PAPER

APPENDIX D - Refereed publications from this research

1. Zou, W., Davey, K.R., 2014 a. A Friday 13th risk model for failure in cross-flow membrane filtration of passion fruit juice. In: Proc. 26th European Modelling and Simulation Symposium-EMSS 2014. Sept. 10-12, Bordeaux, France, paper 106. ISBN: 9788897999447

2. Zou, W., Davey, K.R., 2014 b. A novel Friday 13th stochastic assessment of failure of membrane filtration in juice clarification. In Proc. 44th Australasian Chemical Engineering Conference (Processing Excellence, Powering our future)-CHEMECA 2014. Sept. 27 – Oct. 1, Perth, Australia, paper No. 1259. ISBN/ISSN: 1922107387

3. Davey, K.R., Zou, W., 2015. Fruit juice processing and membrane technology application (*sic*) – A response. Food Eng. Rev. – submitted Oct.

4. Zou, W., Davey, K.R., 2015. An integrated two-step *Fr 13* synthesis - demonstrated with membrane fouling in combined ultrafiltration-osmotic distillation (UF-OD) for concentrated juice. Chem. Eng. Sci. – submitted Nov.

APPENDIX E - A detailed solution to the model synthesis of integrated UF-OD

THE UNIVERSITY OF ADELAIDE
ENGINEERING DESIGN CALCULATIONS

Date		Job No.	Sheet
Scale			
DRG-N BY			
Checked			

a. UF clarification

① Single values of process parameters

$\Delta P = 96\ kPa$ $\quad J^* = 5.62 \times 10^{-6}\ m^3 m^{-2} s^{-1}$

$t = 4500\ s$ $\quad J_{required} = 6.75 \times 10^{-6}\ m^3 m^{-2} s^{-1}$

$k_o = 5.7 \times 10^6\ s\,m^{-2}$

② Cross-flow filtration model

a. $$k_o t = \frac{1}{J^{*2}}\left[\ln\left(\frac{J'}{J_o}\cdot\frac{(J_o - J^*)}{(J' - J^*)}\right) - J^*\cdot\left(\frac{1}{J'} - \frac{1}{J^o}\right)\right] \quad (5.2)$$

b. $$J_o = L\cdot\Delta P \quad (5.3)$$

$$L = 655.6\ L\,m^{-2}h^{-1}bar^{-1}$$

$$J_o = L\cdot\Delta P = 1.821\times10^{-6}\ m^3 m^{-2} s^{-1} kPa^{-1} \times 96\ kPa = 174.816\ m^3 m^{-2} s^{-1}$$

$$\frac{L}{m^2\cdot h\cdot bar} = \frac{L}{m^2\cdot h\cdot bar}\cdot\frac{h}{3600\,s}\cdot\frac{bar}{100\,kPa}\cdot\frac{m^3}{1000\,L} = \frac{m^3}{m^2\cdot s\cdot kPa}\cdot\frac{1}{3.6\times10^8}$$

$$\longrightarrow L = 655.6\ L\,m^{-2}h^{-1}bar^{-1} = 1.821\times10^{-6}\ m^3 m^{-2} s^{-1} kPa^{-1}$$

Substitution of (5.3) into (5.2)

③ $$k_o t = \frac{1}{J^{*2}}\left[\ln\left(\frac{J'}{\Delta P\cdot L}\cdot\frac{L\cdot\Delta P - J^*}{J' - J^*}\right) - J^*\cdot\left(\frac{1}{J'} - \frac{1}{L\cdot\Delta P}\right)\right]$$

$$5.7\times10^6\times4500 = \frac{1}{(5.62\times10^{-6})^2}\left[\ln\left(\frac{J'}{174.816\times10^{-6}}\times\frac{(174.816-5.62)\times10^{-6}}{(J'-5.62\times10^{-6})}\right) - 5.62\times10^{-6}\times\left(\frac{1}{J'} - \frac{1}{174.816\times10^{-6}}\right)\right.$$

$$0.81014 + \frac{5.62\times10^{-6}}{J'} - 0.032 = \ln\left(\frac{J'}{174.816\times10^{-6}}\times\frac{169.196\times10^{-6}}{J'-5.62\times10^{-6}}\right)$$

$$e^{\wedge}\left(0.7784 + \frac{5.62\times10^{-6}}{J'}\right) = \left(\frac{0.9679\times J'}{J'-5.62\times10^{-6}}\right)$$

THE UNIVERSITY OF ADELAIDE
ENGINEERING DESIGN CALCULATIONS

Date		Job No.	Sheet
Scale			
DRG-N BY			
Checked			

For SVA:

$J' = 7.0215 \times 10^{-6} m^3 m^{-2} s^{-1} \approx 7.02 \times 10^{-6} m^3 m^{-2} s^{-1}$

④ Mathematical expression for Fr 13 Simulation:

Substitution for $J_0 = L \cdot \Delta P$ into (5.2) gives:

$$0.00018t = \ln\left(\frac{J'}{L\cdot\Delta P}\cdot\frac{(L\cdot\Delta P)-J^*}{(J'-5.62\times10^{-6})}\right) - 5.62\times10^{-6}\left(\frac{1}{J'}-\frac{1}{L\cdot\Delta P}\right)$$

$$0.00018t = \ln\left(\frac{J'}{1.821\times10^{-6}\Delta P}\cdot\frac{1.821\times10^{-6}\Delta P-5.62\times10^{-6}}{J'-5.62\times10^{-6}}\right) - \frac{5.62\times10^{-6}}{J'} + \frac{5.62\times10^{-6}}{1.821\times10^{-6}\Delta P}$$

$$0.00018t + \frac{5.62\times10^{-6}}{J'} - \frac{3.0862}{\Delta P} = \ln\left(\frac{J'\cdot(1.821\Delta P-5.62)}{1.821\Delta P(J'-5.62\times10^{-6})}\right)$$

$$e^{\wedge}\left(0.00018t + \frac{5.62\times10^{-6}}{J'} - \frac{3.0862}{\Delta P}\right) = \frac{J'\cdot(1.821\Delta P-5.62)}{1.821\Delta P(J'-5.62\times10^{-6})}$$

This equation can be simplified using Matlab or the Software (equation slover)

★

$$J' = \frac{1.13927\times10^{6}\cdot e^{\wedge}(0.00018\cdot t)\cdot\Delta P}{(2.0271\times10^{11}\cdot e^{\wedge}(0.00018t)\cdot\Delta P)-(9.105\times10^{10}\cdot e^{\wedge}(\frac{3.0862}{\Delta P})\cdot\Delta P)+(2.81\times10^{11}\cdot e^{\wedge}(\frac{3.0862}{\Delta P}))}$$

This mathematical expression is used for Fr 13 Simulation.

THE UNIVERSITY OF ADELAIDE
ENGINEERING DESIGN CALCULATIONS

Date		Job No.	Sheet
Scale			
DRG-N BY			
Checked			

b. OD Concentration

① Single Values of process parameters

$A = 1.4\ m^2$

$C_1(CaCl_2) = 8.7\ mol \cdot L^{-1}$ $M = 111\ g \cdot mol^{-1}$; $C_2(CaCl_2) = C_1 \cdot M = 965.79\ kg \cdot L^{-1}$ $C_3(CaCl_2) = C_1 / C_2 = 9.02\ mol\ kg^{-1}$

$P^* = 3.169\ kPa\ (25°C) = 3169\ Pa$ $d_p = 0.2\ um = 0.0000002\ m$

$T = 25°C = 298\ K$ $\delta = 0.000175\ m$

$M_W = 0.018\ kg \cdot mol^{-1}$ $\tau = 2$

$\Delta P = 40000\ Pa$ $\varepsilon = 0.75$

$R = 8.314\ J\ mol^{-1} K^{-1}$ $a_2 = 0.847$; $a_1 = 0.95$

② Synthesis of the equation:

a. $K_1 = [5.16 \times 10^5 (J'_{UF} \cdot A) + 0.47] \times 10^{-5}$

b. $K_2 = [16.46 \cdot e^{\wedge}(-0.203 \cdot C)] \times 10^{-5}$

$= [16.46 \cdot e^{\wedge}(-0.203 \times 9.02)] \times 10^{-5} = 2.638 \times 10^{-5}\ m\ s^{-1}$

c. $K_m = 3169 \times \frac{1.8 \times 10^{-5}}{R \cdot T \cdot \delta} \cdot \left(\frac{3\tau}{\varepsilon d_p \sqrt{8RT/\pi M_W}} + \frac{\Delta P \tau}{\varepsilon (4.46 \times 10^{-6} \cdot T^{2.334}} \right)^{-1}$

$= 3169 \times 4.15153 \times 10^{-5} \times (0.068 \times 10^6 + 40160.6) = 1.2164 \times 10^{-6} \approx 1.22 \times 10^{-6}\ m\ s^{-1}$

$K_{OD} = \left(\frac{1}{K_1} + \frac{1}{K_2} + \frac{1}{K_m} \right) = \left\{ [5.16 \times 10^5 \cdot (J'_{UF} \cdot A) + 0.47] \times 10^{-5} \right\}^{-1} + 0.379 \times 10^5 + 0.82 \times 10^6$

$J_{OD} = (a_1 - a_2) \cdot K_{OD}$

$$J_{OD} = \left[(7.224 \times J_{UF} + 0.47 \times 10^{-5})^{-1} + 8.579 \times 10^5 \right]^{-1} \times 0.102$$

used for F_T 13 Simulation in UF-OD

APPENDIX F - A detailed simulation data of a *Fr 13* risk assessment of integrated UF-OD

Table F-1: Summary comparison of SVA and *Fr 13* simulation of cross-flow UF with a 3 % tolerance

Parameters	SVA	*Fr 13*	Distribution & Formulas
ΔP (kPa)	96	**97.42**	**RiskNormal** (96, 4.8, **RiskTruncate** (81.6, 110.4))
t (s)	4500	**4904.10**	**RiskNormal** (4500, 225, **RiskTruncate** (3825, 5175))
T (^{o}C)	25	25	
L ($m^3\ m^{-2}\ s^{-1}\ kPa^{-1}$)	1.82E-06	1.82E-06	
k_0 ($s\ m^{-2}$)	5.70E+06	5.70E+06	
J^* ($m^3 m^{-2} s^{-1}$)	5.62E-06	5.62E-06	
$J_{required}$ ($m^3\ m^{-2}\ s^{-1}$)	6.75E-06	6.75E-06	
J' ($m^3\ m^{-2}\ s^{-1}$)	7.02238E-06	6.902E-06	Eq. (5.4)
p_1 (risk factor)	-1.04E+00	**0.754**	Eq. (5.13)

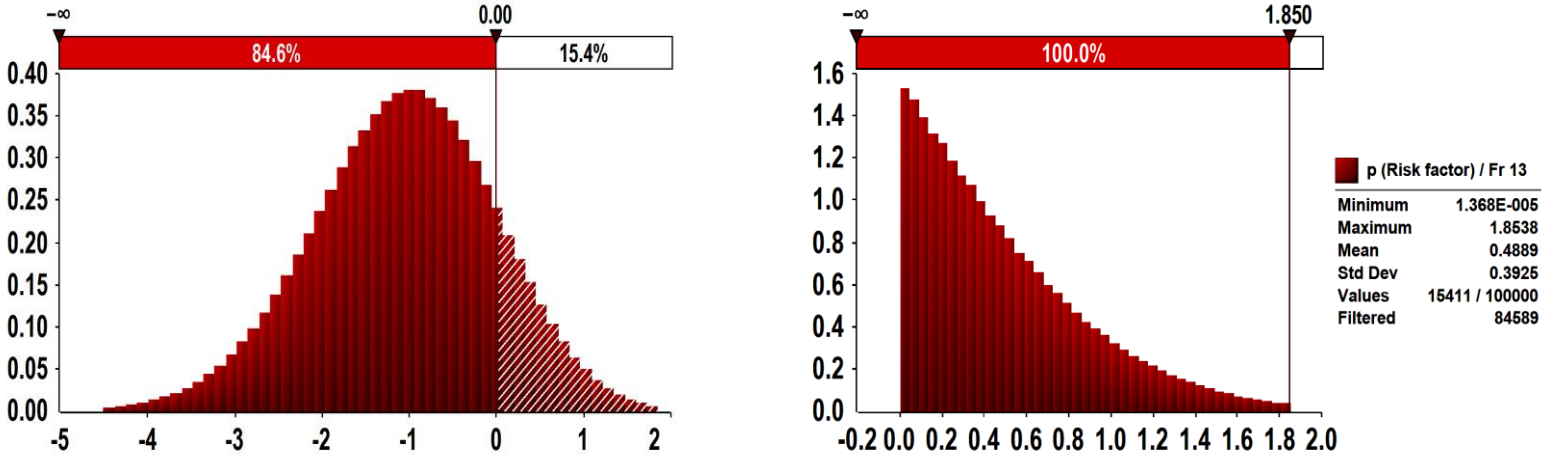

Table F-2: Simulation data of *Fr 13* analysis of integrated UF-OD (selected 10 scenarios are colored 'grey')

Index	$\Delta P_{UF\ 1\text{-}1}$	$t_{UF\ 1\text{-}1}$	$J'_{UF\ 1\text{-}1}$	$Q_{OD\ 1\text{-}2}$	$J'_{OD\ 1\text{-}2}$	$J'_{OD\ 1\text{-}2,\ required}$	p_1	p_2
1	92.0179728	4761.74315	6.94258E-06	9.71961E-06	1.16649E-07	1.1325E-07	0.146977	-0.001582
2	100.987327	4754.40541	6.9449E-06	9.72286E-06	1.1665E-07	1.1325E-07	0.112584	-0.002237
3	105.338163	4815.50192	6.9271E-06	9.69794E-06	1.16644E-07	1.1325E-07	0.376256	0.0027949
4	97.6822151	4800.81525	6.93125E-06	9.70375E-06	1.16646E-07	1.1325E-07	0.314764	0.0016193
5	99.5708395	4736.52386	6.95016E-06	9.73022E-06	1.16652E-07	1.1325E-07	0.034665	-0.003720
6	94.8332104	4742.2862	6.94837E-06	9.72772E-06	1.16651E-07	1.1325E-07	0.061159	-0.003216
7	102.202608	4944.81811	6.89019E-06	9.64626E-06	1.16632E-07	1.1325E-07	0.923132	0.0133062
8	93.9323584	4737.7636	6.94969E-06	9.72957E-06	1.16652E-07	1.1325E-07	0.041597	-0.003588
9	100.582764	4823.5916	6.92469E-06	9.69457E-06	1.16644E-07	1.1325E-07	0.411995	0.0034788
10	85.1995676	4816.87365	6.92633E-06	9.69686E-06	1.16644E-07	1.1325E-07	0.387746	0.0030147
11	104.166264	5156.53334	6.83247E-06	9.56546E-06	1.16614E-07	1.1325E-07	1.778168	0.0299438
12	91.7509469	4778.57721	6.93763E-06	9.71269E-06	1.16648E-07	1.1325E-07	0.22024	-0.000185
13	94.0003372	4889.40158	6.9057E-06	9.66798E-06	1.16637E-07	1.1325E-07	0.693334	0.0088771
14	97.4191395	4904.10446	6.90159E-06	9.66222E-06	1.16636E-07	1.1325E-07	0.754261	0.0100496
15	98.0074017	4893.6288	6.90457E-06	9.6664E-06	1.16637E-07	1.1325E-07	0.710090	0.0091994
16	98.973307	4789.6122	6.93454E-06	9.70836E-06	1.16647E-07	1.1325E-07	0.266058	0.0006890
17	97.5898641	4752.85374	6.9453E-06	9.72342E-06	1.1665E-07	1.1325E-07	0.106637	-0.002350
18	95.20284	4892.57868	6.90482E-06	9.66675E-06	1.16637E-07	1.1325E-07	0.706386	0.0091282
19	102.949158	4987.89691	6.87819E-06	9.62947E-06	1.16629E-07	1.1325E-07	1.100868	0.0167441
20	93.5246678	4760.97159	6.94284E-06	9.71997E-06	1.16649E-07	1.1325E-07	0.143165	-0.001655
21	102.425694	5009.91573	6.8721E-06	9.62094E-06	1.16627E-07	1.1325E-07	1.191133	0.0184941

Index	$\Delta P_{UF\ 1\text{-}1}$	$t_{UF\ 1\text{-}1}$	$J'_{UF\ 1\text{-}1}$	$Q_{OD\ 1\text{-}2}$	$J'_{OD\ 1\text{-}2}$	$J'_{OD\ 1\text{-}2,\ required}$	p_1	p_2
22	94.5640871	4917.52686	6.89774E-06	9.65684E-06	1.16635E-07	1.1325E-07	0.811233	0.0111472
23	93.5050097	4829.07247	6.92298E-06	9.69218E-06	1.16643E-07	1.1325E-07	0.437291	0.0039631
24	102.179002	4819.28516	6.92596E-06	9.69635E-06	1.16644E-07	1.1325E-07	0.393165	0.0031184
25	98.5501017	4839.63607	6.92003E-06	9.68804E-06	1.16642E-07	1.1325E-07	0.48111	0.0048025
26	96.8996679	4865.80424	6.91248E-06	9.67748E-06	1.1664E-07	1.1325E-07	0.592839	0.0069458
27	93.3582967	4930.78936	6.89398E-06	9.65157E-06	1.16634E-07	1.1325E-07	0.866931	0.0122213
28	97.4105138	5007.08938	6.8728E-06	9.62192E-06	1.16627E-07	1.1325E-07	1.180713	0.018292
29	101.833125	4908.08448	6.90053E-06	9.66074E-06	1.16636E-07	1.1325E-07	0.769932	0.0103514
30	94.7646219	4782.10055	6.93666E-06	9.71133E-06	1.16647E-07	1.1325E-07	0.234633	8.92E-05
31	99.4595668	4774.07027	6.9391E-06	9.71473E-06	1.16648E-07	1.1325E-07	0.198577	-0.000599
32	88.6320203	4785.81043	6.93545E-06	9.70963E-06	1.16647E-07	1.1325E-07	0.252593	0.0004319
33	93.2347355	4838.24968	6.92033E-06	9.68846E-06	1.16642E-07	1.1325E-07	0.476601	0.0047161
34	81.8281969	4821.13261	6.925E-06	9.695E-06	1.16644E-07	1.1325E-07	0.407385	0.0033906
35	101.595068	4746.68331	6.94719E-06	9.72606E-06	1.16651E-07	1.1325E-07	0.078695	-0.002882
36	100.134007	4775.41417	6.93871E-06	9.7142E-06	1.16648E-07	1.1325E-07	0.204252	-0.00049
37	85.5757694	4852.72423	6.916E-06	9.68239E-06	1.16641E-07	1.1325E-07	0.540796	0.0059469
38	96.5258736	4743.27623	6.94811E-06	9.72735E-06	1.16651E-07	1.1325E-07	0.065032	-0.003142
39	97.0285568	4888.36696	6.90605E-06	9.66847E-06	1.16638E-07	1.1325E-07	0.688173	0.0087778
40	87.6766304	4786.06106	6.93535E-06	9.7095E-06	1.16647E-07	1.1325E-07	0.254009	0.000459
41	94.7106883	4946.30854	6.88965E-06	9.64551E-06	1.16632E-07	1.1325E-07	0.931106	0.0134602
42	92.880799	4765.4958	6.94149E-06	9.71809E-06	1.16649E-07	1.1325E-07	0.163059	-0.001276
43	104.390683	4753.34339	6.94526E-06	9.72337E-06	1.1665E-07	1.1325E-07	0.107197	-0.00234
44	98.6976718	5090.35396	6.85011E-06	9.59015E-06	1.16619E-07	1.1325E-07	1.516941	0.0248342
45	101.003738	4761.87927	6.9427E-06	9.71978E-06	1.16649E-07	1.1325E-07	0.145179	-0.001616
46	93.3308509	4732.10738	6.95136E-06	9.7319E-06	1.16652E-07	1.1325E-07	0.016954	-0.004057

Index	$\Delta P_{UF\ 1\text{-}1}$	$t_{UF\ 1\text{-}1}$	$J'_{UF\ 1\text{-}1}$	$Q_{OD\ 1\text{-}2}$	$J'_{OD\ 1\text{-}2}$	$J'_{OD\ 1\text{-}2,\ required}$	p_1	p_2
47	90.7883557	4760.90882	6.9428E-06	9.71992E-06	1.16649E-07	1.1325E-07	0.143726	-0.001644
48	107.006272	4837.58168	6.92074E-06	9.68904E-06	1.16642E-07	1.1325E-07	0.470517	0.0045995
49	91.4137342	4843.16697	6.91888E-06	9.68643E-06	1.16642E-07	1.1325E-07	0.498124	0.0051286
50	99.5263016	4764.82172	6.94181E-06	9.71854E-06	1.16649E-07	1.1325E-07	0.158343	-0.001366
51	91.7892295	4783.00072	6.93634E-06	9.71088E-06	1.16647E-07	1.1325E-07	0.239404	0.0001802
52	94.4507925	4883.30323	6.90744E-06	9.67042E-06	1.16638E-07	1.1325E-07	0.667498	0.0083802
53	97.2916567	4800.30862	6.93139E-06	9.70395E-06	1.16646E-07	1.1325E-07	0.312678	0.0015794
54	90.2758677	4736.02397	6.95013E-06	9.73018E-06	1.16652E-07	1.1325E-07	0.035093	-0.003712
55	98.0500124	4939.11276	6.89173E-06	9.64842E-06	1.16633E-07	1.1325E-07	0.900362	0.0128665
56	89.5302184	4920.56152	6.89679E-06	9.6555E-06	1.16635E-07	1.1325E-07	0.825398	0.0114203
57	93.1739369	4804.34971	6.93014E-06	9.7022E-06	1.16645E-07	1.1325E-07	0.331223	0.0019338
58	96.6509873	4940.55866	6.8913E-06	9.64782E-06	1.16633E-07	1.1325E-07	0.906718	0.0129892
59	88.1617989	4921.86445	6.89639E-06	9.65494E-06	1.16634E-07	1.1325E-07	0.831288	0.0115338
60	99.7982883	4783.43778	6.93636E-06	9.7109E-06	1.16647E-07	1.1325E-07	0.239131	0.0001750
61	97.1267667	4911.42396	6.89951E-06	9.65932E-06	1.16635E-07	1.1325E-07	0.785023	0.0106421
62	91.6397752	4973.41819	6.88202E-06	9.63483E-06	1.1663E-07	1.1325E-07	1.044087	0.0156446
63	91.5578801	4749.1131	6.94629E-06	9.72481E-06	1.1665E-07	1.1325E-07	0.092000	-0.002629
64	90.8938834	4745.88059	6.94723E-06	9.72612E-06	1.16651E-07	1.1325E-07	0.078073	-0.002894
65	93.4605158	4923.44778	6.89605E-06	9.65447E-06	1.16634E-07	1.1325E-07	0.836278	0.0116301
66	95.7171889	4849.6985	6.91708E-06	9.68391E-06	1.16641E-07	1.1325E-07	0.524726	0.0056387
67	98.2590207	5030.00946	6.86651E-06	9.61312E-06	1.16625E-07	1.1325E-07	1.273873	0.0201008
68	93.6761052	4758.49167	6.94357E-06	9.721E-06	1.1665E-07	1.1325E-07	0.132310	-0.001862
69	101.964411	4959.32178	6.88613E-06	9.64058E-06	1.16631E-07	1.1325E-07	0.983298	0.0144687

Index	$\Delta P_{UF\ 1\text{-}1}$	$t_{UF\ 1\text{-}1}$	$J'_{UF\ 1\text{-}1}$	$Q_{OD\ 1\text{-}2}$	$J'_{OD\ 1\text{-}2}$	$J'_{OD\ 1\text{-}2,\ required}$	p_1	p_2
70	102.895394	4891.44375	6.90526E-06	9.66737E-06	1.16637E-07	1.1325E-07	0.699781	0.0090011
71	97.6894694	4792.4185	6.9337E-06	9.70718E-06	1.16646E-07	1.1325E-07	0.278511	0.0009268
72	93.5748063	4863.73549	6.91302E-06	9.67822E-06	1.1664E-07	1.1325E-07	0.584961	0.0067945
73	99.7033329	4850.68548	6.91686E-06	9.68361E-06	1.16641E-07	1.1325E-07	0.527933	0.0057002
74	98.8236788	4933.25537	6.89338E-06	9.65074E-06	1.16633E-07	1.1325E-07	0.8758	0.0123924
75	93.3682171	4862.00031	6.91351E-06	9.67891E-06	1.1664E-07	1.1325E-07	0.577658	0.0066543
76	88.7596475	4964.87801	6.88434E-06	9.63808E-06	1.16631E-07	1.1325E-07	1.009741	0.0149801
77	90.5484696	4743.39245	6.94796E-06	9.72714E-06	1.16651E-07	1.1325E-07	0.067295	-0.003099
78	96.4136343	4792.13974	6.93376E-06	9.70726E-06	1.16646E-07	1.1325E-07	0.277636	0.0009101
79	93.5575735	4915.50388	6.89829E-06	9.65761E-06	1.16635E-07	1.1325E-07	0.803047	0.0109894
80	97.7829473	4848.36328	6.9175E-06	9.6845E-06	1.16641E-07	1.1325E-07	0.51851	0.0055195
81	101.674822	4760.41649	6.94314E-06	9.7204E-06	1.16649E-07	1.1325E-07	0.13865	-0.001741
82	85.9163029	4835.90466	6.92084E-06	9.68918E-06	1.16642E-07	1.1325E-07	0.468978	0.00457
83	93.6428764	4811.34696	6.92812E-06	9.69937E-06	1.16645E-07	1.1325E-07	0.361205	0.0025071
84	96.9646018	4804.89525	6.93005E-06	9.70208E-06	1.16645E-07	1.1325E-07	0.332533	0.0019589
85	90.6070189	4789.21198	6.9345E-06	9.7083E-06	1.16647E-07	1.1325E-07	0.266661	0.0007005
86	102.554071	4801.90712	6.93101E-06	9.70342E-06	1.16646E-07	1.1325E-07	0.318328	0.0016874
87	94.1803518	4829.10794	6.92299E-06	9.69218E-06	1.16643E-07	1.1325E-07	0.437251	0.0039623
88	93.9452387	4868.93275	6.91154E-06	9.67615E-06	1.16639E-07	1.1325E-07	0.606885	0.0072155
89	98.480129	4867.07245	6.91215E-06	9.67701E-06	1.1664E-07	1.1325E-07	0.597822	0.0070414
90	95.6427655	4728.57547	6.95245E-06	9.73343E-06	1.16652E-07	1.1325E-07	0.000777	-0.004364
91	101.303226	4730.58778	6.95195E-06	9.73273E-06	1.16652E-07	1.1325E-07	0.008195	-0.004223
92	97.4565491	4826.31483	6.92385E-06	9.69339E-06	1.16643E-07	1.1325E-07	0.424419	0.0037166
93	92.0378074	4748.37024	6.94652E-06	9.72513E-06	1.16651E-07	1.1325E-07	0.088604	-0.002694

Index	$\Delta P_{UF\ 1\text{-}1}$	$t_{UF\ 1\text{-}1}$	$J'_{UF\ 1\text{-}1}$	$Q_{OD\ 1\text{-}2}$	$J'_{OD\ 1\text{-}2}$	$J'_{OD\ 1\text{-}2,\ required}$	p_1	p_2
94	91.2905738	4978.98727	6.88047E-06	9.63266E-06	1.16629E-07	1.1325E-07	1.067124	0.0160905
95	94.2358528	4805.50369	6.92983E-06	9.70176E-06	1.16645E-07	1.1325E-07	0.33589	0.002023
96	97.1298291	4783.32199	6.93635E-06	9.71089E-06	1.16647E-07	1.1325E-07	0.239291	0.0001781
97	88.6665874	4736.83618	6.94985E-06	9.7298E-06	1.16652E-07	1.1325E-07	0.039195	-0.003634
98	95.3081977	4816.12184	6.92676E-06	9.69747E-06	1.16644E-07	1.1325E-07	0.381261	0.0028907
99	103.173108	4777.46268	6.93816E-06	9.71342E-06	1.16648E-07	1.1325E-07	0.212458	-0.000334
100	99.8528004	4775.25045	6.93876E-06	9.71426E-06	1.16648E-07	1.1325E-07	0.203608	-0.000503
101	100.12302	4729.00724	6.9524E-06	9.73336E-06	1.16652E-07	1.1325E-07	0.001526	-0.00435
102	103.06212	4794.43015	6.9332E-06	9.70648E-06	1.16646E-07	1.1325E-07	0.285948	0.0010688
103	85.3116102	4814.46026	6.92703E-06	9.69784E-06	1.16644E-07	1.1325E-07	0.377339	0.0028156
104	93.9778508	4999.56034	6.87482E-06	9.62475E-06	1.16627E-07	1.1325E-07	1.1508	0.0177118
105	93.7088205	5069.17827	6.85575E-06	9.59806E-06	1.16621E-07	1.1325E-07	1.433276	0.0232026
106	87.7876401	4807.72591	6.92905E-06	9.70066E-06	1.16645E-07	1.1325E-07	0.34748	0.0022446
107	93.4664432	4819.91151	6.92563E-06	9.69588E-06	1.16644E-07	1.1325E-07	0.398044	0.0032118
108	96.1614614	4861.60683	6.91367E-06	9.67914E-06	1.1664E-07	1.1325E-07	0.575226	0.0066076
109	92.0294383	4862.90431	6.91322E-06	9.67851E-06	1.1664E-07	1.1325E-07	0.581884	0.0067354
110	92.6575958	4911.97493	6.89927E-06	9.65898E-06	1.16635E-07	1.1325E-07	0.788531	0.0107097
111	101.873985	4737.432	6.94993E-06	9.7299E-06	1.16652E-07	1.1325E-07	0.038108	-0.003654
112	94.0427148	5040.71385	6.86351E-06	9.60892E-06	1.16624E-07	1.1325E-07	1.318338	0.0209651
113	93.0155843	4750.44538	6.94593E-06	9.7243E-06	1.1665E-07	1.1325E-07	0.097379	-0.002527
114	101.155365	5007.35028	6.87279E-06	9.6219E-06	1.16627E-07	1.1325E-07	1.180924	0.0182961
115	96.2374826	4783.28808	6.93634E-06	9.71088E-06	1.16647E-07	1.1325E-07	0.239378	0.0001797
116	90.2775394	4962.38399	6.88507E-06	9.6391E-06	1.16631E-07	1.1325E-07	0.998958	0.0147715
117	105.673475	4889.76236	6.90578E-06	9.66809E-06	1.16637E-07	1.1325E-07	0.692136	0.008854

Table F-3: 3D scatter plot of 14 selected scenarios from Table F-2, six (6) failed scenarios are indicated by marker ▲

$\Delta P_{UF\ 1\text{-}1}$ (kPa)	$t_{UF\ 1\text{-}1}$ (s)	$J'_{UF\ 1\text{-}1}$ ($m^3\ m^{-2}\ s^{-1}$)	p_2
105.3381633	4815.501924	6.9271E-06	0.00279
100.5827645	4823.591601	6.92469E-06	0.00348
97.41913949	4904.104462	6.90159E-06	0.01005
96.89966794	4865.804238	6.91248E-06	0.00695
98.25902073	5030.009456	6.86651E-06	0.0201
105.6734748	4889.76236	6.90578E-06	0.00885
93.23473554	4838.249676	6.92033E-06	0.00472
91.63977518	4973.418189	6.88202E-06	0.01564
97.68946943	4792.418504	6.9337E-06	0.00093
101.3643177	5100.684119	6.84736E-06	0.02563
94.78599064	4868.483722	6.91168E-06	0.00717
95.30116312	4898.587687	6.90311E-06	0.00961
90.14690407	4784.736277	6.9358E-06	0.00033
107.9349195	4873.857055	6.91034E-06	0.00755

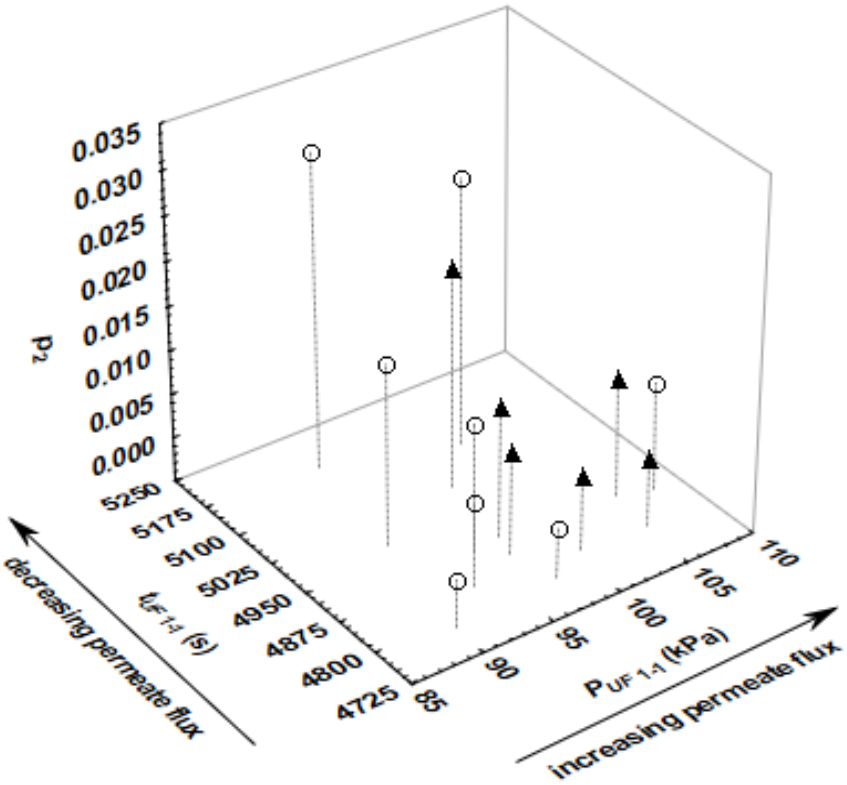

Table F-4: Radar plot of 14 selected scenarios from Table F-2

$\Delta P_{UF\ 1\text{-}1}$ (kPa)	$t_{UF\ 1\text{-}1}$ (s)	$J'_{UF\ 1\text{-}1}$ ($m^3\ m^{-2}\ s^{-1}$)	p_2
105.3381633	4815.50192	6.9271E-06	0.002795
100.5827645	4823.5916	6.92469E-06	0.003479
97.41913949	4904.10446	6.90159E-06	0.01005
96.89966794	4865.80424	6.91248E-06	0.006946
98.25902073	5030.00946	6.86651E-06	0.020101
105.6734748	4889.76236	6.90578E-06	0.008854
93.23473554	4838.24968	6.92033E-06	0.004716
91.63977518	4973.41819	6.88202E-06	0.015645
97.68946943	4792.4185	6.9337E-06	0.000927
101.3643177	5100.68412	6.84736E-06	0.025628
94.78599064	4868.48372	6.91168E-06	0.007174
95.30116312	4898.58769	6.90311E-06	0.009614
90.14690407	4784.73628	6.9358E-06	0.000334
107.9349195	4873.85705	6.91034E-06	0.007555

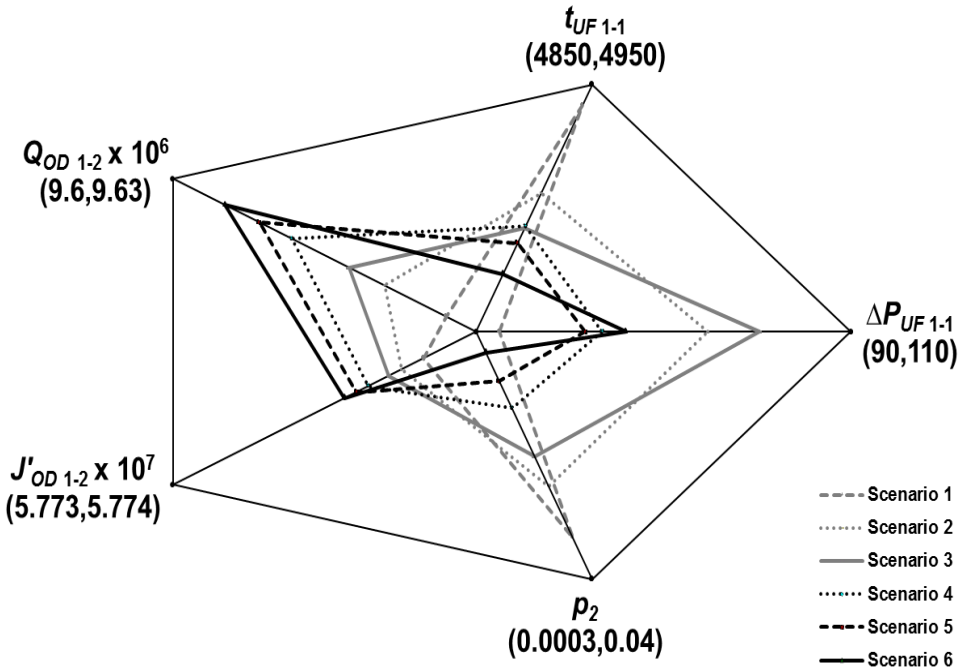

Table F-5: *Fr 13* second-tier simulation of the effect of *%tolerance* on the overall *Fr 13* failures (p_2) in integrated UF-OD

Parameters	SVA	*Fr 13*	Distribution & Formulas
ΔP (kPa)	96	**97.42**	**RiskNormal** (96, 4.8, **RiskTruncate** (81.6, 110.4))
t (s)	4500	**4904.10**	**RiskNormal** (4500, 225, **RiskTruncate** (3825, 5175))
T (^{o}C)	25	25	
L ($m^3\ m^{-2}\ s^{-1}\ kPa^{-1}$)	1.82E-06	1.82E-06	
k_0 ($s\ m^{-2}$)	5.70E+06	5.70E+06	
J^* ($m^3 m^{-2} s^{-1}$)	5.62E-06	5.62E-06	
$J_{required}$ ($m^3\ m^{-2}\ s^{-1}$)	6.75E-06	6.75E-06	
J' ($m^3\ m^{-2}\ s^{-1}$)	7.02238E-06	6.902E-06	Eq. (5.4)
p_1 (risk factor)	-1.04E+00	**0.754**	Eq. (5.13)

%tolerance	Failures (p_1)	Failures (p_2)
1	0	0
1.5	15	9
2	1853	1258
2.5	6198	4208
3	15407	10468
3.5	30208	20511
4	48657	33038
4.5	66916	45435
5	83488	57330

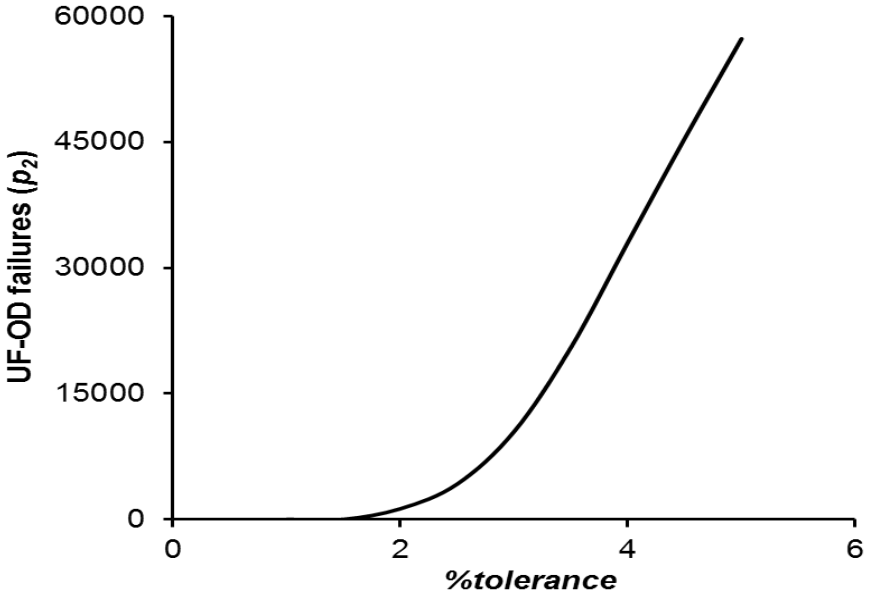

Table F-6: *Fr 13* second-tier simulation of the effect of %stdev on the overall *Fr 13* failures (p_2) in integrated UF-OD

Parameters	SVA	*Fr 13*	Distribution & Formulas
ΔP (kPa)	96	**97.42**	**RiskNormal** (96, 4.8, **RiskTruncate** (81.6, 110.4))
t (s)	4500	**4904.10**	**RiskNormal** (4500, 225, **RiskTruncate** (3825, 5175))
T (^{o}C)	25	25	
L ($m^3\ m^{-2}\ s^{-1}\ kPa^{-1}$)	1.82E-06	1.82E-06	
k_0 ($s\ m^{-2}$)	5.70E+06	5.70E+06	
J^* ($m^3 m^{-2} s^{-1}$)	5.62E-06	5.62E-06	
$J_{required}$ ($m^3\ m^{-2}\ s^{-1}$)	6.75E-06	6.75E-06	
J' ($m^3\ m^{-2}\ s^{-1}$)	7.02238E-06	6.902E-06	Eq. (5.4)
p_1 (risk factor)	-1.04E+00	**0.754**	Eq. (5.13)

Stdev (%)	p_1 (failures)	p_2 (failures)
1	0	0
3	6367	4323
5	15407	10468
7	22164	15049
10	29669	20145
15	36131	24532
20	39518	26832

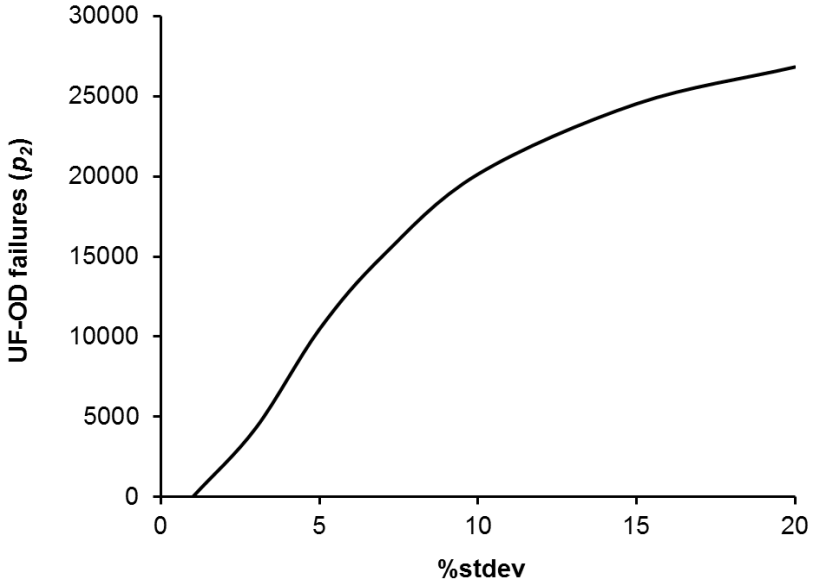

Table F-7: *Fr 13* second-tier simulation of the effect of required operational flux on the overall *Fr 13* failures (p_2) in integrated UF-OD

Parameters	SVA	*Fr 13*	Distribution & Formulas
ΔP (kPa)	96	**97.42**	**RiskNormal** (96, 4.8, **RiskTruncate** (81.6, 110.4))
t (s)	4500	**4904.10**	**RiskNormal** (4500, 225, **RiskTruncate** (3825, 5175))
T (^{o}C)	25	25	
L ($m^3\ m^{-2}\ s^{-1}\ kPa^{-1}$)	1.82E-06	1.82E-06	
k_0 ($s\ m^{-2}$)	5.70E+06	5.70E+06	
J^* ($m^3 m^{-2} s^{-1}$)	5.62E-06	5.62E-06	
$J_{required}$ ($m^3\ m^{-2}\ s^{-1}$)	6.75E-06	6.75E-06	
J' ($m^3\ m^{-2}\ s^{-1}$)	7.02238E-06	6.902E-06	Eq. (5.4)
p_1 (risk factor)	-1.04E+00	**0.754**	Eq. (5.13)

$\%J_{UF\ 1\text{-}1,\ required}$	%stdev			
	5	**7**	**10**	**15**
100	10461	15049	20146	24532
99	0	3198	8911	15677
98	0	10	2134	8362
97	0	0	6	3244
96	0	0	0	295
95	0	0	0	0

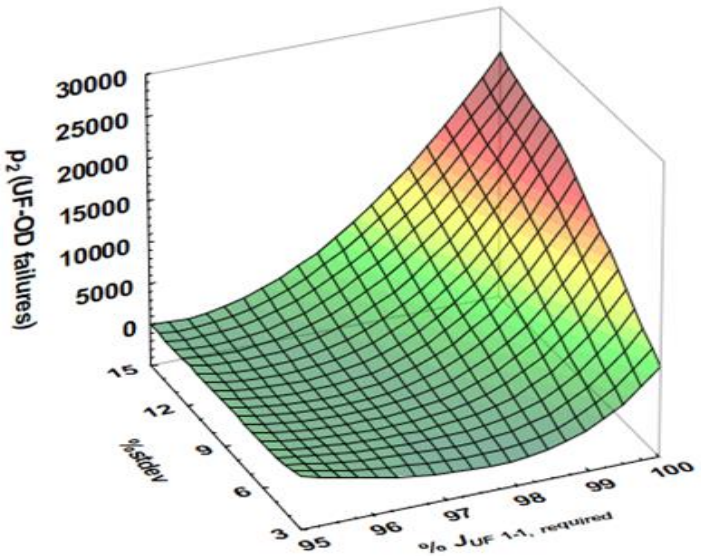

NOMENCLATURE – Chapters 2-4 - Dead-end and cross-flow filtration models

The equation number given after description refers to that in which the symbol is first used or defined.

A	surface area of membranes (m^2) (3.1)
J'	permeate flux in membrane filtration ($m^3\ m^{-2}\ s^{-1}$) (3.1)
$J_{required}$	permeate flux required for successful membrane filtration ($m^3\ m^{-2}\ s^{-1}$) (3.5)
J_0	permeate flux of clean water in membrane permeability test ($m^3\ m^{-2}\ s^{-1}\ kpa^{-1}$) (3.2)
J^*	steady-state permeate flux at the end of cross-flow filtration ($m^3\ m^{-2}\ s^{-1}$) (4.1)
K_n	kinetic fouling constant in dead-end filtrations ($s\ m^{-2}$) (3.1)
K_c	kinetic fouling constant for cake layer formation in dead-end ($s\ m^{-2}$) (3.2)
k_n	kinetic fouling constant in cross-flow filtration ($s\ m^{-2}$) (4.1)
k_0	kinetic fouling constant for cake layer formation in cross-flow ($s\ m^{-2}$) (4.2)
n	number of data
n	adjustment parameter based on principal fouling mode (4.1)
p	risk factor (dimensionless) (3.5)
Q	water volumetric feed flow rate at operational temperature ($m^3\ s^{-1}$) (3.3)
R_T	total resistance of the membranes (psi/gfd-cp) (2.1)
R_m	hydraulic resistance of clean membrane (psi/gfd-cp) (2.1)
R_{ir}	hydraulic resistance of irreversible fouling effects (psi/gfd-cp) (2.1)
R_r	hydraulic resistance of reversible fouling effects (psi/gfd-cp) (2.1)
t	filtration time (s) (3.1)

Greek

ΔP	transmembrane pressure (kPa) (3.3)
μ_T	viscosity of clean-water at operation time (Pa s) (3.3)
$\mu_{T,\,20\,^{o}C}$	viscosity of clean-water at 20 ^{O}C (Pa s) (3.3)

Other

MF	membrane microfiltration
stdev	standard deviation in the normal distribution
%tolerance	assumed practical tolerance over design critical flux (%) (3.5)
UF	membrane ultrafiltration

NOMENCLATURE – Chapter 5 - Integrated two-step UF-OD membrane global model for concentrated pomegranate juice

The first numeric subscript defines the unit item number, the second the order in which it is connected in the global model. The number given after description refers to the equation in which the symbol is first used or defined.

a	water activity (dimensionless) (5.5)
$A_{UF\ 1\text{-}1}$	surface area of membranes for UF (m^2) (Footnote 9)
$A_{OD\ 1\text{-}2}$	surface area of membranes for OD (= 1.4 m^2) (5.7 a)
C	concentration of osmotic agent at processing time (= 9.02 mol kg^{-1}) (5.8)
d_p	membrane average pore diameter (= 0.0000002 m) (5.9)
J_0	permeate flux of clean water in UF membrane ($m^3\ m^{-2}\ s^{-1}$) (5.2)
J^*	permeate flux at UF steady-state (= 5.62 x 10^{-6} $m^3\ m^{-2}\ s^{-1}$) (5.1)
$J'_{UF\ 1\text{-}1}$	permeate flux in a juice clarification for UF($m^3\ m^{-2}\ s^{-1}$) (5.1)
$J'_{OD\ 1\text{-}2}$	permeate flux in a juice concentration for OD ($m^3\ m^{-2}\ s^{-1}$) (5.5)
$J_{UF\ 1\text{-}1,\ required}$	required flux for cross-flow UF clarification (= 6.75 x 10^{-6} $m^3\ m^{-2}\ s^{-1}$) (5.11)
$J_{OD\ 1\text{-}2,\ required}$	required flux for OD concentration (= 1.1325 x 10^{-7} $m^3\ m^{-2}\ s^{-1}$) (5.14)
$k_{UF\ 1\text{-}1}$	kinetic constant of fouling mode for UF (s m^{-2}) (5.1)
$k_{0,\ UF\ 1\text{-}1}$	kinetic constant of cake layer formation for UF (= 5.7 x 10^6 s m^{-2}) (5.2)
$k_{1,\ OD\ 1\text{-}2}$	mass transfer coefficient for feed solution for OD (m s^{-1}) (5.7)
$k_{2,\ OD\ 1\text{-}2}$	mass transfer coefficient for stripping solution for OD (m s^{-1}) (5.8)
$k_{m,\ OD\ 1\text{-}2}$	mass transfer coefficient for membranes for OD (m s^{-1}) (5.9)
$K_{OD\ 1\text{-}2}$	overall mass transfer coefficient for OD (m s^{-1}) (5.6)

L	UF constant for pomegranate juice for J_0 (= 1.821 x 10^{-6} m^3 m^{-2} s^{-1} kPa^{-1}) (5.3) (Footnote 10)
M_w	molecular weight pure water (= 0.018 kg mol^{-1}) (5.9)
n	number of data
n	adjustment parameter based on principal fouling mode (= 0) (5.1)
P^*	vapour pressure of pure water (= 3,169 Pa) (5.9)
p_1	fouling risk factor for UF (dimensionless) (5.11)
p_2	fouling risk factor for combined UF-OD global model (dimensionless) (5.14)
$Q_{UF\ 1\text{-}1}$	volumetric feed flow rate at operational temperature for UF (m^3 s^{-1}) (Footnote 9)
$Q_{OD\ 1\text{-}2}$	volumetric feed flow rate at operational temperature for OD (m^3 s^{-1}) (5.7 a)
R	gas constant (= 8.314, J mol^{-1} K^{-1}) (5.9)
stdev	standard deviation in Normal distribution
$T_{UF\ 1\text{-}1}$	juice temperature in UF (^{O}C) (Footnote 9)
$T_{OD\ 1\text{-}2}$	juice temperature in OD (K) (5.9)
$t_{UF\ 1\text{-}1}$	filtration time for UF (s) (5.2)

Greek

δ	OD membrane thickness (= 0.000175 m) (5.9)
ε	OD porosity (= 0.75 dimensionless) (5.9)
$\Delta P_{UF\ 1\text{-}1}$	transmembrane pressure for UF (kPa) (5.3)
$\Delta P_{OD\ 1\text{-}2}$	membrane driving pressure for OD (Pa) (5.9)
$\mu_{T,\ UF\ 1\text{-}1}$	viscosity of clean-water at operation temperature for UF (Pa s) (Footnote 9)

$\mu_{T,\,20\,^{o}C}$	viscosity of water at 20 ^{O}C (Pa s) (Footnote 9)
τ	tortuosity factor (= 2 dimensionless) (5.9)

Other

OD	membrane osmotic distillation (Fig. 5-1)
stdev	standard deviation in Normal distribution
%tolerance	Practical tolerance over design critical flux, % (5.12)
UF	membrane ultrafiltration (Fig. 5-1)

REFERENCES

Abdul-Halim, N., Davey, K.R., 2015 a. A Friday 13th risk assessment of failure of ultraviolet irradiation for potable water in turbulent flow. Food Control 50, 770-777. http://dx.doi.org/10.1016/j.foodcont.2014.10.036

Abdul-Halim, N., Davey, K.R., 2015 b. Impact of suspended solids on *Fr 13* failure of UV irradiation for inactivation of *Escherichia coli* in potable water production with turbulent flow in an annular reactor. Chem. Eng. Sci. - in revision Oct.

Alves, V.D., Coelhoso, I.M., 2004. Effect of membrane characteristics on mass and heat transfer in the osmotic evaporation process. J. Membrane Sci. 228, 159-167. http://dx.doi.org/ 10.1016/j.memsci.2003.10.004

Amundson, N.R., Aris, R., Varma, A., 1980. The Mathematical Understanding of Chemical Engineering Systems. Pergamon Press, Oxford, UK. pp. 342, 282, 781, 548, 30, 278, 666, 346ff. ISBN: 9780080238364

Aimar, P., Howell, J.A., 1989. Effects of concentration boundary layer development on the flux limitations in ultrafiltration. Chem. Eng. Res. Des. 67, 255-261. ISSN: 02638762

Anon., 2012. Blackett review of high impact low probability risks. Government Office for Science, UK. http://www.bis.gov.uk/assets/goscience/docs/b/12-519-blackett-review-high-impact-low-probability-risks.pdf, viewed Oct. 7, 2015, 10.00 h.

Asao, T., Kumeda, Y., Kawai, T., Shibata, T., Oda, T., Haruki, K., Nakazawa, H., Kozaki, S., 2003. An extensive outbreak of staphylococcal food poisoning due to low-fat milk in Japan: estimation of enterotoxin A in the incriminated milk and powdered skim milk. Epidemiol. Infec. 130, 33-40. http://dx.doi.org/10.1017/S0950268802007951

Aven, T., 2010. On how to define, understand and describe risk. Reliab. Eng. Syst. Safe. 95 (6), 623-631. http://dx.doi.org/10.1016/j.ress.2010.01.011

Aviram, M., Dornfeld, L., 2001. Pomegranate juice consumption inhibits serum angiotensin converting enzyme activity and reduces systolic blood pressure. Atherosclerosis 158, 195-198. http://dx.doi.org/10.1016/S0021-9150(01)00412-9

Boerlage, S.F.E., Kennedy, M.D., Dickson, M.R., El-Hodali, D.E.Y., Schippers, J.C., 2002. The modified fouling index using ultrafiltration membranes (MFI-UF): Characterisation, filtration mechanisms and proposed reference membrane. J. Membrane Sci. 197, 1-21. http://dx.doi.org/10.1016/S0376-7388(01)00618-4

Cassano, A., Jiao, B., Drioli, E., 2004. Production of concentrated kiwifruit juice by integrated membrane processes. Food Res. Int. 37, 139-148. http://dx.doi.org/10.1016/j.foodres.2003.08.009

Cassano, A., Marchio, M., Drioli, E., 2006. Clarification of blood orange juice by ultrafiltration: analyses of operating parameters, membrane fouling and juice quality. Desalination 212, 15-27. http://dx.doi.org/10.1016/j.desal.2006.08.013

Cassano, A., Drioli, E., 2007. Concentration of clarified kiwifruit juice by osmotic distillation. J. Food. Eng. 79, 1397-1404. http://dx.doi.org/10.1016/j.jfoodeng.2006.04.021

Cassano, A., Marchio, M., Drioli, E., 2007. Clarification of blood orange juice by ultrafiltration: analyses of operating parameters, membrane fouling and juice quality. Desalination 212, 15-27. http://dx.doi.org/10.1016/j.desal.2006.08.013

Cassano, A., Conidi, C., Drioli, E., 2011. Clarification and concentration of pomegranate juice (*Punica granatum L.*) using membrane processes. J. Food Eng. 107, 366-373. http://dx.doi.org/10.1016/j.foodeng.2011.07.002

Cassano, A., 2013. Fruit juices. In: A.Y. Tamime, ed. Membrane Processing: Dairy and Beverage Applications. Wiley-Blackwell publishing Ltd, Oxford, UK, pp. 262-280. http://dx.doi.org/10.1002/9781118457009.ch12

Cerf, O., Davey, K.R., 2001. An explanation of non-sterile (leaky) milk packs in well operated UHT plant. Food and Bioprod. Process. (Part C) 79 (4), 219-222. http://dx.doi.org/10.1205/096030801753252289

Chandrakash, S., 2013. A new risk analysis of Clean-In-Place (CIP) milk processing. Master (Research) thesis, The University of Adelaide, pp. 101.

Chandrakash, S., Davey, K.R., 2015. An integrated three-step *Fr 13* failure model - demonstrated with pasteurization of raw milk containing *Mycobacterium avium* subsp. *paratuberculosis* (*MAP*). Chem. Eng. Sci. – in prepn.

Chandrakash, S., Davey, K.R., O'Neill, B.K., 2015. An *Fr 13* risk analysis of failure in a global food process – illustration with milk processing. (Special theme invited research articles). Asia – Pac. J. Chem. Eng. – in proof 24 Mar. http://dx.doi.org/10.1002/apj.1887

Cheryan, M., 1998. Ultrafiltration and Microfiltration Handbook. 2nd ed. CRC Press, Florida, USA. ISBN: 1566765986

Chu J.Y.G., 2015. Synthesis of a new quantitative model and experimental validation for optimisation of energy for conditioning of air in large buildings with unpredictable traffic flows. PhD (Research) thesis. The University of Adelaide - in prepn.

Chu, J.Y.G., Davey, K.R., 2015. A probabilistic *Fr 13* simulation of strategies for cooling of air in buildings with unplanned traffic flow during summer. In: Proc. 3rd Int. Workshop on Simulation for Energy, Sustainable Development & Environment-SESDE 2015, Sept. 21-23, Bergeggi, Italy, Paper 45, pp. P1, 51-59. ISBN: 9788897999614

Constela, D.T., Lozano, J.E., 1997. Hollow fibre ultrafiltration of apple juice: macroscopic approach. LWT-Food Sci. Technol. 30, 373-378. http://dx.doi.org/10.1006/fstl.1996.0192

Cui, Z.F., Jiang, Y., Field, R.W., 2010. Fundamentals of pressure-driven membrane separation processes. In: Z.F. Cui, H.S. Muralidhara, ed. Membrane Technology: A Practical Guide to Membrane Technology and Applications in Food and Bioprocessing. Butterworth-Heinemann, UK, pp. 1-18. ISBN: 9781856176323

Davey, K.R., 2015 a. A novel Friday 13th risk assessment of fuel-to-stream efficiency of a coal-fired boiler. Chem. Eng. Sci. 127, 133-142. http://dx.doi.org/10.1010/j.ces.2015.01.031

Davey, K.R., 2015 b. Failure modelling of a generic process with feed-stream, reactor, separator and recycle with purge – A Friday 13th risk assessment. Chem. Eng. Sci. – in prepn.

Davey, K.R., 2011. Introduction of fundamental and benefits of Friday 13th risk modelling technology for food manufacturers. Food Aust. 63 (5), 192-197. ISSN: 1032598

Davey, K.R., 2010. A novel proposal to advance the discipline and to quantitatively safeguard important hygienic bio-processes. In: Proc. 40th Australasian Chemical Engineering Conference (Engineering at The Edge)-CHEMECA 2010, Sept. 26-29, Adelaide, Australia, Paper 0495. ISBN: 9780858259713

Davey, K.R., Cerf, O., 2003. Risk modelling - An explanation of Friday 13th syndrome (failure) in well-operated continuous sterilization plant. In: Proc. 31st Australasian Chemical Engineering Conference (Product and Processes for the 21st Century)-CHEMECA 2003, Sept. 28–Oct. 1, Adelaide, Australia, Paper 61. ISBN: 0863968295

Davey, K.R., 2001. Models for predicting the combined effect of environmental process factors on the exponential and lag phases of bacteria growth – Development and application and an unexpected correlation. In Proc. 6th World Conference of Chemical Engineering Conference, Sept. 23-27, Melbourne, Australia, pp. 170ff. ISBN: 0734022018

Davey, K.R., Chandrakash, S., O'Neill, B.K., 2015. A Friday 13th failure assessment of Clean-In-Place removal of whey protein deposits from metal surface with auto-set cleaning times. Chem. Eng. Sci. 126, 106-115. http://dx.doi.org/10.1016/j.ces.2014.12.013

Davey, K.R., Chandrakash, S., O'Neill, B.K., 2013. A new risk analysis of Clean-In-Place milk processing. Food Control 29 (1), 248-254. http://dx.doi.org/10.1016/j.foodcont.2012.06.014

Davey, K.R., Lavigne, O., Shah, P., 2016. Establishing an atlas of risk of pitting of metals at sea - demonstrated for stainless steel AISI 316L in the Bass Strait. Chem. Eng. Sci. 140, 71-75. http://dx.doi.org/10.1016/j.ces.2015.10.008

Davey, K.R., Zou, W., 2015. Fruit juice processing and membrane technology application (*sic*) – A response. Food Engineering Reviews – submitted Oct. 28, 2015.

De Bruijn, J.P.F., Venegas, A., Martinez, J.A., Bórquez, R., 2003. Ultrafiltration performance of Carbosep membranes for the clarification of apple juice. LWT-Food Sci. Technol. 36, 397-406. http://dx.doi.org/10.1016/S0023-6438(03)00015-X

De Carvalho, L.M.J., 2008. A study of retention of sugars in the process of clarification of pineapple juice (*Ananas comosus*, L. Merril) by micro- and ultra-filtration. J. Food Eng. 87 (4), 447-454. http://dx.doi.org/10.1016/j.jfoodeng.2007.12.015

Domingues, R.C.C., Ramos, A.A., Cardoso, V.L., Reis, M.H.M., 2014. Microfiltration of passion fruit juice using hollow fiber membranes and evaluation of fouling mechanisms. J. Food Eng. 121, 73-79. http://dx.doi.org/10.1016/j.jfoodeng.2013.07.037

D'Souza, N.M., Mawson, A.J., 2005. Membrane cleaning in the dairy industry: A review. Crit. Rev. Food Sci. Nutr. 45 (2), 125-134. http://dx.doi.org/10.1080/10408690490911783

Echavarria, A.P., Torras, C., Pagán, J., Ibarz, A., 2011. Fruit juice processing and membrane technology application. Food Eng. Rev. 3, 136-158. http://dx.doi.org/10.1007/s12393-011-9042-8

Espamer, L., Pagliero, C., Ochoa, A., Marchese, J., 2006. Clarification of lemon juice using membrane process. Desalination 200, 565-567. http://dx.doi.org/10.1016/j.desal.2006.03.458

Field, R.W., Wu, D., Howell, J.A., Gupta, B.B., 1995. Critical flux concept for microfiltration fouling. J. Membrane Sci. 100, 259-272. http://dx.doi.org/10.1016/0376-7388(94)00265-Z

Field, R.W., Wu, J.J, 2011. Modelling of permeability loss in membrane filtration: Re-examination of fundamental fouling equations and their link to critical flux. Desalination 283, 68-74. http://dx.doi.org/10.1016/j.desal.2011.04.035

Foust, A.S., Wenzel, L.A., Clump, W.C., Maus, L., Andersen, L.B., 1980. Principles of Unit Operations. 2nd ed. John Wiley and Sons, New York, USA. ISBN: 0471268976

Ghasem, N., Henda, R., 2008. Principles of Chemical Engineering Processes. CRC Press, UK. ISBN: 9781420080193

Giaccone, V., Ferri, M., 2005. Microbiological quantitative risk assessment and food safety: An update. Vet. Res. Commun. 29 (Suppl.2), 101-106. http://dx.doi.org/10.1007/s11259-005-0020-6

Goulas, A., Grandison, A.S., 2008. Application of membrane separation. In: T.J. Britz, R.K. Robinson, ed. Advanced Dairy Science and Technology. Wiley-Blackwell publishing Ltd, Oxford, UK, pp. 35-74. http://dx.doi.org/10.1002/9780470697634.ch2

Haimes, Y.Y., 2009. On the complex definition of risk: A systems-based approach. Risk Anal. 29 (12), 1647-1654. http://dx.doi.org/ 10.1111/j.1539-6924.2009.01310.x

Haimes, Y.Y., 2004. Risk Modeling, Assessment, and Management, 2nd ed., John Wiley & Sons Inc., New Jersey, USA. ISBN: 0471480487

Hausmann, A., Duke, M.C., Demmer, T., 2013. Principles of membrane filtration. In: A.Y. Tamime, ed. Membrane Processing: Dairy and Beverage Applications. Wiley-Blackwell publishing Ltd, Oxford, UK, pp. 17-51. http://dx.doi.org/10.1002/9781118457009.ch2

Hermia, J., 1982. Constant pressure blocking filtration laws: Application to power-law non-newtonian fluids. Trans. Ind. Chem. Eng. 60, 183-187. http://dx.doi.org/10.1007/978-94-009-5091-75

Hogan, P.A., Canning, R.P., Peterson, P.A., Johnson, R.A., Michaels, A.S., 1998. A new option: osmotic distillation. Chem. Eng. Prog. (July), 49-61.

Law, A.M., 2011. How to select simulation input probability distributions. In: Proc. the 2011 Winter Simulation Conference-WCS 2011. Dec. 11-14, Phoenix, USA, pp. 1394-1406. ISBN: 9781457721090

McCabe, W.L., Smith, J.C., Harriott, P., 2001. Unit Operations of Chemical Engineering. 6th ed. McGraw-Hill, New York, USA. ISBN: 0070393664

Milazzo, M.F., Aven, T., 2012. An extended risk assessment approach for chemical plants applied to a study related to pipe ruptures. Reliab. Eng. Syst. Safe. 99, 183-192. http://dx.doi.org/10.1016/j.ress.2011.12.001

Mirsaeedghazi, H., Emam-Djomeh, Z., Mousavi, S.M., Ahmadkhaniha, R., Shafiee, A., 2010. Effect of membrane clarification on the physicochemical properties of pomegranate juice. Int. J. Food Sci. Tech. 45 (7), 1457-1463. http://dx.doi.org/10.1111/j.1365-2621.2010.02284.x

Mulder, M., 1996. Basic Principles of Membrane Technology. 1st ed. Kluwer Academic Publishers, USA. ISBN: 9780792342489

Nandi, B.K., Das, B., Uppaluri, R., 2012. Clarification of orange juice using ceramic membrane and evaluation of fouling mechanism. J. Food Process. Eng. 35, 403-423. http://dx.doi.org/10.1111/j.1745-4530.2010.00597.x

Notermans, S., Mead, G.C., 1996. Incorporation of elements of quantitative risk analysis in the HACCP system. Int. J. Food Microbiol. 30, 157-173. http://dx.doi.org/10.1016/0168-1605(96)00997-x

OREDA., 2015. Offshore and Onshore Reliability Database, OREDA 2015 Handbook, DNV.GL.http://blogs.dnvgl.com/software/2015/06/new-edition-oreda-2015-handbook/ viewed Oct. 23, 2015, 16.00 h.

Ozilgen, M., 1998. Food Process Modeling and Control: Chemical Engineering Applications. CRC Press, UK. ISBN: 9056991434

Patil, R.A., 2006. Novel application of quantitative risk assessment modelling to a continuous fermenter. Master (Research) thesis, The University of Adelaide, pp. 122.

Patil, R.A., Davey, K.R., Daughtry, B.J., 2005. A new quantitative risk assessment of a fermenter for Friday 13th syndrome. In: Proc. 32nd Australasian Chemical Engineering Conference (Smart Solution-Doing More with Less)-CHEMECA 2005. Sept. 25-29, Brisbane, Australia, Paper 79. ISBN: 9781604235142

Razi, B., Aroujalian, A., Fathizadeh, M., 2012. Modeling of fouling layer deposition in cross-flow microfiltration during tomato juice clarification. Food Bioprod. Process. 90, 841-848. http://dx.doi.org/10.1016/j.fbp.2012.05.004

Ravindra Babu, B., Rastogi, N.K., Raghavarao, K.S.M.S., 2008. Concentration and temperature polarization effects during osmotic membrane distillation. J. Membrane Sci. 322, 146-153. http://dx.doi.org/10.1016/j.memsci.2008.05.041

Ravindra Babu, B., Rastogi, N.K., Raghavarao, K.S.M.S., 2006. Mass transfer in osmotic membrane distillation of phycocyanin colorant and sweet-lime juice. J. Membrane Sci. 272, 58-69. http://dx.doi.org/10.1016/j.memsci.2005.07.034

Roorda, J.H., Van der Graaf, J.M., 2001. New parameter for monitoring fouling during ultrafiltration of WWTP effluent. Water Sci. Technol. 43 (10), 241-248.

Rosen, E.M., 2009. Steady state chemical process simulation: a state-of-the-art-review. In: R.G. Squires, G.V. Reklaitis, ed. Computer Applications to Chemical Engineering. America Chemical Society, USA. ISBN: 9780841205499

Saxena, A., Tripathi, B.P., Kumar, M., Shahi, V.K., 2009. Membrane-based techniques for the separation and purification of proteins: An overview. Adv. Colloid. Interfac. 145, 1-22. http://dx.doi.org/10.1016/j.cis.2008.07.004

Schafer, A.I., Andritsos, N., Karabelas, A.J., Hoek, E.M., Schneider, R., Nystrom, M., 2005. Fouling in nanofiltration. In: A.I. Schafer, T.D. Waite, A.G. Fane, ed. Nanofiltration-principles and Applications. UK: Elsevier, pp. 169-239. ISBN: 1856174050

Sinnott, R.K., 2005. Chemical Engineering Design. 4th ed. Elsevier, Butterworth Heinemann, UK. ISBN: 0750665386

Snedecor, G.W., Cochran, W.G. 1989. Statistical Methods, 8th ed. Iowa State University Press, Iowa, USA, pp. 194. ISBN: 9780813815619

Suddath, C. 2009. A brief history of Friday the 13th. Time (Feb). http://www.time.com/time/nation/article/0,8599,1879288,00.html, viewed 20 April, 2015, 4:14 pm.

Sullivan, M. 2004. Statistics – Information Decision Making Using Data. Pearson Education, New Jersey, USA. ISBN: 0130618640

Todisco, S., Peña, L., Drioli, E., Tallarico, P., 1996. Analysis of the fouling mechanism in microfiltration of orange juice. J. Food. Process. Pres. 20, 453-466. http://dx.doi.org/10.1111/j.1745-4549.1996.tb00759.x

Vaillant, F., Millan, P., O'Brien, G., Dornier, M., Decloux, M., Reynes, M., 1999. Cross-flow microfiltration of passion fruit juice after partial enzymatic liquefaction. J. Food. Eng. 42, 215-224. http://dx.doi.org/10.1016/S0260-8774(99)00124-7

Vose, D., 2008. Risk Analysis-A Quantitative Guide. 2nd ed. John Wiley and Sons, Chichester, UK, pp. 64, 59, 34, 41-43, 19, 201-205 ff, 379 ff. ISBN: 9780470512845

Vose, D.J., 1998. The application of quantitative risk assessment to microbial food safety. J. Food Protect. 61 (5), 640-648. ISSN: 0362028X

Wilson, E.L., Burns, D.J.W., 1983. Kiwifruit juice processing using heat treatment techniques and ultrafiltration. J. Food Sci. 48, 1101-1105. http://dx.doi.org/10.1111/j.1365-2621.1983.tb09170.x

Zambra, C., Romero, J., Pino, L., Saavedra, A., Sanchez, J., 2015. Concentration of cranberry juice by osmotic distillation process. J. Food. Eng. 144, 58-65. http://dx.doi.org/10.1016/j.jfoodeng.2014.07.009

Zou, W., Davey, K.R., 2014 a. A Friday 13th risk model for failure in cross-flow membrane filtration of passion fruit juice. In: Proc. 26th European Modeling and Simulation Symposium–EMSS 2014. Sept. 10-12, Bordeaux, France, paper 106. ISBN: 9788897999447

Zou, W., Davey, K.R., 2014 b. A novel Friday 13th stochastic assessment of failure of membrane filtration in juice clarification. In: Proc. 44th Australasian Chemical Engineering Conference (Processing Excellence, Powering our Future)-CHEMECA 2014. Sept. 28 – Oct. 01, Perth, Australia, Paper No. 1259. ISBN: 1922107387

Zou, W., Davey, K.R., 2015. An integrated two-step *Fr 13* synthesis - demonstrated with membrane fouling in combined ultrafiltration-osmotic distillation (UF-OD) for concentrated juice. Chem. Eng. Sci. – submitted Nov.